Virginia Journal of Science
Volume 69, Issue 1 & 2
Spring & Summer 2018
doi: 10.25778/2DS9-MP13

Reproductive Correlates of a Perineal Gland in the Hispid Cotton Rat

Robert K. Rose[1] and Julie A. Winchell[1,2]
Department of Biological Sciences, Old Dominion University
Norfolk, Virginia 23529-0266

[2]Current addresses:
City of Cleburne Environmental Services, Cleburne, Texas 76033
4224 CR 801, Joshua, Texas 76058

ABSTRACT

During studies of the annual cycle of reproduction in the hispid cotton rat (*Sigmodon hispidus*) in southeastern Virginia, we discovered an anal (more specifically, perineal) gland that is present only in males during the breeding season. The perineal gland encircles the lower end of the rectum and has ductal connections to the urethra, through which its secretions probably are delivered. This fatty gland is highly developed in breeding males but, like the testes and seminal vesicles, regresses during the winter non-breeding season. The prominence and cyclicity of the perineal gland suggests that it somehow facilitates normal reproduction. The combined mass of testes, seminal vesicles, and perineal gland constitutes only about 0.01 percent of the body mass of large males during the non-breeding season, but as much as 4.8 percent of body mass during the breeding season. Thus, males devote a large amount of energy to growing and maintaining these glands in anticipation of and during the breeding season. Despite two field trials, the function of the perineal gland and the nature of its secretion are unknown.

INTRODUCTION

The hispid cotton rat, *Sigmodon hispidus,* the biology of which was reviewed by Cameron and McClure (1988), is a native rodent of old fields and early successional habitats in the southeastern US. Seasonal breeders everywhere, in southeastern Virginia cotton rats breed from March to October (Rose and Mitchell, 1990; Bergstrom and Rose, 2004). The onset of male reproductive capacity, using the criterion of convoluted cauda epididymides (Jameson, 1950), extends beyond the interval of female reproductive readiness by 2-4 weeks on both ends. During studies of reproduction in *S. hispidus,* one of us (RKR) noted, in adult males during the breeding season, the presence of a large subcutaneous anal organ, hereafter called the perineal gland because it encircles the rectum near the base of the tail. Although large in breeding males, this organ is indiscernible in non-breeding males, in females, and in juveniles.

In order to evaluate its nature, we examined the gross anatomy and seasonal changes of the perineal gland throughout the annual cycle. The objectives of our study were to: (1) describe the anatomy and seasonal cyclicity of the gland, (2) determine the relationship between the gland and the reproductive system, and (3) if possible, determine the method of delivery and information content of the glandular product(s). To accomplish these goals, we recorded changes in the statuses of the perineal gland, testes, and seminal vesicles by the necropsy of monthly samples of adult-sized males. We learned that the perineal gland is a seasonally cyclical multilocular gland, by inference is under androgen control, and probably delivers its secretions via the urethra.

MATERIALS AND METHODS

Specimens of cotton rats for necropsy were obtained using Fitch live traps (Rose, 1994), baited with Purina Sweetena®, a mixture of oats, corn, millet, and molasses, placed about 5 m apart on transect lines in old field habitat. Monthly samples of potentially adult males (> 50 g) were obtained from four old fields in southeastern Virginia. After chloroform euthanasia, standard body measurements including lengths of tail, hind foot, ear, and body (total length minus tail length) and weights of body, paired testes, seminal vesicles, and perineal gland were determined using a Mettler analytical balance. In all, 129 males were necropsied, 90 from the breeding season and 39 from the non-breeding season.

To prepare tissues for histological examination, a subset of wild-caught animals was anesthetized with chloroform in the lab, after which an intraperitoneal injection of 1.0 ml of tribromo-ethanol (1 g/40 ml) was used to maintain anesthesia during perfusion. The thoracic cavity was opened, a cannula was placed in the left ventricle for introduction of perfusate, and the inferior vena cava was cut to allow the exit of fluids. The tissues were flushed with heparinized buffered saline and then perfused with a solution of 4 percent paraformaldehyde in 0.1 M phosphate buffer solution (Glaubert, 1975). After the cotton rat had succumbed, the perineal region was dissected away from the lower torso and stored in 10 percent formaldehyde fixative for 24 h. Then, after the pelvic girdle and lower spine were carefully removed, the block of tissue was placed in 10 percent formalin until prepared for embedding about 20 h later.

Fully developed perineal glands could not be sectioned successfully because their waxy contents prevented adequate fixation, causing the paraffin sections to shatter. The most readable slides were prepared from a 75-g male with scrotal testes and a partially enlarged perineal gland that allowed dehydration and fixation. After the bones had been removed, the remnant was divided into three smaller pieces before dehydration. The caudal piece included the majority of the perineal gland, the central piece included a large portion of the penile shaft, and the most craniad piece, which extended well into the pelvic cavity, included the external penis, seminal vescicles, and preputial glands. These pieces were placed for dehydration in successive 30-minute baths of 25, 50, 70, and 80% ethanol before being embedded overnight in paraffin in an Autotechnicon-2A automated tissue processor. The paraffin blocks were thin-sectioned with an American Optical 820

microtome. The 10μ sections were stained with either a modified Periodic Acid Schiffs (PAS) or a Mayer's hematoxylin and eosin (H & E) stain (Luma, 1968).

The first field study, using the homogenate from whole perineal glands placed on filter paper and inserted into experimental traps, was conducted on a 6 by 5 grid with each trap being placed 7.5 m apart. Before the experiment, the plot was trapped, and animals ear-tagged and released, for 19 days in September and early October to determine a population estimate (MNA), sex ratios, and reproductive status. The perineal homogenate was produced using the frozen perineal glands of necropsied mature males; 12.3 g of glands from several males was homogenized in 45 ml of a 70% ethanol:30% phosphate-buffered saline (PBS) solution which contained 200 mg/l of L-ascorbic acid. (The ethanol was used as an organic solvent to solubilize any lipids, the PBS was used to stabilize the pH, and the L-ascorbic acid inhibited oxidation. This three-ingredient solution on filter paper triangles was used as the control for the experiment.) Both homogenate and control solutions were then stored at -20 ºC until used in the field studies. Later these mixtures were used to saturate 4 cm by 5 cm triangles of Watman #11541 filter paper, which were then placed inside traps; traps were checked daily and papers were replaced every third day. The field experiment was run for 10 days near the end of the breeding season, during which captured animals were evaluated for their reproductive status and body weight.

The second field study, conducted near the end of the breeding season the next year, examined the effect of chemically separated fractions of the perineal gland homogenate on wild populations of cotton rats. Perineal gland and muscle tissue from the flanks of male cotton rats (as control) were homogenized separately in PBS (1g/4ml). These homogenates were extracted three times with a 9:1 chloroform:methanol solution; the methanol/water fraction was kept at -20 ºC until use, whereas the chloroform fraction was evaporated off under a gentle nitrogen stream and then reconstituted to a volume of methanol equal to the volume of the top fraction. For the field study, a 15 by 6 grid (7.5-m interval) was established and animals were trapped, marked, and evaluated as before. Fifteen traps were assigned to each of the six treatments in a stratified random fashion. Each trap was baited with a 0.1 g sample of either perineal gland or muscle homogenate, or a chloroform or methanol extract (extracted from 0.1 g of homogenized tissue). These samples, on #10 Watman filter paper triangles, were placed in traps as before. The traps were checked daily for 10 days; fresh papers were added after the fifth night.

The SAS statistical package (SAS Institute, Inc., 1985) was used for standard statistics, general linear model analysis of variance (ANOVA), stepwise regression, and correlation analysis. Unless otherwise stated, the $P < 0.05$ level of significance was used.

RESULTS

During the breeding season, the adult male cotton rat possesses a large perineal gland (Fig. 1) located dorsal to the testes, under the tail, and just anterior to the anus. The testes must be excised in order to see the position of the gland in relation to the rectum, penis, and gracilis muscles of the hind legs. The anterior-most aspects of the gland

originate at the base of the penis, and when fully developed, the gland sometimes extends dorsoposteriorly to the fourth caudal vertebra.

The perineal gland is divided on each side into three unequal parts, which together encircle and are loosely attached by fascia to the rectum (Fig. 1, numbers 3A, 3B, 3C). The segment located anterior and ventral to the rectum is large (Fig. 1, 3C) and has strong, definite attachments to the base of the penis. The other smaller lobe-shaped segments (Fig. 1, 3A, 3B) lie dorsal to the rectum and caudad to the attachment points of the largest segment. One region, distinctly separable from the largest mass of the gland (Fig. 1, 3A), has a lobular appearance and dorsally flanks each side of the rectum. It is held to the largest glandular mass by a single fibrous tubule (observed but not characterized histologically) and loosely by fascia elsewhere. Due to its placement and description, these 3A lobes may not be part of the perineal gland but rather Cowper's glands, as described in the porcupine (Mirand and Shadle, 1953). (Cowper's glands are accessory to the testes and produce the vehicle to transport sperm.)

The size, weight, and shape of the perineal gland, which literally rings the rectum (Fig. 2), can vary dramatically depending on breeding status, which is determined by the maturity of the animal as well as the season. When a large (> 80 g) male is in the non-breeding condition, the gland is greatly reduced and often difficult to detect. As the breeding season approaches, the gland enlarges, revealing three definite bisymmetrical regions on each side (Fig. 1), as described above.

Histology of the perineal gland

The excised perineal gland of a large male in breeding condition is approximately the size and shape of an asymmetrical Lifesaver®. The gland is fatty and waxy, and resistant to penetration by the fixing and dehydrating agents used to prepare histological tissues for staining, and thus sections cut from such tissues were not revealing. After much trial and error, we succeeded in making tissue sections from the growing glands of young males but not from those of fully mature cotton rats.

The low magnification photograph of the cross-section of the pelvic region (Fig. 3) shows the rectum (#1), two lateral (perineal) glandular regions (2A, 2B) with their muscular investments lying lateral to the rectum and below the urethra (#3), and two other areas of glandular tissues also lateral to the urethra (#4). The glandular tissue shows bilateral symmetry, with portions lying either lateral or dorso-lateral to the rectum and ventral to the urethra. The glandular areas contain small tubules that coalesce to form larger tubules or ducts, which in turn lie within a neck-like projection of the gland, possibly connecting with the urethra. Two additional structures, which flank the urethra, contain ductal fibrous connective tissue with squamous epithelium and some vasculature. These appear to provide structural support for the perineal gland. The vicinity of the gland is highly vascularized, with large extravascular and sinusoidal spaces. Although the perineal gland and the rectum are closely apposed, no connections were detected.

Higher (31X) magnification (Fig. 4) revealed the tri-partite gland surrounded by a prominent investment of smooth muscle. The bulbous portion of the gland contains

secretory acinar cells, connective tissue, and small tubules. The neck-like projection of the gland has narrowing ducts extending towards the penis, all surrounded by smooth muscle. H & E staining revealed tubules filled with a pink mucinous material similar in appearance to colloidal tissue of the thyroid gland. The material is further characterized using a PAS hematoxylin stain, creating a bright pink similar to stained glycoproteins or glycolipids.

At high power (not shown), the tissue is seen as a multi-lobular, compound tubuloacinar gland with several distinct bundles separated by septa and connective tissues. Individual lobules are surrounded by fibrous connective tissue and the entire group of lobules is enclosed by smooth muscle. Tubules within and between lobules are lined with epithelium progressing from columnar to more cuboidal in shape. The non-tubular regions reveal the mucin-filled acini, resembling alveoli. Each acinar (secretory) cell has a large granular cytoplasm and a flattened nucleus located near the basal lamina. Overall, the acinar cells are similar in appearance to the acini of salivary gland tissue.

At the head-like junction of the perineal gland with the penis (not shown), the gland contains reduced numbers of acinar cells with more connective tissue and glandular tissue such as that found in the more lobular portions of the gland. However, as this head abuts the penis, the nature of the glandular tissue within the muscular wall of the penis is different from tissue outside of the muscular wall, consisting of densely staining columnar tissue with larger nuclei and little cytoplasm when compared to the glandular tissue outside of the muscle. These glandular areas are also surrounded by blood-filled sinusoids. This type of tissue extends cranially up the dorsal portion of the penis and can also be seen in low-magnification cross sections from the second, more craniad block of tissue in the same plane as the vas deferens (photograph not shown).

Seasonality of the perineal gland

In order to illustrate the seasonal variation and relative importance of the perineal gland, standard statistics were determined separately for the entire sample and for the non-breeding and breeding seasons (Table 1). The results showed the relative uniformity in both lengths of body measurements and body weights among the three groups, but drastic and significant differences in the weights of testes ($F = 101.34$, $P < 0.001$), seminal vesicles ($F = 45.48$, $P < 0.01$), and perineal glands ($F = 45.65$, $P < 0.01$) between non-breeding and breeding seasons. The striking seasonal change in the weight of the perineal gland illustrates its potential importance. Even with the inclusion of young (short and light) males, the mean weight of the perineal gland in the breeding season (813 ± 65.2 mg SE) comprised about 0.8 percent of the grand mean weight for the 90 males. The perineal gland weighed as much as 1.4 percent of total body weight in the largest males.

To further examine the seasonal variability of the perineal gland, a stepwise regression analysis was run using perineal gland weight as the dependent variable. Of the six independent variables (weights of body, testes, and seminal vesicles, and lengths of body, hind foot, and ear), only the three weights met the significance level for entry into the model. However, body weight was dropped from the model after it was determined

to be 'not significant' when only the three organ weights were entered into the model. Thus, this analysis confirmed that the perineal gland and the reproductive organs (testes and seminal vesicles) show seasonal changes, whereas body weight and the linear measurements do not. The analysis of variance with stepwise regression, having an r^2 = 0.9272 ($P < 0.0001$), indicates the close association of these three organs, the predictive model for which is: Perineal gland mass = -18.670 + 0.443 (testes mass) + 0.398 (seminal vesicles mass).

Relationship of the perineal gland to reproductive organs

Pearson's correlation coefficient was used to assess the seasonal relationships of the perineal gland, testes, and seminal vesicles, including their relationships to other body measurements. Perineal gland weights were compared with body measurements and with weights of the body, testes, and seminal vesicles. All correlations except those with ear and hind foot measurements were highly ($P < 0.001$) correlated. The strongest correlations were between the perineal gland and the testes and seminal vesicles. The testes, producers of androgens, showed a positive and highly significant correlation with perineal gland weight ($r = 0.933$, $P < 0.001$). The seminal vesicles, secondary sex organs responsive to androgens produced by the testes and producers of seminal fluid, also showed a similar significant correlation to the perineal gland ($r = 0.930$, $P < 0.001$).

In order to more closely examine the changes in the perineal gland during the breeding season, perineal gland weights were compared to reproductive organ weights for monthly samples. Not only did the mean monthly weights of the perineal gland change dramatically throughout the year (Fig. 5), but the weights of the testes and seminal vesicles went through similar cyclical changes. Substantial growth in all three organs began in February. However, testes weight increased earlier and more rapidly than the related organs, increasing 13-fold from January to February. From February to March, testes weight increased only 1.8 times, whereas perineal gland and seminal vesicles increased 5- and 7-fold, respectively. Later, the changes in all three organs were more synchronous.

Weights of the perineal gland, testes and seminal vesicles all decreased in mean values during July (Fig. 5), probably due to the recruitment of spring-born males into the population. In August, the mean organ weights rebounded nearly to their previous high levels (with mean body weight also increasing from 87.5 g to 108 g), but then a rapid reduction in the sizes of all three organs was seen in October. Mean testes weight decreased sharply in October, and regression continued so that from November to January, the paired testes weights of all males ranged from 30-50 mg, and the related organs were tiny, if detectable. All three organs remained low in weight until the following February, when the cycle began anew.

Preliminary field studies

We made two attempts, only partly successful, to learn the information content of the product of the perineal gland by placing derivatives of the gland into the natural environment and evaluating the responses of wild cotton rats.

The first study, using a homogenate of perineal gland obtained from several adult males placed on filter paper pieces and randomly introduced as a treatment in half of the traps, resulted in a significant difference in the responses to treatment versus control traps: 26 males were captured in traps with the perineal gland homogenate but only 4 males in the control traps ($X^2 = 16.14$, $df = 1$, $P < 0.0001$). But no significant differences were seen in females (homogenate: $n = 11$ and control: $n = 9$).

The intriguing results of this first field test prompted a second field study the next autumn, when an attempt was made to learn more details of the chemical nature of the active component(s) in the secretion. Perineal gland homogenates and both fractions from a chloroform:methanol extraction of perineal gland homogenate were used. A homogenate from hind leg muscle of adult males and the extracted fractions from the muscle homogenate were used as controls. These six treatments (perineal gland homogenate with its chloroform and methanol fractions, muscle homogenate with its similar chloroform and methanol fractions, and controls) were placed in traps in the field as before. Despite 196 captures of cotton rats over 10 days of trapping, no homogenate or extract was better than any other at attracting or repelling either sex. Thus, the results of the second field study were inconclusive, and failed to give further clues as to the information content of the glandular product.

DISCUSSION

In a review of 20th century investigations on the role of chemical communication in rodents, Johnson (2003) reports that studies, mostly conducted on lab mice, indicate secretions usually are a mix of 50 or more different chemical compounds and that scent overmarking behavior reveals that many rodents can evaluate and respond to changes in their olfactory environment. In their study of scent communication in hispid cotton rats in Texas, Gregory and Cameron (1989) found that dominant males marked more often with urine than subordinates or females, but both sexes seemed to mark their environments with feces.

In order to determine the anatomy, method of delivery of secretory products, cyclical nature, and probable function of the perineal gland in *Sigmodon hispidus*, we examined several aspects of this previously undescribed organ. The subcutaneous location and close association of the perineal gland to the rectum and penis (Figs 1 and 2) indicated three possible routes of delivery for any glandular products: through the skin, in feces, or via the urethra, all used by rodents. Although many species of arvicoline rodents possess enlarged sebaceous glands whose products are extruded onto specialized hairs or skin pads, as in the caudal gland of *Dicrostonyx groenlandicus* (Quay, 1968), the large size of the gland in *Sigmodon*, a sigmodontine rodent, the presence of only loose fascial attachments to the skin, and the lack of skin or hair specializations near the gland suggested no delivery through the skin. In addition, the flimsy fascial attachments to the

rectum made a fecal delivery (as occurs in *Microtus agrestis*— Khan, 1984, or in *Thrichomys aperoides*—Talamoni et al., 2014) doubtful. The third possible route, urethral delivery through the urinary tract, as seen in the beaver (Svendsen, 1978) or in three *Rattus* species in Australia (Mallick, 1992), seems the most plausible delivery route of glandular products. In fact, dissection revealed strong ligamentous attachments of the gland to the penis, further supporting the hypothesis of a close association of the perineal gland to the reproductive and lower urinary tract. However, no duct connecting the gland to the urethra could be found during the gross dissection of several males.

During necropsy, a distinctive pungent odor was associated with the developed perineal gland of breeding males. A similar odor often emanated from live traps or was detected when handling reproductive males in the field, to the extent that the sex of the animal could accurately be predicted before examining the genitalia.

A histological study of maturing males, i.e., those with partially enlarged perineal glands, supported the notion of a urinary delivery route. Several difficulties arose when preparing tissues for histology, relating to the oily or waxy texture of the gland, the massive size of a fully enlarged gland, and the large blocks of pelvic regions that would be needed to confirm attachment or association of other organs. However, one interpretable series of cross sections of the perineal region was obtained from the area near the attachment of the perineal gland to the penis. Although no connections or attachments between the perineal gland and the rectum or skin were seen, an attachment to the penis was evident. A neck-like projection at the end of a bulb-shaped section of the gland extended towards the penis. The medial end formed a glandular mass that abutted the muscular band of the penis, and glandular tissue extended into the penis toward the urethra.

The entire gland is surrounded by an investment of smooth muscle (see Figs 3 and 4) and the septated multilobular acinar bundles within the bulb of the gland contain small tubules which coalesce into a large tubule or duct through the neck-like portion of the gland. Together with evidence of a tubule within the muscular band of the penis near the urethra, these findings suggest an active method of delivery (controlled by smooth muscle contractions) that probably injects the product of the gland through a duct leading into the urethra and the urine. Further histology is needed to confirm the existence of this ductal opening into the urethra and to determine the nature of the histological changes that occur at different phases of the male reproductive season. For the present, a urethral entry of glandular products and placement via the urine seems most likely.

Seasonality of the perineal gland

The cyclicity of the perineal gland corresponds closely with the seasonal weight changes of the reproductive organs (Figure 5). As with the responses of testes and seminal vesicles to the approaching breeding season, the perineal gland enlarges from a tiny organ that cannot be dissected away from the surrounding tissues to a large oily gland whose mass comprises up to 1.4% of the total body weight in some males. Together with the testes (up to 1.8%) and seminal vesicles (up to 1.6%), these organs can

comprise up to 4.8% of the total body weight of large males and thus their enlargement requires substantial energy costs, for growth before and for maintenance during the breeding season. In contrast, during the non-breeding seasons these three organs might sum to 75 mg at the most, which is less than 0.01% of body weight for a 100-g male. A 90% reduction in energy costs for organ maintenance is likely to be associated with the regression of these three organs. Because seasonal regression of the sex organs serves as an energy-saving adaptation in small mammals to enhance winter survivability (e.g., Blank, 1992), the regression of the perineal gland would further increase these energy savings. However, this additional energy reduction can be adaptive only if the necessary products or functions of the perineal gland are no longer needed during the non-breeding months of winter. Thus, the regression of this gland in late autumn further indicates that the perineal gland and its secretions serve reproduction in some capacity.

The synchronous regression and recrudescence of perineal gland and seminal vesicles suggests that both are under androgen control. Because androgens are required for growth and maintenance of accessory sex organs, for external secondary sexual characteristics, and for some pheromone-producing glands (Bronson, 1989), we would expect (and saw—Fig. 5) the growth of the testes to precede the enlargement of the seminal vesicles and perineal gland. The mean weight of testes showed a dramatic increase in February, whereas the increases in mean weights of the perineal gland or seminal vesicles, small in February, were not substantial until March (Fig. 5). The converse was true at the end of the breeding season in October, when the weights of seminal vesicles and perineal gland dropped dramatically while the testes weights declined more gradually. A similar pattern of growth and regression in the preputial gland of muskrats was shown by Beer and Meyer (1951) to be under androgen control. Seminal vesicles have been shown to be under androgen control in other rodents (e.g., Tamarkin et al., 1976), so their enlargement is expected after testicular recrudescence, with its related increase in androgen production. Likewise, the regression of seminal vesicles occurs as androgen production drops in autumn (before the reduction in testes weight). Because changes in weights are synchronous with those of the seminal vesicles, we believe that the perineal gland is under the same androgen control as the seminal vesicles. Further support for this hypothesis is seen in the androgen control of specialized sebaceous glands. In several families of mammals, glandular reduction by castration and either growth or maintenance of the gland after castration by androgen therapy have been demonstrated in the anal and chin glands of rabbits (Mykytowycz, 1965), in the proctodeal gland of the short-tailed vole (Khan, 1984), in the supracaudal gland of the guinea pig (Martan, 1962), and in the ventral gland of the Mongolian gerbil (Thiessen et al., 1968). The perineal gland in *S. hispidus* probably is another example.

The only deviation from the spring increase and fall decrease in organ weights occurred as a dip in the mean weights of all three organs in July (Fig. 5). In his studies of the kangaroo rat, *Dipodomys merriami,* a species with sexual dimorphism in a dorsal skin gland, Quay (1953) observed a similar pattern when the mean area of the gland showed a drop in May but recovery in June. The decreases in mean organ weights during July in *S. hispidus* and in May in *D. merriami* corresponded to the times when spring-born animals of both species are first entering the reproductive populations. This introduction of

young, small males undergoing their sexual maturation would tend to decrease the mean weights for the month, thereby explaining the July dip in *S. hispidus*. In brief, the July decreases in mean organ weights are not due to real reductions in organ weights of individuals but are explained by the changing composition of the population as young-of-the-year males entered the breeding population.

Features of the anatomy, preliminary histological studies and similarities in patterns of growth and regression strengthen the evidence of a link between the perineal gland and reproductive functions in male cotton rats. Statistical analyses confirmed these relationships. All three organs (testes, seminal vesicles, perineal gland) showed significant differences of the mean organ weights of males between breeding and non-breeding seasons. In addition, high correlations of the perineal gland to those of the testes and seminal vesicles (both $P < 0.001$) indicated a high probability for the gland to be associated with the reproductive system. Finally, the linkage of the pattern of recrudescence and regression of the perineal gland to that of the reproductive organs (Fig. 5) was further illustrated by the significant results from the ANOVA with stepwise regression.

The field study using the exudate of whole perineal glands produced significant exploratory behavior in males but not in females, perhaps suggesting that males were guarding females or seeking to find and expel other males from their territories. When the exudate was divided into polar and non-polar portions and these odors were placed in traps, no responses were seen in either sex in the second field study. In brief, more lab and field studies are needed to determine the nature and function of the chemicals produced by the perineal gland, and their role in normal reproduction.

In conclusion, the perineal gland showed seasonal cycling and a strong relationship to the reproductive system in the male hispid cotton rat, *Sigmodon hispidus*. The gland, probably under the same androgen control as the seminal vesicles, enlarges from an indiscernible organ to one weighing up to 1.4% of total body weight in large breeding males. The energy expenditure for growth and maintenance of the perineal gland at a time when reproductive energy requirements are great suggests the importance of the gland and the necessity for its products as part of successful reproduction. Our studies suggest that the glandular product is deposited into the environment in the male's urine. Perhaps this product signals the presence of a reproductive male and serves as a territorial marker, but its message is still unclear.

ACKNOWLEDGMENTS

This study was conducted under the guidelines of the American Society of Mammalogists for use of mammals for research (latest: Sikes et al., 2016) and before the Old Dominion University Animal Care and Use Committee evaluated studies using wild mammals for research. We thank Drs. P. Williams and K. Carson for their advice and encouragement, J. Merritt, P. Loose, C. Pague, A. Yoder, and M. Adams for assistance with different lab and field aspects of our studies, A. White and S. Mautner for assistance with the figures, and our department for facilities and equipment.

LITERATURE CITED

Beer, J. R., and R. K. Meyer. 1951. Seasonal changes in the endocrine organs and behavior patterns of the muskrat. Journal of Mammalogy 32:173-191.

Bergstrom, B. J., and R. K. Rose. 2004. Comparative life histories of Georgia and Virginia cotton rats. Journal of Mammalogy 85:1077-1086.

Blank, J. L. 1992. Phenotypic variation in physiological response to seasonal environments. Pp. 186-212 *in* Mammalian Energetics, T. E. Tomasi and T. H. Horton, eds., Comstock Publishing Associates, Ithaca, New York. 276 pp.

Bronson, F. H. 1989. Mammalian reproductive biology. University of Chicago Press, Chicago. 325 pp.

Cameron, G. N., and P. A. McClure. 1988. Geographic variation in life history traits of the hispid cotton rat, *Sigmodon hispidus.* Pp. 33-64 *in* Evolution of life histories in mammals (M. S. Boyce, Ed.). Yale University Press, New Haven, Connecticut.

Glaubert, A. M. 1975. Fixation, dehydration, and embedding of biological specimens. North-Holland Publication Company, New York.

Gregory, M. J., and G. N. Cameron. 1989. Scent communication and its association with dominance behavior in the hispid cotton rat (*Sigmodon hispidus*). Journal of Mammalogy 70:10-17.

Jameson, E. W., Jr. 1950. Determining fecundity in male small mammals. Journal of Mammalogy 31:433-436.

Johnson, C. E. 2003. Chemical communication in rodents: from pheromones to individual recognition. Journal of Mammalogy 84:1131-1162.

Khan, T. Y. 1984. An account of the structure and development of the proctodeal (anal) gland of *Microtus agrestis* with particular reference to the social environment. Unpublished Ph.D. thesis, University of London.

Luma, L. G. (ed.) 1968. Manual of histologic staining methods of the Armed Forces Institute of Pathology, 3rd edition. McGraw-Hill, New York.

Mallick, S. A. 1992. Urine-marking in three species of *Rattus*. Wildlife Research 19:89-93.

Mirand, E. A., and A. R. Shadle. 1953. Gross anatomy of the male reproductive system of the porcupine. Journal of Mammalogy 34:210-219.

Mykytowycz, R. 1965. Further observations on the territorial function and histology of the submandibular cutaneous (chin) glands in the rabbit *Oryctolagus cuniculus* (L.). Animal Behaviour 13:400-412.

Quay, W. B. 1953. Seasonal and sexual differences in the dorsal skin gland of the kangaroo rat (*Dipodomys*). Journal of Mammalogy 34:1-14.

Quay, W. B. 1968. The specialized posterolateral sebaceous glandular regions of microtine rodents. Journal of Mammalogy 49:427-445.

Rose, R. K. 1994. Instructions for building 2 live traps for small mammals. Virginia Journal of Science 45:151-157.

Rose, R. K., and M. H. Mitchell. 1990. Reproduction in the hispid cotton rat, *Sigmodon hispidus* Say and Ord (Rodentia:Muridae), in southeastern Virginia. Brimleyana 16:43-59.

Sikes, R. S., and the Animal Care and Use Committee of the American Society of Mammalogists. 2016. Guidelines of the American Society of Mammalogists for

the use of wild mammals in research and education. Journal of Mammalogy 97:663-688.
Svendsen, G. E. 1978. Castor and anal glands of the beaver (*Castor canadensis*). Journal of Mammalogy 59:618-620.
Talamoni, S. A., M. A. C. Assis, M. M. F. Freitos, H. P. Godinho, and N. Bazzoli. 2014. Seromucous anal gland in a New World hystricomorph rodent *Thrichomys aperoides* (Lund 1839). Acta Zoologica 95:133-136.
Tamarkin, L., J. S. Hutchison, and B. D. Goldman. 1976. Regulation of serum gonadotropins by photoperiod and testicular hormones in the Syrian hamster. Endocrinology 99:1528-1533.
Thiessen, D. D., H. C. Friend, and G. Lindzey. 1968. Androgen control of territorial marking in the Mongolian Gerbil. Science 160:432-434.

Table 1. Means (± *SE*) and weights (mg) of perineal gland, testes, seminal vesicles, and body, and linear measurements (mm) for adult male cotton rats (> 50 g) collected each month throughout the year. The non-breeding season includes the months of November through January (when the perineal gland is too small to detect) and the breeding season extends from February through October. Body length is total length minus tail length.

	Annual $N = 129$		Non-breeding season $N = 39$		Breeding season $N = 90$	
Variables	Mean	Range	Mean	Range	Mean	Range
Perineal gland	568 ± 55.7	1-2342	1.0 ± 0.0	0	813 ± 65.2	1-2342
Testes	776 ± 63.6	20-2311	44.5 ± 2.7	20-104	1093 ± 68.4	38-2311
Seminal vesicles	579 ± 64.6	1-3080	6.8 ± 0.8	1-15	827 ± 80.0	1-3080
Body weight	97 ± 2.3	51-168	88.3 ± 3.2	52-121	101 ± 2.8	51-168
Body length	145 ± 1.3	116-185	137.3 ± 1.8	114-160	148 ± 1.7	116-185
Hind foot length	30.2 ± 0.1	26-35	29.9 ± 0.3	26-35	30.1 ± 0.1	26-35
Ear length	17.8 ± 0.1	14-21	17.9 ± 0.1	15-19	17.7 ± 0.1	14-21

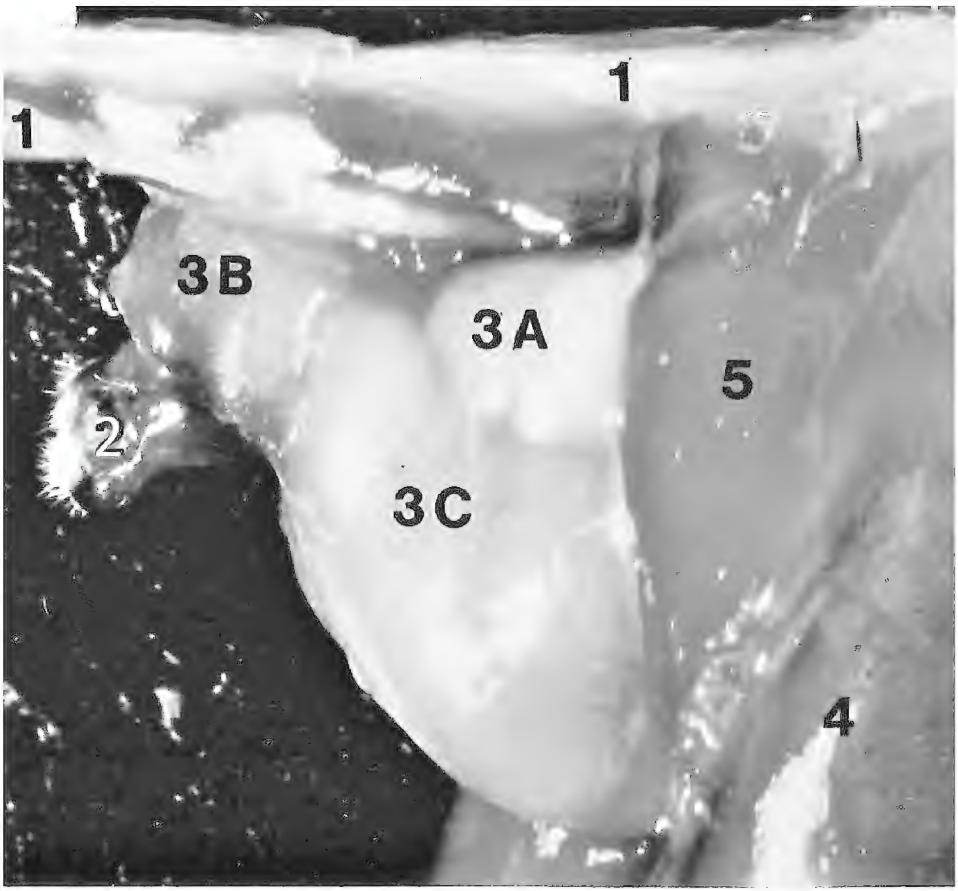

Figure 1. The location of a fully developed perineal gland in the male hispid cotton rat, *Sigmodon hispidus*. The testes have been removed to enable the parts lying dorsal to the testes to be identified: tail (1), anus at end of rectum (2), the three right lobes of the perineal gland (3A, 3B, 3C), and skeletal muscles of the thigh (4, 5).

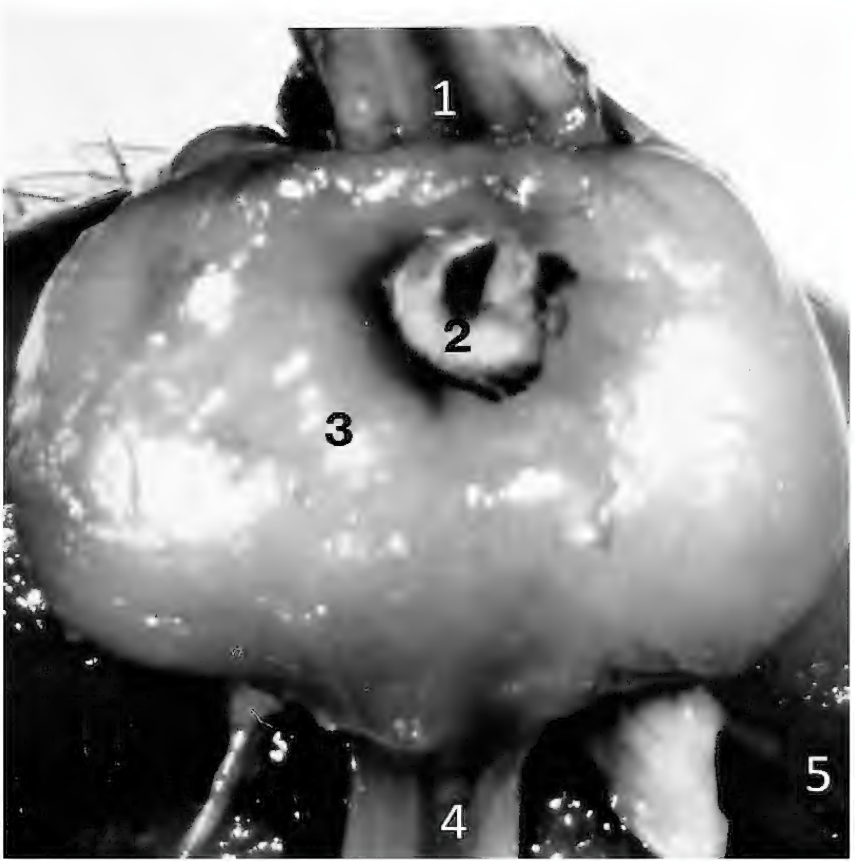

Figure 2. A posterior view of the perineal gland showing the tail (1), cross section of rectum (2), perineal gland (3), penile shaft (4) and muscle of the thigh (5).

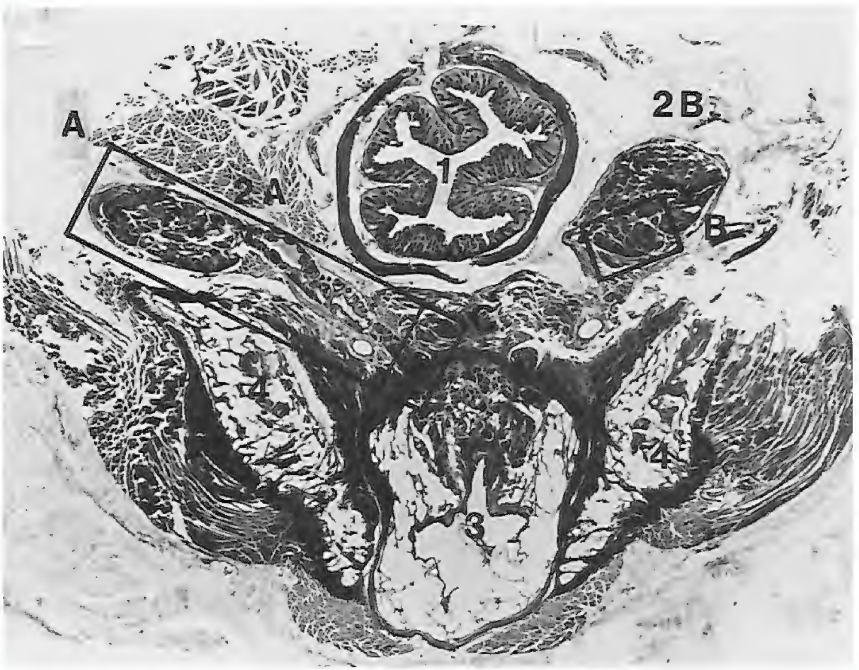

Figure 3. Histological cross-section of the pelvic region of a mature male cotton rat showing the rectum (1), regions of the perineal gland (2), urethra (3), other regions of the perineal gland (4).

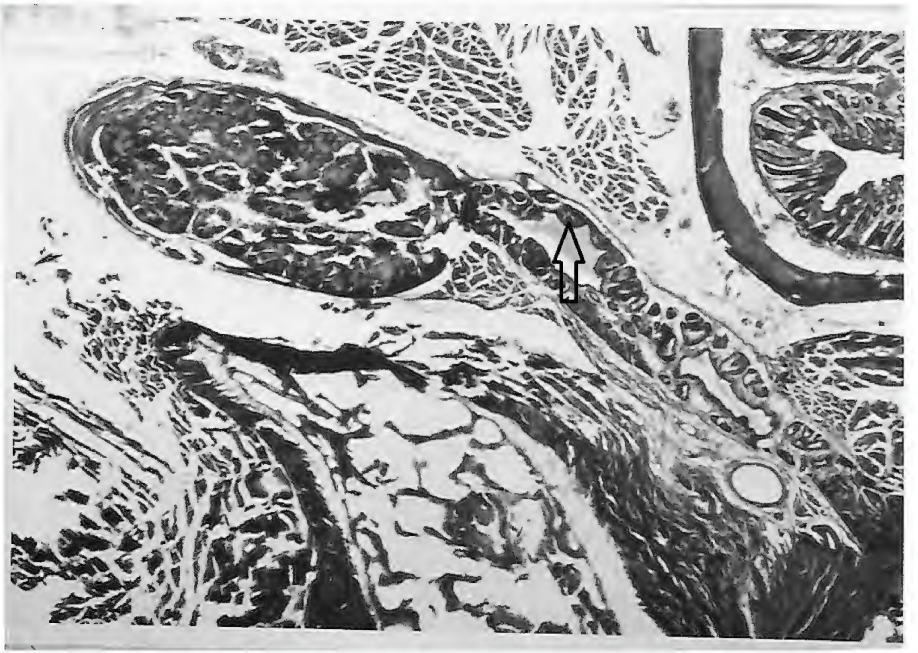

Figure 4. Higher magnification of the rectangular "A" region of Figure 3, showing the acinar cells in the bulbous secretory area of a lobe of the perineal gland, and the neck-like middle section (with arrow pointing to an acinar cell) ending in a tube extending towards the penis.

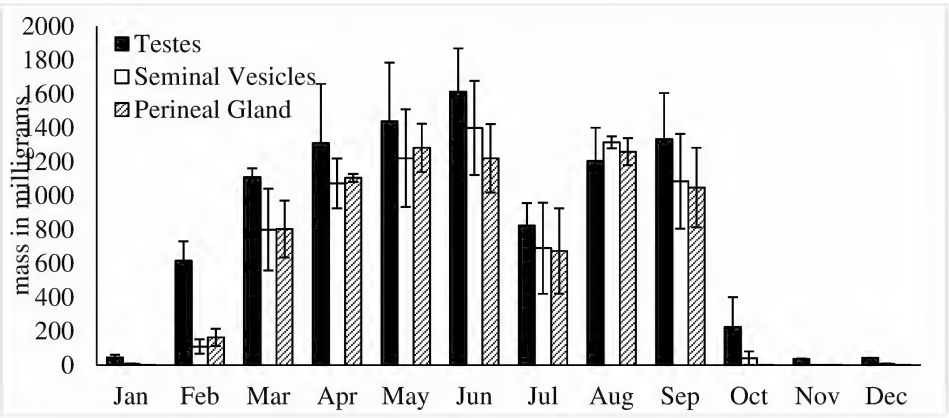

Figure 5. Comparison of mean monthly weights ± *SE* of paired testes, seminal vesicles, and perineal gland. $n = 129$. Notice that testes mass almost always is greater than the others, except for August, which signals rapid changes to come in autumn.

Virginia Journal of Science
Volume 69, Issue 1 & 2
Spring & Summer 2018
doi: 10.25778/tetn-ty74

PROCEEDINGS OF THE 96TH ANNUAL MEETING

Virginia Academy of Science
Longwood University, Farmville, Virginia
May 23-25, 2018

Contents

Agriculture, Forestry, and Aquaculture

GROWTH RESPONSE OF ALFALFA (*MEDICAGO SATIVA*) TO AZOMITE ON DIFFERENT SOIL-TYPES. Ariel M. Coleman & Vitalis W. Temu. Virginia State University (VSU). The growth response of Alfalfa (*Medicago sativa*) to AZOMITE, a naturally occurring hydrated sodium calcium aluminosilicate containing other minerals and trace elements, was assessed in a greenhouse trial at VSU. Alfalfa seedlings were transplanted onto un-amended Borne, Bojac, Emporia, and Cullen soils in 7*45 cm tubes and watered as needed. At full bloom stage, plants were clipped and fertilized with 0, 0.5, 1, or 1.5 g AZOMITE/700g soil in four tubes/soil-type. At flowering, regrowth heights, stem thickness, forage biomass, and specific leaf dry weights were recorded. Data were analyzed as a randomized complete block design for effects of soil-type and treatment.

AZOMITE application improved the measured responses on all soil-types except Emporia that was too acidic for growing alfalfa. Yields ranged from 0.7 g to 2.4 g for Bojac and Cullen at 0 and 1 g AZOMITE/tube, respectively, with plant heights and specific leaf weights in similar patterns. The yield response was greater on Cullen > Bojac > Bourne receiving ≥1 g/tube but marginal increase for the 1.5 g application rate was not significant. The 1.5 g AZOMITE rate increased soil pH from 4 to ≥ 5 for Bojac and Cullen but not Bourne or Emporia. Results indicate that AZOMITE application can improve alfalfa yields on nonacidic soils and that its prolonged use on slightly acidic soils may minimize the costs for subsequent liming. Data on forage quality response to AZOMITE is needed. Author contact: Vitalis W. Temu, vtemu@vsu.edu

CAGE AQUACULTURE IN VIRGINIA. M. David Crosby, Cooperative Extension, Virginia State University. In Virginia, it is estimated that there are over 80,000 farm ponds. In 1985, it was thought that this aquatic resource could be used to develop the aquaculture industry in Virginia. The Aquaculture Program at Virginia State University has provided workshops, technical assistance to potential aquaculture producers, fish farmers associations and aquaculture coops like Virginia Aquafarmers Network (VAN) since the start of the program in 1985. Potential fish farmers are taught how to construct a simple 4x4 ft. round fish cage that could grow 250-350 fish in their farm ponds. For first-time cage aquaculture producers, rainbow trout (*Oncorhynchus mykiss*) are recommended. Catfish (*Ictalurus punctatus*) and hybrid striped bass (*M. chrysops* × *M. saxatilis*) are also used for cage aquaculture. It is recommended that the pond have electrical access to operate an aerator for cage production. However, this is not needed for one-acre ponds doing cage aquaculture at low production levels. Since 2015, farm pond owners are being introduced to the use of airlift pump system for cage production. The use of an airlift pump for trout production has shown that it improves production by increasing the water exchange into the cage. Virginia fish farmers are starting to adopt airlift pump system for cage production. Marketing and fingerling and feed cost are still significant issues for many cage producers. Author contact: dcrosby@vsu.edu

PROSPECTS FOR COUNTERSEASONAL HYDROPONIC ROMAINE (*LACTUCA SATIVA* VAR. *LONGIFOLIA* L.) AND BOSTON (*LACTUCA SATIVA* VAR. *CAPITATA* L.) LETTUCE PRODUCTION IN VIRGINIA. Tim C. Durham, Ag Program, Ferrum College. Hydroponic lettuce represents an attractive emerging market in Virginia. Romaine cultivar 'Ideal Cos' (weekly) and Boston cultivars 'Harmony' (week one) and 'Ermosa' (thereafter) were grown using the Nutrient Film Technique from January through April 2018. Eight, one-week staggered growing cycles were initiated at a temperature of 68 °F, pH 6.4, 200 ppm nitrogen, and an EC of 2.3 mmhos cm^{-1}. Weekly plantings were duplicated, divided into 24 h supplemental-plus-ambient and ambient-alone light regimes, and harvested 56-61 days from seeding in rockwool. Continuous light induced morphological and tactile artifacts (compactness, blistering, and brittleness) and increased incidence and severity of tipburn. However, this treatment also exhibited greater resiliency during an unplanned power outage. Overall, supplemental light induced a statistically significant increase in biomass for both varieties ($P<0.0001$, Fisher's LSD). This corresponded to a 35.8% (R) and 42.9% (B) increase, respectively. Initially, marketability (>150 g) was enhanced by supplemental light until

reaching near parity with natural light with the onset of longer days in April. For romaine, biomass per unit area (kg m^{-2}) ranged weekly from 43.7% to 109.7% of that previously reported in field studies. Despite this variability, the price premium, particularly during counterseasonal windows, suggests that hydroponic lettuce is a viable option. However, further optimization, including an assessment of diminishing return thresholds (nutrition and photoperiod-by-cultivar interactions) is warranted. (Supported by VA Tobacco Region Commission grant). Author contact: tdurham@ferrum.edu

TRANSMUTING CASSAVA FROM STAPLE FOOD TO INDUSTRIAL CROP: THE BANGLADESH CASE. Francoise Djibodé-Favi[1], Mark Klingman[1], Ronald Bowen[1], Md. Shamsul Kabir[2] & Md Eleash Mridha[3], [1]Agriculture Research Station, Virginia State University, [2]Asia Farmer-to-Farmer Regional Director, Wrinrock International Bangladesh, [3]Director PRAN Agro Business Limited (PABL), PRAN-RFL Center Bangladesh. Cassava (*Manihot esculenta* Crantz) is not a staple in Bangladesh and PABL/PRAN (PRAN Agro Business Limited), a food processor and Agribusiness Company has decided to grow cassava and transform the tuber part into gluten-free starch needed for its baking and the clothing industries. I trained youth involved in this project. PABL provide input and buy-back from cassava farmers. Thirty-two PABL staff and producers attended six days of in-class training (Tanghail). PABL staff and executives were also trained at the company's headquarters (Dhaka) for three hours. On-farm visits were made to assess the existing status of cassava production, problems, and to make improvement recommendations. Participants are located in the Districts of Tanghail (54%), Habiganj (33%) and Comilia (7%). No participant (100%) had any prior formal training on cassava production. Producers were recruited during an on-farm visit or by cell phone call. Trainees (100%) believe they improved their knowledge about cassava production two days post-training. They (100%) also believe cassava should be grown on ridges but only 8% want to adopt that practice. The participants (100%) want to obtain improved cassava varieties to increase tuber yield and starch content. Therefore, all of them want a cassava research center in Bangladesh. They all plan to use the training modules and believe in early control of cassava pests. Author contact: ffavi@vsu.edu

AUXILIARY INFORMATION IN SUPPORT OF OPERATIONAL FOREST INVENTORY. Patrick C. Green & Harold E. Burkhart, Dept. of For. Res. Env. Cons., Virginia Tech. Accurate, up-to-date information is critical for informed forest management decisions and financial reporting obligations. Field inventory is a common practice to estimate standing conditions such as tree density, dominant height, and merchantable timber volume. Ground-based forest inventory requires significant time and monetary resources to meet precision requirements; however, budgetary and logistical constraints often limit resource availability forcing less precise estimates. Remotely-sensed auxiliary information derived from unmanned aerial vehicles (UAV) is being investigated to support forest inventory during early stand survival. Promising results were obtained for spruce (*Picea* spp.) seedling detection from red/green/blue (RGB) imagery collected with a fixed-wing UAV. The best results were achieved using the Determinant of the Hessian blob detection method which identified 97 when 96 seedlings were present on a control plot. Our results, along with additional sources of auxiliary information such as Lidar and National Agriculture Imagery Program (NAIP) data, will

be extended to common inventory points in managed loblolly pine *(Pinus taeda* L.) including: one to two years after forest establishment, crown closure (~ age 10), pre- and post-thinning (~ age 15), pre- and post-additional thinning, and near final harvest (~ age 25). Stand level estimates of population parameters will be developed to improve precision of estimates at similar operating costs. (Supported by Forest Modeling Research Cooperative (FMRC) Va. Tech.) Author contact: pcgreen7@vt.edu

CHALLENGES IN RAISING BARBADOS BLACKBELLY SHEEP (*OVIS ARIES*): GENETICS, PATHOLOGIES, AND MARKETING. Roman J. Miller, Knoll Acres, Rockingham County and Dept. of Biol., Eastern Mennonite University. Successfully raising Barbados Blackbelly (BB) sheep in Virginia generates three key challenges: (1) maintaining genetic purity and diversity in a small heritage breed of hair sheep; (2) guarding against prevailing diseases that frequently trouble sheep; and (3) managing production and marketing that enhance sustainability and economic success. Genetic purity and diversity is enriched by maintaining two different unrelated lines of genetic offspring: Winston and Ivan family lines. Maximizing closed flock conditions, upholding a healthy environment, periodic disease testing, and routine vaccinations and deworming exhibit strategies that prevent debilitating diseases. Limiting production to available farm resources promotes sustainability. Maximizing efforts to market lambs, primarily as registered quality breeding stock for regional and international buyers, but secondarily for meat consumption sales in local retail markets, supports economic sustainability. Based on over 25 years of experience in raising sheep and 10 years of experience in raising BB sheep, I have found that the unique traits of this breed (prolific breeders, excellent mothers, easy birthers, versatile eaters, healthy hardiness, mild flavored meat, and easy maintenance) enhance productivity and profitability for the small farm shepherd. Author contact: romanjaymiller@gmail.com

HOW SCIENCE IMPACTS PEOPLE, FARMERS AND FARM POLITICS. Wayne F. Pryor & Norman L. Hyde, Virginia Farm Bureau Federation. Virginia farmers constantly adapt to new technology allowing them to be better stewards of the land. Smartphones, the Internet, no-till planting, precision agriculture and global-positioning technology contribute to their success. Improved seed genetics, dairy cows bred to be more productive and irrigation improvements allow farmers to increase production and provide better stewardship of the land. Drones are just the latest technology being adapted in the field. Farmers and Farm Bureau recognize the need for and embrace technological change. Farmers need support from local Cooperative Extension and Virginia's land-grant universities, Virginia Tech and Virginia State University. And that takes funding from the Virginia General Assembly. Farm Bureau has lobbied for agriculture research and outreach programs since they began more than a century ago. Farm Bureau also is a long-standing supporter of fair taxation for farmland, particularly in fast-developing communities, through the Virginia Land-Use Taxation program. Farm Bureau's latest scientific challenge is negative public opinion. Biotechnology is used to improve seeds and plants. Political opponents and firms who stand to gain from limiting the use of biotechnology have coined the negative phrase GMO's to describe modern agricultural practices. Sympathetic journalists and social media have greatly increased the influence of these opponents. More than 1,500 studies over the past 20 years have shown

no negative health or environmental impacts from GMO crops or food derived from them. Farm Bureau will continue working to engage and talk with consumers to change misconceptions. Author contact: nhyde@vab.com

POTTED SINGLE STEM RASPBERRY PRODUCTION UNDER HIGH TUNNEL CONDITION AT VIRGINIA STATE UNIVERSITY'S RANDOLPH FARM. A.R. Rafie, College of Agriculture, Virginia State University. In 2017, research was conducted to evaluate yield and fruit size for three newly-introduced raspberry varieties, 'Imara', 'Kweli', and 'Kwanza', grown in a high tunnel and using a single stem (cane) production system. Bare-rooted plants were planted individually in seven-gallon capacity pots filled with 50% mushroom compost and 50% hardwood mulch. Plants were irrigated using a micro-sprinkler once daily April-June, twice daily July-October, and once daily in November. Each pot was fertilized in May with 0.2 ounces of slow-release Osmocote and with 0.2 ounces of MicroStart60 3-2-3 NPK fertilizer every two weeks starting in June. A simple trellis system with two levels of wire set at 3' and 4' height was set up using 5' tall T-posts and 12-gauge galvanized wire. Harvest started in July 10 and continued until December 12. Varieties 'Imara', 'Kweli', and 'Kwanza' produced 1,650.9 grams, 1,315.6 grams, and 483.5 grams of fresh marketable raspberry per plant, respectively. 'Imara' had the highest yield. Fruit size (weight of 10 fruits) among varieties during the production season did not differ significantly; however, all three tended to produce larger fruits in late season (November). Author contact: arafie@vsu.edu

ESTIMATION OF CARRYING CAPACITY IN LOBLOLLY PINE (*PINUS TAEDA* L.). Sheng-I Yang & Harold E. Burkhart. Department of Forest Resources and Environmental Conservation, Virginia Polytechnic and State University. For a plant species, carrying capacity is the maximum size of population under limited site resources on a long-term basis. This study was aimed at estimating carrying capacity in loblolly pine plantations. Maximum stand basal area that can be sustained over a long period of time is an informative expression of carrying capacity. To quantify stand basal area carrying capacity, one method is to calculate the estimate from a fitted cumulative basal area-age equation; another method is to obtain the estimate implied by maximum size-density relationships (MSDRs), denoted implied maximum stand basal area. Data for analyses were from a loblolly pine spacing trial, established in the two physiographic regions (Piedmont and Atlantic Coastal Plain), and maintained by the Forest Modeling Research Cooperative at Virginia Tech, which provides a sound empirical basis for evaluating potential carrying capacity. Estimates from four MSDR measures, including Reineke's self-thinning rule, competition-density rule, Nilson's sparsity index and diameter-based relative spacing index, were compared with estimates from the Chapman-Richards equation fitted to the maximum stand basal area observed on plots from the spacing trial. The result indicated that diameter-based relative spacing index greatly mitigated the undesirable property of other three MSDR measures, which overestimated the maximum stand basal area in the young stands. Author Contact: siyang23@vt.edu

Posters

GENETIC DIVERSITY WITHIN AND ACROSS APPLE (*MALUS PUMILA*) VARIETIES. John Christman III & Janet Steven, Christopher Newport University. Commercial apples are produced asexually by grafting which can limit genetic diversity. Despite this, previous research done on apples have found them to be quite diverse, but this is usually done across many varieties. If diversity is not maintained, crops face potential destruction from pressures such as pests, diseases, and climate change. The goal of this study was to develop an understanding of the level of genetic diversity that exists across different apple varieties and within apple varieties. DNA was extracted from leaf tissue samples that were collected from two orchards (5 samples from different trees from 20 different varieties for a total of 100 samples). Next, 7 different microsatellites were used to genotype the samples via PCR. Then variation was quantified across all varieties and within each variety. The genetic data from this research shows that across varieties at most loci, apples are genetically diverse. However, since apples are reproduced asexually, it would be expected that each locus only have 1-2 alleles within a variety. The data does show that there is some diversity within varieties, and that each individual apple variety is not equally diverse. This is most likely due to somatic mutations in branches. This research shows that despite grafting, diversity can be maintained in apple populations through the cultivation of many varieties. Other crops could also benefit from the production of a diverse array of varieties. Author contact: janet.steven@cnu.edu

COMPARATIVE CULTURE AND YIELD OF HYDROPONIC AND FIELD GROWN ROMAINE (*LACTUCA SATIVA* VAR. LONGIFOLIA L.) AND BOSTON (*LACTUCA SATIVA* VAR. CAPITATA L.) LETTUCE. Kateri L. Smith, Sean T. Trollinger & Tim C. Durham, Ag Program, Ferrum College. Lettuce is increasingly viewed as a "superfood" or nutraceutical. As such, hydroponics represents an attractive option to capitalize on robust year-round demand. Data generated from eight Nutrient Film Technique hydroponic growing cycles were compared to previously published field reports. Hydroponic romaine and Boston were almost universally smaller, with a threefold greater planting density. However, our data suggests that hydroponic productivity per unit area (kg biomass m^{-2}) is at least comparable, albeit more spatially intensive. Temporally, days to harvest were comparable at ~56 days. Minimal pest and disease pressure was noted, and no prophylactic or curative sprays were necessary. The closed nature of the system effectively eliminates point and non-point source pollution. These features contrast with environmental externalities often associated with typical field practices. Compared to field-grown lettuce, hydroponics has the potential to occupy 1/3 the footprint and command up to 5x the unit price year-round. The protected environment effectively doubles the length of the growing season. Minimal labor is required, and no operational costs for field preparation are incurred. Though further holistic analysis is warranted (particularly in energetics and the origination of electricity needs from a legacy versus "clean" energy portfolio), the overall sustainability footprint for hydroponics appears to be competitive. As such, it represents a suitable platform for new market entrants, with the capacity to scale as necessary. (Supported by: VA Tobacco Region Commission grant). Author Contact: hsmith2@ferrum.edu

Astronomy, Mathematics and Physics with Materials Sciences

KAN EXTENSIONS IN CLASSICAL ANALYSIS. Marco Aldi, Department of Mathematics and Applied Mathematics, Virginia Commonwealth University. The most common approach to the foundations of classical analysis is based on the epsilon-delta formalism developed in the 19th century by Weierstrass. While the traditional framework is efficient, it is not easily mastered by beginners, partly because the conceptual content of definitions of basic concepts such as limits and integrals is somewhat obscured by the notation. We describe a novel and conceptual approach to the foundations of classical analysis based on the notion of Kan extension from category theory. We show that all basic concepts of calculus can be naturally interpreted in terms of Kan extensions. Additionally, we demonstrate how our framework yields conceptual proofs of some of the key theorems in classical analysis. Author contact: maldi2@vcu.edu.

A PHYSICAL MODEL OF THE TOROIDAL DIPOLE. J. Del Carpio Arispe[1], A. Gutarra-leon[2], B. S. Murphy[3], N. Gaul[4], A. Hanelli[5] and W. Majewski[1], [1]Northern Virginia Community College, [2]George Mason University, [3]Virginia Polytechnic Institute, [4]University of Virginia, [5]California Institute of Technology. We have investigated two laboratory models of the third elementary electromagnetic dipole, known as the toroidal dipole. Its magnetic realization is a circumferentially magnetized ring constructed of neodymium. The electric model of the dipole is a well-known toroidal coil connected to a DC voltage. The electric and magnetic toroids produce only inner magnetic field, inside the torus, and interact only on contact with the electric current density or with a time-dependent electric field. We studied the characteristics of a permanent-magnet toroid and observed the influence of electric and magnetic fields on it. A static toroidal dipole moment of this magnetic toroid was measured in interaction with the external current. In practical applications a magnetic toroid can be used as a magnetic field curl-meter or an ammeter. The role of toroidal dipoles in particle physics and in technology is mentioned. (Supported by NVCC Educational Foundation). Author contact: Walerian Majewski, wmajewski@nvcc.edu

THE DISTANCE TO TWO VARIABLE STARS OF DIFFERENT TYPE BY THE PERIOD-LUMINOSITY METHOD OF MISS HENRIETTA SWAN LEAVITT. Amber Bonevich, Charles Crook, & Tom Mosca III, Rappahannock Community College. In 1912, Henrietta Swan Leavitt established the Period-Luminosity relation for Cepheid-type variable stars. Having exhausted their supply of hydrogen, these pulsating variable stars enlarge and shrink as gravity combats diminishing energy production. In 1924 Edwin Hubble observed a Cepheid star in the Andromeda "nebula," which by its distance established the existence of a galaxy outside the Milky Way, and signaled the birth of modern cosmology. We recalculated the distance to Delta Cephei. Using a 150 mm refracting, robotic telescope in Mayhill, NM, we imaged Del Cep on successive nights, arriving at a period estimate of 5.5 days and average observed luminosity of 3.9. Using distance = 10^((m-M+5)/5) with "m" average observed luminosity, and "M" absolute luminosity calculated from the period-luminosity relationship, we arrived at a distance of 316 parsecs. The commonly accepted distance is 272 parsecs. The difference may be attributable to intervening dust clouds, and the roughness of our period estimate due to

limited observations (the actual period is closer to 5.3 days). Estimating the distance to a second variable star of the RR Lyrae type is an ongoing component of the project. Funding for this project was made possible through a Rappahannock Community College Educational Foundation, Inc. professional development grant. Author contact: Tom Mosca III, tmosca@rappahannock.edu

STUDIES ON THE AGING OF THE Mu2e COSMIC RAY VETO SYSTEM. Peter J. Farris, Robert C. Group & Yuri Oksuzian, Dept. of Physics, University of Virginia. The Muon-to-Electron Conversion experiment (Mu2e) operates at extremely high sensitivities, requiring a means of reducing experimental background. The Cosmic Ray Veto system (CRV) is a particle detector that will surround the Mu2e apparatus to veto penetrating particles that present background. The CRV must have a detection efficiency of 99.99% throughout the expected three-year lifetime of the Mu2e experiment. The CRV is comprised of extruded polystyrene scintillating strips which degrade over time, decreasing the efficiency of the CRV. Using a standard accelerated aging technique, several scintillator samples were heated to increase their rate of degradation. The scintillators exhibited non constant decay rates: during the first two years the average aging rate is 4% per year but over the first ten years the average rate is 2.3% per year. This falls below the current estimate for the CRV aging rate of 3% per year of ten years. Fermilab is operated by Fermi Research Alliance, LLC under Contract No. De-AC02-07CH11359 with the US Department of Energy. Author contact: pjf4qr@virginia.edu

THE ELECTRODYNAMIC WHEEL. N. Gaul[1], B. Murphy[2], J. Del Carpio Arispe[3], A. Gutarra-leon[4], V. Cordrey[5], S. Samiei[1] and W. Majewski[3] , [1]University of Virginia, [2]Virginia Polytechnic Institute, [3]Northern Virginia Community College, [4]George Mason University, [5]College of William and Mary. We constructed three circular neodymium magnet array wheels in both Halbach and non-Halbach configurations with strong alternating-polarity magnetic fields on the outer rims of the wheels. Such systems are referred to as electrodynamic wheels (EDW). A Halbach array is a series of magnets which have their magnetic dipole directions rotated by 90 degrees at each adjacent position. Our non-Halbach array created somewhat weaker alternating fields around the rim with magnetic dipole moments arranged circumferentially with reversing polarity. Our experiments measured the lift and drag forces produced by these spinning wheels on conducting plates which play a role of the tracks, at varying rotation speeds of the wheels. These forces were compared with theoretical predictions for the ratio of lift to drag. We found that the lift to drag ratios for both measured wheels followed the predicted linear relationship as functions of angular velocity of the rotating magnetic field. (Supported by NVCC Educational Foundation, Virginia Academy of Science and the Society of Physics Students). Author contact: Walerian Majewski, wmajewski@nvcc.edu

HIGGS FIELD'S VACUUM EXPECTATION VALUE FROM THE MUON DECAY. A. Gutarra-leon[1], J. Del Carpio Arispe[2], B. Murphy[3], N. Gaul[4] and W. Majewski[2]. [1]George Mason University, [2]Northern Virginia Community College, [3]Virginia Polytechnic Institute, [4]University of Virginia. A cosmic ray (atmospheric) muon decays into an electron and two neutrinos. By detecting the delay time between arrival of the

muon and an appearance of the decay electron in our scintillation detector, we measured the muon's average lifetime at rest in the material of our detector. From the lifetime, using the Standard Model of Fundamental Particles' relations and an experimental value for masses of W boson M_W and of the muon m_μ, we calculated the vacuum expectation value of the Higgs field to be $v = 207\ GeV/\sqrt{\hbar c}$, as well as the universal weak and electric charges. We measured the sea-level fluxes of both low-energy (below 140 MeV) and high-energy muons. We also found the shapes of the energy spectra of low-energy muons and of their decay electrons. We attempted to measure the stopping power of muons in lead shielding. (Supported by NVCC Educational Foundation, the Society of Physics Students and the Chancellor of the Virginia Community College System). Author contact: Walerian Majewski, wmajewski@nvcc.edu

GEOMETRIC PROBABILITY FOR A PAIR OF POINTS LOCATED IN TWO SPHERES. Nicole W. Marzolf & Michelle L. Parry, Dept. of Chem. and Phys., Longwood Univ. Many calculations in physics depend on the separation distance between points such as the gravitational and electrostatic forces between particles. In this presentation, we considered a pair of uniformly distributed spheres separated by some center to center separation distance. An analytic solution for the probability density was determined for the distribution of distances between points chosen from each sphere. The results of this analytic solution were compared to a Monte Carlo simulation in order to check for consistency. We also calculated the electrostatic energy in a pair of uniformly charged spheres using the probability density function and compared this to the well-known result. The results of the analytic solution reduced the complexity of this last calculation from a six-dimensional integral to a one-dimensional integral. (Supported by: Collegiate Undergraduate Research and Inquiry Opportunities (CURIO) Grant, Office of Student Research (OSR), Longwood Univ.) Author contact: Michelle Parry, parryml@longwood.edu

APPLIED ACOUSTICS: A TALE OF SELF-HEALING POLYMERS, WHITE DWARF STARS, BASEBALL BATS AND THE RESONANCES THAT BIND THEM. Kenneth A Pestka II, Dept. of Physics, Longwood University. This work includes a survey of experimental applied physical acoustic methods and techniques used to improve the characterization of physical systems including baseball bats, self-healing thermoplastic polymers, crystallized white dwarf stars and others. This work will focus on methods that take advantage of resonant behavior within these systems and will emphasize the experimental technique of resonant ultrasound spectroscopy and its broad applicability. Author Contact: pestkaka@longwood.edu

DETERMINING THE EFFICIENCIES OF INFRARED PHOTOVOLTAIC DEVICES. Aaron T. Swecker[1], Christopher H. Jackson[1], Oleksandr Kokhan[2], Brian C. Utter[3], & Giovanna Scarel[1], [1]Department of Physics and Astronomy and [2]Department of Chemistry and Biochemistry, James Madison University and [3]Deptartment of Physics and Astronomy, Bucknell University. In our research, we attempt to determine if relationships exist between a laser's wavelength and power and our photovoltaic devices capacitances when the devices are exposed to infrared light. Specifically, using a model based on the law of conservation of energy, in this presentation we discuss our results in

finding a rough estimate for the efficiency of capacitors with respect to increasing capacitance and wavelength. We also briefly talk on how we plan to better determine the efficiencies of our capacitors in the future. (Supported by: Office of Naval Research Awards N000141410328 and N000141512158, JMU Center for Material Science, JMU 4-VA Consortium: 2016-2017, JMU Department of Physics and Astronomy). Author contact: Aaron Swecker, sweckeat@dukes.jmu.edu

ELECTRON-PHONON COUPLING, LEADING TO CHARGE DENSITY WAVES IN 2*H*-TaS_2. Kapila Wijayaratne[1], Junjing Zhao[1], Utpal Chatterjee[1], Christos Malliakas[2], Mercouri Kanatzidis[2] & Duck Young Chung[3], [1]University of Virginia, [2]Northwestern University & [3]Argonne National Lab. Charge density wave (CDW) phase is an exciting phenomenon exhibited by many low dimensional layered materials. However, when it comes to the CDW formation in the class of material called transition metal dichalcogenides (TMD), the underlying microscopic mechanism is in still debated. Peierls like Fermi surface nesting, which is the traditional explanation of CDW has been considered as a candidate mechanism. But Angle-Resolved Photoemission Spectroscopy (ARPES) measurements on 2H-TaS_2 show that the CDW vector is not compatible with expected Fermi surface nesting vectors. Pronounced many-body renormalizations were observed in the electronic dispersion, which are manifested by the presence of multiple slope changes (`kinks'). The temperature independence of the kink energies implies that a strong electron-phonon coupling is present which was further observed to be momentum-dependent. The similar results gained on 2H-$TaSe_2$ and 2H$NbSe_2$ rationalize the possible universality of the momentum-anisotropic strong electron-phonon coupling of incommensurate CDW order in 2H polytype of TMDs. Work at UVa was supported by the National Science Foundation and the Jefferson Trust. Work at ANL was supported by the U.S. Department of Energy. Author Contact : Kapila Wijayaratne, kw4tn@virginia.edu

Posters

INDUCTIONAL MAGNETIC LEVITATION. B. Murphy[1], J.Del Carpio Arispe[2], A. Gutarra-leon[3], N. Gaul[4] and W. Majewski[2], [1]Virginia Polytechnic Institute, [2]Northern Virginia Community College, [3]George Mason University, [4]University of Virginia. We constructed three circular neodymium magnet array wheels in both Halbach and non-Halbach configurations with strong alternating-polarity magnetic fields on the outer rims of the wheels. Such systems are referred to as electrodynamic wheels (EDW). A Halbach array is a series of magnets which have their magnetic dipole directions rotated by 90 degrees at each adjacent position. Our non-Halbach array created somewhat weaker alternating fields around the rim with magnetic dipole moments arranged circumferentially with reversing polarity. Our experiments measured the lift and drag forces produced by these spinning wheels on conducting plates which play a role of the tracks, at varying rotation speeds of the wheels. These forces were compared with theoretical predictions for the ratio of lift to drag. We found that the lift to drag ratios for both measured wheels followed the predicted linear relationship as functions of angular velocity of the rotating magnetic field. We expand here on our construction of a Halbach EDW with tightly-spaced magnets. (Supported by NVCC Educational Foundation,

Virginia Academy of Science and the Society of Physics Students). Author contact: Walerian Majewski, wmajewski@nvcc.edu

MEASURING TOROIDAL DIPOLE MOMENT. A. Gutarra-leon[1], J. Del Carpio Arispe[2], B. Murphy[3], N. Gaul[4] and W. Majewski[2], [1]George Mason University, [2]Northern Virginia Community College, [3]Virginia Polytechnic Institute, [4]University of Virginia. We have investigated two laboratory models of the third elementary electromagnetic dipole, known as the toroidal dipole. Its magnetic realization is a circumferentially magnetized ring constructed of neodymium. The electric model of the dipole is a well-known toroidal coil connected to a DC voltage. The electric and magnetic toroids produce only inner magnetic field, inside the torus, and interact only on contact with the electric current density or with a time-dependent electric field. We studied the characteristics of a permanent-magnet toroid and observed the influence of electric and magnetic fields on it. A static toroidal dipole moment of this magnetic toroid was measured in interaction with the external current. In practical applications a magnetic toroid can be used as a magnetic field curl-meter or an ammeter. The role of toroidal dipoles in particle physics and in technology is mentioned. Experimental details explained. (Supported by NVCC Educational Foundation). Author contact: Walerian Majewski, wmajewski@nvcc.edu

A HOME RUN: THE ACOUSTIC AND PHYSICAL ANALYSIS OF WOODEN BASEBALL BATS. Derek Holmberg & Kenneth A Pestka II, Dept. of Physics, Longwood University. In this work we present the results of multiple physical acoustic experiments used to model and asses the behavior of several wooden baseball bats composed of four different types of wood. We will show through acoustic analysis that dynamically excited bats are affected by their composition and geometry. The macroscopic elastic behavior of four different wood species commonly used in baseball bat construction will also be investigated by testing real baseball bats made from the wood types. In addition, full-scale 3D bat models, which are generated using the finite element modeling software Femap with NX Nastran and incorporate the measured bat properties (such as the elastic constants and Young's Moduli), will be presented. We found the longitudinal Young's Moduli of each of our wood types by using the calculated densities and longitudinal sound speeds through our wood samples. Once the Young's Moduli had been determined, several simple baseball bat models were constructed using the Femap software. The first several fundamental modes of vibration of the bats were found and analyzed. An analysis of the physical bats' properties versus the Femap models will be performed during the summer. Author Contact: derek.holmberg@live.longwood.edu

USING RESONANT ULTRASOUND SPECTROSCOPY TO DETERMINE ELASTIC CONSTANTS OF MULTIPLE SAMPLES OF A SELF-HEALING POLYMER. Jacob W. Hull & Kenneth A. Pestka II, Longwood University. Self-healing polymers such as poly ethylene co-methacrylic acid (EMAA) are thermoplastic polymers that restore their original structure after being damaged. In this work we will present the experimental results of a specific self-healing polymer with 60% of the methacrylic acid groups neutralized by sodium (EMAA-0.6 Na), known as DuPont

Surlyn 8920. In this work we will present the resonant spectrum from multiple samples of EMAA-0.6 Na as well as the methods in which the resonances were found and how the resonant spectrum is used to determine the elastic constants of the samples. Author Contact: Jacob Hull, jacob.hull@live.longwood.edu

SPIDER BALLOONING: SIMULATING TAKE-OFF, FLIGHT, AND SETTLING. Jessica L. Masterson, Jordan M. Hines & Iordanka N. Panayotova, Dept. of Mathematics, Christopher Newport University, Newport News, VA 23606. A fascinating mechanism for aerial dispersal called "ballooning" can be observed in spiders (Araneae). Field and laboratory studies of spider ballooning have many limitations. A three-dimensional numerical model, created by I.N. Panayotova and collaborators, was used to simulate the effect of physical parameters such as the mass of the spider and the length of the dragline, on the speed and distance traveled. This study showed that the spider's speed is directly proportional to the spider's mass, but inversely proportional to the length of the spider's dragline. The settling velocity during free-fall is a non-linear function of the mass, and a quadratic function of the dragline's length. Interestingly, the settling velocity levels up with large masses and with long draglines. In flight, instability of the air kept the spider and drag-line aloft for long periods, making large distances possible. For a wind speed of 0.1 m/sec headed upward at 60 degrees above horizontal, a spider with a mass of 1 mg can launch. Complex transport dynamics was observed when wind was present. When eddies were present some entangling at the end of the dragline was observed, however the entangling did not affect the spider's ability to disperse. (Partially supported by the Research LENS Travel Fund provided by the Office of Undergraduate Research and Creative Activity at Christopher Newport University) Author contact: iordanka.panayotova@cnu.edu

THE PARKER SOCHACKI METHOD OF TAYLOR SERIES GENERATION WITH A-PRIORI ERROR ESTIMATES. Joseph D. Rudmin, James Madison University. The Parker Sochacki Method (PSM) is a simple, fast, powerful, and accurate method of solving systems of ordinary differential equations (ODE's). The system of differential equations is broken down into unary and binary operations, then everything is treated as a Taylor series, and series coefficients are equated. While popular interpolative methods such as Runge-Kutta can miss narrow poles, the a-priori absolute error estimate of PSM locates all poles and provides domains of convergence. PSM can always be cast in polynomial form, which allows separation of variables in almost all physical systems, facilitating exploration of hidden symmetries. PSM is implicitly symplectic. Author contact: rudminjd@jmu.edu

ORBITAL SELECTIVITY AND PARTICLE-HOLE ASYMMETRY OF THE CHARGE DENSITY WAVE ENERGY GAP IN TRANSITION METAL DICHALCOGENIDES. Kapila Wijayaratne[1], Junjing Zhao[1], Jasper van Wezel[2] & Utpal Chatterjee[1], [1]University of Virginia & [2]University of Amsterdam. Angle Resolved Photoemission Spectroscopy (ARPES) study of the incommensurate Charge Density Wave (CDW) material, *2H*-TaS_2, is presented in comparison to a similar layered transition metal dichalcogenide (TMD) *2H*-$NbSe_2$. Similarities were observed in the selective appearance of CDW energy gap about some specific symmetry points in the

momentum space, particle-hole asymmetry of this gap and the persistence of a pseudogap above CDW transition temperature. As per differences, in *2H*-TaS_2, the gap was significant for all momentum locations about a symmetry point, while in the case of *2H*-$NbSe_2$ the gap opened up only in specific momentum locations. Analysis of momentum and temperature dependence of the electronic band dispersion shows many body renormalization due to a phononic origin. As the model of Fermi surface nesting was unable to explain above observations, a tight binding model with emphasis on orbital selectivity and strong electron-phonon coupling was utilized. In the light of similar behaviors exhibited by other related material, we suggest that this model can be generalized for a wide spectrum of CDW materials beyond TMDs. Study was supported by the National Science Foundation, U.S. Department of Energy, Jefferson Trust and Netherlands Organization for Scientific Research. Author Contact : Kapila Wijayaratne, kw4tn@virginia.edu

Biology with Microbiology and Molecular Biology

Not available

Biomedical and General Engineering

MEMORY INFLUENCES INSTABILITIES IN ELECTRICAL RYTHMS IN A FRACTION-ORDER CARDIOMYOCYTE MODEL. Tien Comlekoglu & Seth H. Weinberg, Dept of Biomedical Engineering, VCU. Cardiomyocyte electrical behavior is typically approximated with ideal resistor-capacitor circuit networks. However, non-ideal circuit components may more appropriately model excitable cell properties. These non-ideal circuit components are governed by fractional-order dynamics and contribute capacitive memory effects that result in a history dependence to the transmembrane potential. Prior work finds that in a minimal model driven solely by voltage instabilities, membrane capacitive memory acts to shorten the action potential duration (APD) and suppresses alternans, a beat to beat alternation in the APD. We now investigate the effect of membrane capacitive memory in a model that incorporates both intracellular calcium cycling and transmembrane voltage dynamics. Two parameterizations corresponding to both calcium driven and voltage driven alternans mechanisms were studied. Simulations were performed for fractional orders ranging from 1 to 0.85 with cycle lengths between 200 and 600 ms. APD was shortened at smaller fractional orders, which is consistent with prior work. The peak intracellular calcium concentrations per beat were also decreased at smaller fractional orders. Membrane capacitive memory suppressed alternans in the calcium driven at decreasing fractional orders. However, intermediate fractional orders between 0.9 and 0.95 introduced calcium instabilities in the voltage driven parameterization, which served to promote alternans in the APD. Our results suggest that membrane capacitive memory plays a role in both suppression and formation of alternans in both calcium and voltage driven alternans regimes. Author contact: comlekoglutn@mymail.vcu.edu

DEVELOPING SMART SURFACES ON ORTHOPEDIC IMPLANTS BASED ON BIOMIMETIC DESIGNS. Drew T. Elliott[1], Brandon R. Knouse[2] & Rupak Dua[2], [1]Department of Biology, Hampden-Sydney College, [2]Department of Chemistry,

Hampden-Sydney College. The development of effective arthroplasty implants must consider antibiotic resistance of local bacteria as well as osseointegration. This project addresses these concerns by engineering grade 5 titanium (Ti) surface inspired by nanoarrays found on cicada wings through alkaline hydrothermal treatment (AHT) as a function of time (four and eight hours). Additionally, the surface of AHT treated Ti plates were also functionalized with bone morphogenetic protein-2 (BMP-2) in an effort to increase the rate of osseointegration. Outcomes for anti-bacterial properties were assessed through bacterial cell viability assay kit for three bacterial strains namely *Staphylococcus aureus*, *Pseudomonas aeruginosa* and *Escherichia coli* in static and dynamic environment. SEM analysis showed that Ti plates that underwent 4hr AHT were densely covered with 250nm spikes while 8hr AHT plates were covered with spikes of length 900nm which were more uniformly distributed, thinner, and had a pointed end. 4 hour and 8 hour AHT plates that underwent functionalization, showed that the BMP-2 was incorporated within the nano-spikes. Under static conditions all 4 treatment groups had significantly more non-viable bacteria on their surface ($p<0.05$) when compared with the control group. In summary, we showed that the nano-structures generated on titanium by the hydrothermal treatments showed bactericidal properties for both gram-positive and gram-negative bacteria and also for motile/non-motile bacterial strains. Author contact: : Rupak Dua, rdua001@fiu.edu

POLYMER APPLICATION TO CUT-SLOPES TO MAINTAIN STRUCTURAL STABILITY. Madison, R, Gilmore[1,2]., Brian, Schieber[1]., Katie, Smith[1]., Alex, Hasty[1]., Julia Huchens[1]., Caryn, Martin[2]., Kyle, Gipson[1]., & Yonathan, Admassu[2]., [1]Dept. of Engineering and [2]Dept. of Geology & Environmental Science. Undercutting induced rockfalls (UCIR) cause millions of dollars in property damage and are a safety risk to motorists worldwide, especially from cut-slopes along roadways through mountainous areas. Current prevention methods to reduce the danger of UCIR include shotcreting, fences and rock bolts. The goal of this research is to maintain the structural stability of a cut-slope by minimizing the effects of weathering using a polymer application. This study focuses on the Conemaugh formation in Ohio, which is comprised of weak sedimentary rocks like mudstones, shales and siltstones. Durability properties of rock samples with and without the polymer application were estimated using an absorption test and determining the slake durability index. The results from these tests show that synthetic and natural polymers (like polyurethane and pine tree rosin used in this study) can be used to decrease the effects of weathering on mudstones. Author gilmormr@dukes.jmu.edu.

EFFECTIVENESS OF SUBJECTIVE RATING OF EYE TRACKING TASKS IN DETECTING MILD TRAUMATIC BRAIN INJURY. Mary A. Kannan & Paul A. Wetzel, Dept. of Biomedical Engineering, Virginia Commonwealth University, Richmond VA, 23220. Persistent and chronic post concussive symptoms (PCS) following a mild traumatic brain injury have been well-documented. Standard exams may not show all the deviations from normal and patients are often unaware of changes in cognitive ability. For this study, 71 post-concussive participants and 75 normative population participants were enrolled. The Eyelink 1000 eye tracking system recorded eye movements at 500 Hz. Participants were subjected to various eye movement tasks,

designed to produce responses from the saccadic and smooth pursuit systems, which are controlled by different parts of the brain and utilize different control pathways. The purpose of this study is to assess subjective rating of impairment in eye movements as a measure for PCS, the sensitivity of human raters to impairment due to PCS, and a rating scale of impairment as a tool in the assessment PCS. All subject identifiers were removed and three experienced eye tracking analyzers were asked to subjectively rate each eye tracking file on a scale from 1 (highly impaired) to 5 (not impaired). Significant differences in impairment scores between the control and PCS groups were found ($p \leq 0.001$). High inter-rater reliability was found (Cohen's Kappa > 0.6), indicating that raters were generally observing the same differences in eye movement responses.

HIP CONTACT STRESSES DURING A SIT-TO-STAND TRANSFER. Patrick A. Jones, Nathan J. Veilleux & Jennifer S. Wayne, Department of Biomedical Engineering, Virginia Commonwealth University. During normal daily activity, the femoroacetabular (hip) joint experiences large reaction forces which can lead to changes in the native anatomy over time. Computational modelling of a sit-to-stand loading activity can be used to accurately assess joint contact stresses over the course of the motion and illustrate where anomalies may occur. A computational model of the hip was developed from patient CT scans with anatomically and mechanically accurate cortical and trabecular bone solid bodies. Articular cartilage was generated on these 3D bodies by mapping 2D grayscale images correlating to regional mean thickness values provided by previous experimental studies. A series of finite element studies were conducted to examine the role of subchondral bone thickness in the model. Ranging from 0.1mm to 1mm, cartilage contact stress was not impacted by the thickness of the subchondral bone, permitting simplification of the models for next phase work. Further work will include the application of kinematic constraints for discrete time points of a sit-to-stand transfer to the finite element model to determine the displacement of the femur necessary to correctly position the joint. These displacements will be used in a finite element study to determine the resultant deformations and stresses present in the acetabular and femoral articular cartilage, thereby providing more information about the mechanical impacts of a sit-to-stand transfer on the hip. Author Contact: jonespa6@vcu.edu.

SANDCASTLE WORM INSPIRED BIOADHESIVE FOR MUSCULOSKELETAL TISSUE REPAIR. Philip J. Mollica III[1] & Rupak Dua[2], [1]Department of Biology, Hampden-Sydney College, [2]Department of Chemistry, Hampden-Sydney College. Bone and tissue adhesives are beneficial and are mostly used as supplement to standards methods of musculoskeletal tissue repair which may include sutures, pins, screws etc. However, the adhesive that can do the repair all by itself is still a huge challenge in the medical industry. This research project aims to develop a synthetic glue inspired by Sandcastle worm's glue which is strong, quick setting, and functional in an aqueous environment. Attempts were made to synthesize the analog of Sandcastle's glue negatively charged proteins. This was accomplished by synthesizing the analog of DOPA monomer (dopamine methacrylamide, DMA) using a borate-dopamine complex and reacting it with methacryloyl chloride at pH >9. The resulting product was washed with ethyl acetate, and recrystallized from hexane. Characterization of this compound was done using ^{1}H and C-13 NMR spectroscopy. Spectrum results showed that DOPA analog

was synthesized successfully, however it still has some impurities. Synthesis process of DMA needs to be modify to get the pure monomer analog before it can be used for polymerization with other monomeric analogs to yield negatively charged protein analog. We would like to thank Virginia Academy of Science for funding this project through Undergraduate Research Award. Contact: Rupak Dua, rdua001@fiu.edu

THE LINC COMPLEX CONTRIBUTES TO EPITHELIAL ACINI HOMEOSTASIS Vani Narayanan, & Daniel E. Conway, Department of Biomedical Engineering, Virginia Commonwealth University, Richmond, VA, 23284. Mechanical forces, both at cell-cell junctions and cell-matrix adhesions, have been shown to be important for regulating homeostatic processes of the epithelium, such as proliferation, collective cell migration, and 3D organization. More recently the nuclear LINC (linker of the nucleoskeleton and cytoskeleton) complex has emerged as another critical structure and mechanosensitive region of the cell. We hypothesized that the LINC complex was necessary for epithelial function. With the help of a previously developed Nesprin-2G force biosensor, nuclear forces were estimated to be significantly higher in 3D as compared to 2D monolayers. Interestingly, acini displayed a lower force across Nesprin-2G on day 3 as compared to day 7 of morphogenesis, indicating that pressure increases during acinar formation. To disrupt the LINC complex, we developed an MDCK II cell line expressing a tetracycline inducible dominant negative (DN) KASH, a peptide that disrupts the endogenous nesprin-SUN interactions and blocks nuclear-cytoskeleton interactions. Expression of DN KASH in MDCK 3D acinar cultures resulted in rapid filling of the central lumen with cells, suggesting that the LINC complex is necessary for acinar equilibrium. The lumen occlusion occurs without measurable increases in cellular proliferation, suggesting either a defect in cell division, apoptosis, migration, or cellular polarity. Cells expressing DN KASH exhibited slower migration speeds in response to a scratch wound cell migration assay, consistent with prior reports in fibroblasts. . Taken together our results indicate that the LINC complex is a critical structure in the epithelium.

INTERCELLULAR SODIUM NANODOMAIN SIGNALING REGULATES REPOLARIZATION IN CARDIAC TISSUE. Madison B Nowak,[1] Steven Poelzing[2], & Seth H Weinberg[1], [1]Department of Biomedical Engineering, Virginia Commonwealth University and [2]Virginia Tech Carilion Research Institute, Virginia Polytechnic University. Ventricular fibrillation is a life-threatening condition caused by irregular electrical signals generated in the heart. Action potentials (AP) in the heart are initiated by an influx of sodium (Na^+) ions via voltage-gated Na^+ channels. Mutations in the gene encoding the Na^+ channel protein can result in a gain-of-function, creating a "late" Na^+ current and prolonging AP duration (APD). Imaging studies have shown that Na^+ channels are highly clustered at the cell intercalated disc (ID), facilitating the formation of Na^+ nanodomains in the intercellular space between cells. In this work, we performed new simulations to predict the effects of changing the width of both intercellular cleft and interstitial space on APD in cardiac tissue. In our 1D model, cardiac tissue was represented by a 50-cell strand of electrically coupled cardiomyocytes. Each cell was discretized into 10 axial and 2 ID patches, with Na^+ channel localization at the ID varied from 10 to 90%. Simulations of mutant phenotype cardiac tissue with a wider

intercellular cleft of 50 nm demonstrated consistent early-afterdepolarizations (EADs), driven by enhanced late Na^+ current. Consistent with our prior work, for high Na^+ channel ID localization, we found that APD increases with increasing cleft width. Interestingly, regardless of the Na^+ channel localization, we found that APD only minimally depended on interstitial widths. This supports the prediction that Na^+ in the intercellular cleft is a key regulator of EAD promotion.

COMPUTATIONAL ASSESSMENT OF SURGICAL REPAIRS FOR LISFRANC INJURIES. M. Tyler Perez & Jennifer S. Wayne, Dept. of Biomedical Eng., Virginia Commonwealth University. While Lisfranc injuries in the midfoot are less common than other ankle and midfoot injuries, the outcomes of surgical repairs of these injuries remain poor. Existing literature has compared the different surgical procedures but has not concluded with a recommended procedure. This study uses a computational biomechanical model to evaluate the foot before and after a Lisfranc injury. Using SolidWorks™ a healthy human foot model was created whereby biomechanical function was dictated by accurate 3D articular anatomy, ligament restraints, and muscle loading. The model has proved to match experimental results for separation of the medial cuneiform and second metatarsal in a normal cadaver foot. While the dorsal diastasis for a foot with a Lisfranc injury is within one standard deviation of the experimental data, the plantar diastasis is larger. A possible source of difference is that the cadaver foot had the plantar ligaments cut but the plantar soft tissue was left intact which could resist diastasis. Meanwhile the model had no plantar components to resist diastasis. When muscle forces are added into the model, there was less diastasis for the normal foot but greater diastasis for the Lisfranc injury model. This suggests that cadaver experiments may underestimate the change in diastasis as a result of the injury. The remaining work for this model is to investigate the reasons for differences between the experimental and model results and investigate the impact of 4 surgical procedures. Author contact: perezmt@vcu.edu

INFLUENCE OF HEART RATE VARIABIITY ON CARDIAC ELECTROMECHANICAL DYNAMICS. Vrishti M. Phadumdeo & Seth H. Weinberg, Dep. Of Biomedical Engineering, Virginia Commonwealth Univ. Heart rate continuously varies because of circadian rhythm, stochasticity, and autonomic regulations, which is referred to as heart rate variability (HRV). Clinically, low HRV correlates with a greater risk for cardiac arrhythmias. Alternans, a beat-to-beat alternation in intracellular Ca and action potential duration (APD) is a risk factor for arrhythmias. We study the effects of HRV on electromechanical properties and relationship between APD and Ca. A nonlinear discrete-time model governing APD and intracellular Ca signaling coupled with a stochastic pacing period is used to model a single cardiac myocyte and HRV. Our results show that HRV decreases APD and Ca variability at pacing periods, where alternans is present. Additionally, greater HRV weakens the correlation between APD and peak Ca and disrupts the alternating pattern in both APD and peak Ca. The efficacy of these results is dependent on the sarcoplasmic reticulum Ca uptake rate. These results show that HRV disrupts alternans, suggesting that it is an anti-arrhythmogenic factor. Author contact: Vrishti Phadumdeo, phadumdeovm@vcu.edu

NANOPARTICLES FORMED FROM PORCINE LUNG EXTRACELLULAR MATRIX GUIDE PRO-REGENERATIVE MACROPHAGE PHENOTYPE IN VITRO AND IN VIVO. Alexandria Ritchie, Patrick A. Link, Michael S. Valentine & Rebecca L. Heise, Dept. of BME, VCU. During ventilator induced lung injury, pressure in the lungs causes damage to the alveoli. In response, macrophages are recruited. M1-like macrophages promote inflammation while M2-like macrophages promote tissue regeneration. This study demonstrates the ability of nanoparticles derived from the extracellular matrix of porcine lung (PLECM) to induce a pro-regenerative macrophage phenotype. We used nanoparticles to study the impact on bone marrow-derived monocyte phenotypes of young mice in vitro, and on the lungs, in vivo. Cells were kept naïve, activated to become M1 or M2, or had nanoparticles added. Cells were activated by altering the growth media to include LPS and IFNy for M1 activation or IL-4 and IL-13 for M2. In vivo, mice were injected with nanoparticles and cells from the lungs were isolated. Cells were stained and run through the flow cytometer. Cells that exhibited markers +CDllc (in vitro) or +CD80 (in vivo)/-CD206 were designated as M1. Those that were -CD11c (in vitro) or –CD80 (in vivo) were designated as M2. Data suggests that cells activated with PLECM nanoparticles have a high percentage of -CD11c/+CD206 expression. Thus, nanoparticles from PLECM induce a pro-regenerative macrophage phenotype and may promote regeneration. Author Contact: rlheise@vcu.edu

IMPROVING THE BARRIER FUNCTION OF A RECELLULARIZED LUNG. Keerthana Shankar, Bethany M. Young & Rebecca L. Heise. Department of Biomedical Engineering, VCU. Lung transplantations are the current standard treatment for many lung diseases, but are hindered by a lack of donors. They are also an expensive procedure with a survival rate that rapidly decreases 5 years post transplantation. As an alternative, we explored bioengineering lungs *in vitro* through an acellular tissue scaffold repopulated with new cells. Though other groups have transplanted bioengineered lungs *in vivo*, these lungs fail due to edema. While decellularization of the lung preserves the 3D architecture of the extracellular matrix (ECM), it also decreases the concentration of ECM proteins. This disruption of the ECM causes changes in cell phenotype, affects cell attachment and maturation, and leads to lung failure. To address this, we used a hydrogel coating to replenish lost ECM proteins within the acellular scaffold and a bioreactor to seed mouse lung epithelial cells (MLE12). Immunoblotting confirmed presence of the ECM proteins found in intact lung within the fabricated ECM hydrogel. Preliminary experiments of repopulated rat lung on a shaker showed higher DNA concentration within the ECM hydrogel coated lung when compared to the control. The addition of the hydrogel also resulted in greater E-Cadherin expression and barrier resistance suggesting that the reintroduction of the ECM proteins also improved epithelial barrier function. Using a bioreactor, we were successfully able to repopulate the vasculature and alveoli of a hydrogel coated rat lung with endothelial and epithelial cells, respectively. Though full coverage was not yet achieved, these results suggest that the ECM plays a significant role in the development of a functional lung *in vitro*. Author contact: shankark@vcu.edu

THE IMPACT OF AGING AND MECHANICAL STRETCH ON MONOCYTE RECRUITMENT AND MACROPHAGE POLARIZATION IN EXPEIMRENTAL VENTILATOR-INDUCED LUNG INJURY. Michael S. Valentine, Patrick Link,

Franck Kamga Gninzeko, Joe Herbert, and Rebecca Heise, Dept. of BME, Virginia Commonwealth University. Alveolar overdistension and cyclic atelectasis are injury mechanisms that occur in ventilator-induced lung injury (VILI) and lead to loss of alveolar barrier integrity and pulmonary inflammation. Age is thought to be a predictive factor in the severity of VILI; however, the relationship and mechanisms between age and the severity of VILI are unknown. Individually, mechanical stretch and aging influence monocyte recruitment and macrophage polarization. Bone-marrow derived monocytes (BMDMs) were harvested from mice (C57Bl6/J) from 2 different age groups; 8 weeks (young) and 20 months (old). An in vitro invasion assay was performed with conditioned media (CM) from primary cultured alveolar epithelial type II (ATII) cells cyclically stretched (15% change in surface area) for 24 hours or static controls. In vivo, young and old mice were subjected to pressure-controlled ventilation (PIP: 35-45 cmH20, RR: 90 breaths/min, PEEP:0 cmH20) for 2 hours using a Scireq Flexivent. Flow cytometry was performed and data were assessed on a BD LSRFortessa-X20 flow cytometer using BD FACSDIVA software. Age and mechanical injury impacted monocyte recruitment and synergistically altered macrophage polarization. Better understanding age-dependent factors associated with macrophage plasticity is essential for developing treatments or therapies for related lung injury. (Supported by: NIH 1R01AG041823-01A1). Author contact: msvalentine@vcu.edu

PROXIMAL VERSION ESTIMATION WITHOUT THE DISTAL FEMUR. Nathan J Veilleux & Niraj V Kalore & Jennifer S Wayne, Department of Biomed. Eng., Virginia Commonwealth Univ., Richmond VA. 23220. The success of total hip replacement surgery depends on proper anteversion of the femoral stem. Femoral version is defined as the angle between the femoral neck and condyles in a horizontal plane. An excessively retroverted or anteverted femoral stem will lead to impingement and stem loosening, shortening the life of the hip implant. However, there is no accurate way for surgeons to measure femoral version, since the femoral condyles aren't visible during the surgery, nor are they included in preoperative CT scans. This means that a new technique for estimating version that only uses the proximal femur must be developed. CT scan data for 80 entire femurs and 215 proximal femurs has been provided by the VCU Department of Radiology. Each CT scan has been converted into a 3D model in the program Mimics. These surfaces have been imported into MATLAB, where a program has been developed that is able to detect all named landmarks of the femur. The locations of 13 of these landmarks on the proximal femur have been passed into a statistical shape model. The distances and angles between these points have been fed into a linear model to predict version. The difference between true version and version predicted by this model was $0.00° \pm 5.13°$ with a maximum overestimation and underestimation of 11.80° and 15.35°, respectively. This model and its prediction of femoral version are a substantial improvement over pre-operative 2D or intra-operative visual estimation measures.

Posters

EXPEDITING IMAGE ANALYSIS FOR NOVEL BIOLOGICAL APPLICATIONS WITH AN AUTOMATED MATLAB ALGORITHM. William M. Armstrong[1], Callie J. Miller[1] & Marta K. Bechtel[2], [1]Deptartment of Engineering,

[2]Deptartment of Biology, James Madison University. Image analysis involves decomposing an image into its most basic components in order to extract statistical data. With image analysis, it is possible to quantify how something changes as opposed to just visualizing the change. For example, the quantification of the number of cells in a set of consecutive images can be used to find the rate of cell division over the time course of the experiment. Counting the number of cells in an image by eye, however, is physically intensive and prone to error. To combat this, we have developed a MATLAB algorithm for automated image analysis to allow quantification of biological images with applications including, amount of actin expression, cell enumeration, cell nucleus area, and orientation angle of actin filaments. The program provides an easy to use graphical user interface to allow the end user to operate the program with little to no prior experience in image analysis tools or techniques. Author contact: William Armstrong, armstrwm@dukes.jmu.edu

USING MATLAB TO QUANTIFY EXTRACELLULAR MATRIX FIBER ALIGNMENT BY MIGRATING CELLS. Christine M. Gatto[1], Kristopher E. Kubow[2], and Callie J. Miller[1] [1]Department of Engineering, [2]Department of Biology, James Madison Univ. The extracellular matrix (ECM) is the non-cellular part of tissues and organs that is composed of water, proteins, and polysaccharides. One of the most significant roles of the ECM is to serve as a medium for cell migration. Cells move through the ECM by adhering to the various fibers comprising the ECM. Experimentalists have shown that when the cell adheres to these fibers, the fibers move closer together, becoming more aligned. Understanding how cells align ECM fibers could be used to prevent the spread of diseases because if diseased cells cannot move from their location, then the cells cannot spread the disease or infect other cells. It is not clear how a cell's ability to align fibers will impact its movement through the ECM, however, the hypothesis is that the ability of cells to align fibers in the ECM is related to how fast they are able to move through ECM. Identifying how aligned ECM fibers are currently depends on a "by-eye" analysis which varies from researcher to researcher. The ability to quantify the degree of alignment of ECM fibers would greatly benefit experimental studies perturbing cells moving through the ECM that are studying the alignment of ECM fibers by migrating cells. In order to quantify co-alignment of ECM fibers, we have developed an image analysis algorithm to identify and quantify the start and end locations of fibers in an experimental image. Author contact: gattocm@dukes.jmu.edu

THE EFECT OF COLD WORKING ON THE MECHANICAL PROPERTIES AND MICROSTRUCTURE OF LOW CARBON STEEL. Christine M. Gatto. Rob J. Prins. Heather A. Kirkvold, Dept. of Engineering, James Madison University. The purpose of this research is to understand how cold work affects the mechanical properties and microstructure of a low carbon steel. This research will contribute to the materials group at James Madison University by improving our understanding of the connection between microstructures and material properties. In order to conduct this experiment pieces of low carbon steel are processed using a roll. The roll applies cold work by squeezing the steel, thereby deforming it so that it becomes thinner, longer, and slightly wider. To calculate the exact amount of cold work applied by the roll, two measurements are needed: the original cross-sectional area and the cross-sectional area after

deformation. Once the desired amount of cold work is reached, the pieces are tested in order to determine what effect the cold work has on mechanical properties. The tests that are conducted are hardness and tensile tests. The expected results of this research are that the hardness and the yield strength will both increase as cold work increases. In order to examine the microstructures, the specimens are mounted into pucks, polished, etched, and viewed under a microscope to see how cold work affects the microstructure of the steel. The expectation is that the degree of grain elongation in the microstructure will increase with an increase in cold work. Author Contact: gattocm@dukes.jmu.edu

STRETCH AND STIFFNESS INDUCED-SENESCENCE IN VENTILATOR INDUCED LUNG INJURY. Franck J. Kamga Gninzeko, Michael S. Valentine, Sahil R. Chindal, & Rebecca L. Heise. Dept. of Biomedical Engineering, Virginia Commonwealth Univ. Acute lung injury (ALI) and acute respiratory distress syndrome (ARDS) are among the most severe forms of lung injury. To remedy to ALI and ARDS, patients are often placed on a mechanical ventilator. However, mechanical ventilation itself can lead to ventilator induced lung injury (VILI). The biotrauma, volutrauma and atelectrauma observed in VILI create a stressful environment which may induce cellular senescence contributing to the inflammatory process. *We hypothesize that mechanical stretch and substrate stiffness increase cellular senescence in non-aged cells. We further hypothesize that LPS may synergistically increase this mechanically-induced senescence.* To test this hypothesis, Mouse lung epithelial 12 cells were cyclically stretched at 15%, at 0.86 Hz for 24 hours and on a separate set up MLE12 were seeded on 1 kPa and 24 kPa for 24 hours with and without LPS. Gene expressions were performed at the end of each experiments. Stretch with the addition of LPS significantly increased P21 gene expression compared to other groups; stiffness and LPS also led to increase gene expression in some senescence markers. In conclusion, using a two-hit model of VILI, we were able to show upregulation of senescence associated markers. This suggests that even though stretch and stiffness may induce senescence, the addition of LPS in conjunction with mechanical stretch and stiffness may also lead to cellular senescence. In a nutshell, these results may lead to a better understanding of the role of mechanical stretch and stiffness induced senescence in the context of lung injury. Author contact: Franck Kamga Gninzeko, kamgagninzefj@vcu.edu

THE EXTRACELLULAR MATRIX MEDIATES TIME DEPENDENCY OF EPITHELIAL-MESENCHYMAL TRANSITION. Kristin P. Kim, Lewis S. Scott & Christopher P. Lemmon, Dept. of Biomedical Engineering, Virginia Commonwealth Univ. Epithelial-Mesenchymal Transition (EMT) is a process of phenotypic adaptation of epithelial cells that regulate mobility in developmental, physiological, and pathological processes. Mechanical and chemical signaling of the extracellular matrix provide feedback loops that maintain the migratory states of EMT. In this study, we investigate the role of the extracellular matrix protein fibronectin on the time dependency of EMT. We induce EMT using transforming growth factor beta 1 (TGF- β) and analyze the relative expression of known EMT markers. The inhibition of the extracellular matrix restricts EMT progression, indicated by a decrease in mesenchymal markers. This inhibition can by overwhelmed by high stimulations by TGF- β. These findings suggest that fibronectin has a role in the maintenance of EMT induced by a low, sustained

stimulation of added TGF- β. In future studies, we will investigate the potential of fibronectin inhibition to reverse EMT in both low and high concentration TGF- β conditions. This targeting of the extracellular matrix may have the potential for treatment of EMT in disease states such as cancer and fibrosis. Author contact: kimkp@vcu.edu

WESTERN BLOTTING OF UNFOLDED PROTEIN RESPONSE COMPONENTS IN AN INDUCIBLE CELL LINE MODEL OF SEVERE CONGENITAL NEUTROPENIA. Kari J. Knepp[1], Bhavuk Garg[1], Hrishikesh M. Mehta[1] & Seth J. Corey[1,2], [1]Division of Pediatric Hematology, Oncology, and Stem Cell Transplantation, Department of Internal Medicine, VCU School of Medicine, Children's Hospital of Richmond at VCU; [2]VCU Massey Cancer Center. Severe Congenital Neutropenia (SCN) is a bone marrow failure syndrome characterized by extremely low number of neutrophils. SCN patients, due to a lack of neutrophils are unable to mount an effective innate immune response. Previous studies have shown SCN to be associated with *ELANE* mutations. *ELANE* encodes neutrophil elastase (NE). Granulocyte Colony Stimulating Factor (GCSF) treatment rescues the low levels of neutrophils; however, prolonged treatment with GCSF leads to Acute Myeloid leukemia (AML). Using an inducible-ELANE expression system consisting of wild type (wt), point mutation (G185R) and deletion mutation (d10aa) isoforms, in a murine myeloblast cell line 32D and GCSF treatment we investigated the effect of *ELANE* mutations and GCSF in granulopoiesis and survival. We evaluated stress and apoptosis related molecules using immunoblotting and observed an induction of stress related protein CHOP with *ELANE* expression which is counteracted by GCSF treatment. Similar results are observed with the expression of phospho-eIF2α. Also, we observed induction of Mcl-1 and BIM isoforms upon GCSF administration. These could be products of cleavage or alternative splicing which are known to be pro-apoptotic. Together these results indicate a stress-related response upon mutant *ELANE* expression which is resolved by GCSF treatment. R25GM102795. kjh2976@email.vccs.edu

POROUS HYDROGEL AND OTC MUSCLE SUPPLIMENT FOR MUSCLE RENERGATION Tyler A. McGaughey, Kristin M. Fischer, & Michael J. Wolyniak. Department of Biology Hampden Sydney College. Patients that have lost major sections of tissue from events like major trauma, may require clinical intervention, but this still results in decreased muscle functionality. Tissue engineering (TE) is an attractive option because a new section of tissue can be grown *in vitro,* but most tissues fail to reach maturity in a timely fashion. If the myoblasts are introduced into a cross-linked hydrogel scaffold with a 10% static tension and Muscle Milk® (MM) added, then myoblast maturation rates will improve. A 10% (w/v) gelatin solution cross-linked with 1% (w/v) microbial transglutaminase (mTG) maintained its 3D shape for two weeks. Fluorescent murine myoblasts (C2C12) were embedded in the gelatin hydrogels and a 10% static tension over 7 days caused a significant number of myoblasts to produce projections, indicating the beginning of maturation. A cell study was carried out to investigate the effects of a quarter (0.35% (w/v)) and an eighth (0.18% (w/v)) of the recommended daily value of MM on C2C12 myoblast maturation. However on days 7 and 14, the supplement inhibited cellular growth. A cross-linked 3D, hydrogel scaffold was successfully developed that promoted myoblast maturation through a 10% static tension while the

MM had a negative impact on cell growth. Future work will enzymatically degrade the MM prior to cell culture. (Supported by the VAS Small Project Research Grant) Author contact: Kristin Fischer, kfischer@hsc.edu

INTERCELLULAR SODIUM NANODOMAIN SIGNALING REGULATES REPOLARIZATION IN CARDIAC TISSUE. Mario J. Mendez, Christopher A. Lemmon, & Seth H Weinberg, Department of Biomedical Engineering, Virginia Commonwealth University. Epithelial to mesenchymal transition (EMT) is a fundamental biological process that plays a central role in embryonic development, tissue regeneration, and pathological conditions, such as cancer metastasis. EMT is the transdifferentiation of an epithelial cell to a mesenchymal stem cell; losing the characteristic cell-cell adhesion of an epithelial cell and gaining the increased cell motility of a mesenchymal cell. Recent work has demonstrated the existence of bistability in the EMT system, with an intermediate or partial (pEMT) state that retains some characteristics of the primary epithelial state but also shows features of mesenchymal state. Prior work has demonstrated that transforming growth factor-beta (TGF-beta) is a major and potent inducer of this cellular transition. In our study, we used a mathematical model of the core regulatory network describing TGF-beta-induced EMT, which consists of coupled reversible and irreversible bistable switches. We performed simulations to determine critical parameters that govern two key features of the EMT process: (1) hysteresis in the TGF-beta-dependence of the transition from epithelial to the pEMT states and (2) the reversibility of the pEMT to mesenchymal state transition. We found that the presence of hysteresis depended on critical properties of the microRNA-34 signaling pathway. In contrast, we found that mesenchymal reversibility depended on properties of the endogenous TGF-beta production. Model predictions demonstrate that both the reversibility and sensitivity of TGF-beta-mediated EMT is governed by complex interactions between these coupled switches. Author contact: mendezmj@mymail.vcu.edu

Botany

AGRICULTURE AS SCIENCE: HOW VIRGINIA CROPS CAN BE USED TO INVESTIGATE FUNDAMENTAL QUESTIONS OF PLANT BIOLOGY. Anne B. Alerding, Dept. of Biol., Virginia Military Institute. Soybean is the top agricultural field crop in Virginia and brings over $200,000,000 into the state's economy annually. Soybean yield in Virginia reaches only 25% of its maximum, and production research has traditionally focused on yield gains associated with crop responses to herbivory, disease, and weather. My research program is returning soybean research to its botanical roots by addressing fundamental resource allocation decisions occurring within the plant during seed filling. Soybean fruits are produced in racemes, which are situated at nodes along the main stem and branches. Branch initiation occurs later in vegetative development, setting the stage for resource competition between juvenile branching stems and producing fruits within the shoot. We are exploring temporal and spatial patterns of secondary vascular tissues and lateral growth of stems in relation to production of fully mature and aborted pods and seeds. These investigations required novel research approaches to quantify vegetative growth, including developing image analysis

procedures (ImageJ-Fiji) and complete biomass compositional analysis of protoplasmic and cell wall chemicals. Our results are uncovering new botanical discoveries with in the fields of breeding, histochemistry, cell biology, and physiology. (Supported by: Virginia Soybean Board, Grant-in-Aid of Research, Jackson Hope Foundation). Author contact: Anne B. Alerding, alerdingab@vmi.edu

THE UNIVERSITY OF RICHMOND HERBARIUM MYXOMYCETE COLLECTION. W. John Hayden & S. M. Hayden, Dept. of Biol., Univ. of Richmond. The University of Richmond Herbarium (URV) includes a small special collection of ca 1500 myxomycete specimens, largely the product of Robert F. Smart and his students. Smart, at UR from 1929 to 1969 and a myxomycete specialist, gathered specimens from Arkansas (Mississippi Co.), Mississippi (Tate Co.), and Massachusetts (Middlesex, Norfolk, and Suffolk counties). Most of Smart's collections, however, are from Virginia; the University of Richmond campus and the Mountain Lake Biological Station (Giles Co.) are areas he sampled particularly thoroughly. Most of Smart's specimens date from the early 1930s, but he continued to add specimens to the herbarium, sporadically, into the 1940s. Among Smart's students, two were particularly prolific collectors of myxomycetes: A. Howell collected primarily in Prince George Co. and the city of Petersburg in the mid-1930s and W. T. Allman gathered myxomycetes mostly from Greenville, Henrico, and Sussex counties in the early 1940s. The myxomycete collection was static from 1945 to the early 1980s at which time W. J. and S. M. Hayden began to collect myxomycetes, primarily from Chesterfield, Henrico, and Powhatan counties, as well as other locations. Recent curatorial work on URV myxomycetes has focused on preparing the collection for digital archiving of label data. To this end many "indet." specimens were identified, critical location data was added to original labels, and, as necessary, many specimens were remounted and/or equipped with new printed labels. Author contact: W. John Hayden, jhayden@richmond.edu

EASTERN HEMLOCK (*TSUGA CANADENSIS*) DECLINE AND FOREST DYNAMICS AT SHENANDOAH RETREAT, VIRGINIA. A. Ingle & J. Kincaid, Environmental Studies Program, Shenandoah University, Winchester, VA 22601. Eastern hemlock (*Tsuga canadensis*) is a shade tolerant, coniferous tree species native to the Appalachian Mountains. Throughout its range extending from Maine to Alabama, *T. canadensis* is declining because of the hemlock wooly adelgid (HWA, *Adelges tsugae*), a non-native insect pest. Previous research suggests *T. canadensis* decline is altering forest dynamics, nutrient cycling, and surface water quality. Existing research also has documented a lack of studies examining forest responses to HWA-induced mortality of *T. canadensis* in southern states such as Virginia. The overall goal of this research is to characterize *T. canadensis* mortality and forest dynamics in the study area. A 20x50 meter plot consisting of 10x10 meter quadrats was established at the study site. Within the plot, all seedlings (stems 5 cm to $\leq$ 1 m tall), saplings (stems $>$ 1 m tall to $<$ 5 cm dbh), trees and snags (stems $\geq$ 5 cm dbh) were documented. Tree cores were extracted from all *T. canadensis* stems in the plot. Tree ring evidence suggests *T. canadensis* at Shenandoah Retreat has experienced significant decline since the 1990s, with the growth of one tree declining by 84.6%. Forest structural evidence indicates a lack of *T. canadensis* recruitment, which will likely result in a shift in overstory composition. The

presence of *Ailanthus altissima* in the seedling class is cause for concern because this non-native species aggressively colonizes canopy gaps and outcompetes native species. Author contact: Alan Ingle, aingle16@su.edu

THE FLORA OF VIRGINIA PROJECT: A 2017-2018 PROGRESS UPDATE. Marion B. Lobstein, Professor Emeritus, Northern Virginia Community College. The Foundation of the Flora of Virginia Project (FFVP) released the mobile version of *Flora of Virginia* App for Android and iOS systems at the September 30, 2017 tristate meeting of the Virginia, Maryland, and West Virginia Native Plant Societies. This App contains an easy-to-use graphic key for use by the general public as well as inclusion of the dichotomous keys and descriptions at family, genus, and species level. The background chapters from the *Flora of Virginia*, a glossary, botanical illustrations, photographs, and county range maps from the Digital Atlas of the Virginia Flora are also features included in the App. Additional information on conservation ranks for rare or threatened species and scores for level of invasiveness for invasive species are also provided in the App. Preparation of versions of this App for computers, both Macintosh and personal computers is actively underway. Author contact: Marion B. Lobstein, mblobstein@earthlink.net

INDUCTION OF SOMATIC EMBRYOGENESIS FROM LEAF AND PETIOLE TISSUE OF AFRICAN VIOLETS (*SAINTPAULIA RUPICOLA* B.L. BURTT). T. Warner Lowry & Michael H. Renfroe, Dept. of Biol., James Madison Univ. The *in vitro* propagation of plants through somatic embryogenesis is a promising method for the production of plants in species that are endangered, commercially valuable, or otherwise difficult to propagate through traditional horticultural methods. Leaf and petiole explants of critically endangered African violets (*Saintpaulia rupicola* B.L. Burtt) were cultured on Murashige and Skoog (MS) basal media that was supplemented with either 2μM, 5μM, or 8μM thidiazuron (TDZ). These concentrations were used for induction media followed by a growth medium, and for induction media alone. None of the petiole explants grew or developed any organs while in culture for 12 weeks. All leaf explants that did grow and develop adventitious shoots first developed callus from which adventitious shoots were able to differentiate. Callus isolated from the leaf explants was placed on basal MS medium and differentiated into adventitious shoots. This provides evidence that TDZ may be used for the induction of adventitious shoot growth and that these concentrations of TDZ do not induce somatic embryogenesis in *S. rupicola.* Author contact: T. Warner Lowry, lowrytw@dukes.jmu.edu

A NEW NAME FOR JMU'S HERBARIUM AND AN UPDATE ON ITS DIGITIZATION PROJECT. Conley K. McMullen. James Madison University. In 1964, Norlyn Bodkin joined the Department of Biology at Madison College. The herbarium, which was housed in Burruss Hall consisted of two cabinets and perhaps 2,500 specimens. As the department's plant taxonomist, Bodkin enthusiastically took on the role of curator of the collection. By the time he retired from teaching in 1998, there were well over 13,000 specimens. In addition, during Bodkin's tenure the herbarium was recognized in *Index Herbariorum* as JMUH. The growth of the collection resulted primarily from Bodkin's own collections, those of his field botany classes, and those of many undergraduate and graduate students. Although most specimens are from Virginia

and West Virginia, several other states and countries are represented. The oldest specimens, gifted to JMU in 2007 by The Natural History Museum in London, England, were collected in Portsmouth, Virginia, by German botanist Ferdinand Ignatius Xavier Rugel in 1840. In addition to herbarium specimens, the facility includes a small library, which contains a variety of Floras, botany textbooks, identification keys and journals. On June 6, 2016, in recognition of his contributions to the botanical sciences, this facility was officially named the Norlyn L. Bodkin Herbarium. The Bodkin Herbarium now provides students with a modern, fully equipped, efficient teaching and research facility with well over 18,000 specimens. In July of 2014, digitization of the specimens began. At this time, 9070 specimens have been photographed, and label information of 5357 of these has been databased. Author contact: Conley K. McMullen, mcmullck@jmu.edu

A FLORISTIC SURVEY OF VASCULAR PLANTS OF THE BLUE RIDGE CENTER FOR ENVIRONMENTAL STEWARDSHIP, PURCELLVILLE, LOUDOUN COUNTY, VIRGINIA. Elizabeth K. McMurchie & Andrea Weeks, School of Systems Biology and Dept. of Biology, George Mason University, Fairfax, VA 22030. A floristic survey and analysis of community composition were conducted during the 2017 growing season at the Blue Ridge Center for Environmental Stewardship (BRCES), Purcellville, Virginia. The BRCES is a 900 acre park located in the "Between the Hills" region of Loudoun County between the Blue Ridge and Short Hill Mountains. The park contains several wetlands, including Gordon Pond, Piney Run, Sweet Run and an unshaded seep adjacent to Sweet Run, as well as a wetland that has developed in place of a formerly dammed pond. Parts of two meadows, Demory Field and Sawmill Field, as well as a powerline cut, are maintained for native grasses and meadow plants. In 2014, the mostly wooded western 600 acres of the park were transferred to the Virginia Department of Conservation and Recreation to form Loudoun County's first State Park. In this study, vascular plants of 468 taxa at the species level belonging to 308 genera and 101 families were identified. Twenty-eight species identified were new records for Loudoun County. Two species, *Pycnanthemum torrei* and *Viola macloskeyi* var. *pallens*, are considered rare at the state level under the Virginia Natural Heritage Resources designation S2 (imperiled) and S3 (vulnerable), respectively. Eleven plots were used to determine community types as defined by the Virginia Natural Heritage Program. Author contact: Elizabeth K. McMurchie, emcmurch@masonlive.gmu.edu

GLOBAL DIVERSIFICATION IN THE FERN GENUS CRYPTOGRAMMA. Jordan S. Metzgar. Dept. of Biol. Sci., Va. Polytechnic Inst. & State Univ. We examined diversification, biogeographic history and polyploidy within the parsley ferns (*Cryptogramma*) across multiple time scales. *Cryptogramma* is a small circumboreal genus of rock ferns in the large, diverse family Pteridaceae and is most closely related to the Asian genus *Coniogramme* and the monotypic Central American genus *Llavea*. We generated a combined six locus plastid sequence alignment and a low-copy nuclear marker alignment for 40 accessions. Phylogenetic analysis of these datasets demonstrate that all three genera are reciprocally monophyletic, with *Cryptogramma* and *Coniogramme* most closely related to one another. This analysis also recovered the monotypic *Cryptogramma* section *Homopteris* and sect. *Cryptogramma* as reciprocally monophyletic. Within sect. *Cryptogramma*, the strongly supported phylogeny supported

recognizing most described species as reciprocally monophyletic clades that are mostly allopatric and can be delineated by a few morphological characters. The nuclear DNA phylogeny supported the hypothesis that the allotetraploid *C. sitchensis* originated from a hybridization event between the Asian *C. raddeana* and the Beringian *C. acrostichoides*, and the plastid DNA phylogeny revealed that *C. acrostichoides* was the maternal parent. In contrast, the tetraploid *C. crispa* appears to have originated as an autopolyploid from an undiscovered or extinct ancestor. Author contact: Jordan S. Metzgar, metzgar@vt.edu

HEMP AND THE POLITICS OF AGRICULTURE. Michael H. Renfroe, Dept. of Biol., James Madison Univ., Harrisonburg, VA 22807. Hemp was introduced as a crop in Virginia in the 1600s. The Shenandoah Valley was the leading region of national hemp production in the late 1700s. Production of industrial hemp in the United States was essentially outlawed by the passage of the Marihuana Tax Act of 1937. Shortages of hemp fiber during World War II led to the authorization of hemp production for a limited time. The Controlled Substances Act of 1970 designated all forms of *Cannabis sativa* as a Schedule One controlled substance. This effectively outlawed production of industrial hemp because the legislation failed to distinguish non-psychoactive industrial hemp from psychoactive marijuana. The Agricultural Act of 2014 authorized universities to engage in industrial hemp research provided states authorized and regulated the research programs. Virginia authorized university-based research in 2015. Numerous other states are engaged in research on industrial hemp. Most other industrialized countries produce and process industrial hemp resulting in millions of dollars of hemp products being imported into the United States. However, our famers are not able to grow industrial hemp and supply the raw materials that would stimulate a manufacturing economy surrounding hemp. Despite attempts to remove the non-psychoactive oil and fiber crop from the Controlled Substances list, political controversy continues to limit the potential for the production of industrial hemp in the United States. Author contact: Michael H. Renfroe, renfromh@jmu.edu

DOMINANT TREES OF THE VIRGINIA COASTAL PLAIN: 1607 VS. TODAY. Stewart Ware, Dept. of Biol., Coll. of William & Mary, Williamsburg, VA 23187-8795. Pines are the most abundant of the top ten forest trees in Virginia's central Coastal Plain. It has been suggested that this was true when Europeans first arrived, perhaps including some longleaf pine. However, Capt. John Smith listed 15 trees of potential economic value present in 1607—1609, and did not include pine in the list. He said the dominant trees were oaks and hickories, and that pitch and tar had little economic potential, "there being only here and there a tree suitable for the purpose." Presumably aborigines rarely abandoned cultivated sites where pines might have invaded. Further, pre-settlement ground fires apparently were not intense enough to kill canopy hardwoods and provide light for pine establishment, but were sufficient to exclude fire intolerant beech and red maple, not listed by Smith but usually present today. Author contact: Stewart Ware, saware@wm.edu

AN UPDATE ON THE SERNEC HERBARIUM DIGITIZATION PROJECT IN VIRGINIA. Andrea Weeks, Dept. of Biology, George Mason University. Fairfax, VA 22030. In 2014, 11 Virginian herbaria (GMUF, FARM, VPI, LYN, VMIL, URV, LFCC,

JMUH, VCU, BDWR, AVCH) began creating publicly-accessible online databases (www.sernecportal.org). To date, the project has gathered 220,258 records of Virginian herbarium specimens, including 126,516 images. A study conducted to assess the research impact of these data revealed that adding GMUF data to global portals improved locality data by 34% for individual taxa in Virginia, on average. The crowd-sourcing platform Notes from Nature (www.notesfromnature.org), which allows the public to transcribe specimen label information into database fields, has so far created 24,000 fully transcribed specimens for GMUF. Analysis of transcription activity in the past year revealed that 1096 individuals created 42,540 label transcriptions and that the 10 most active participants created 56% of these. This indicates that the public outreach of Notes from Nature is broad, but the success of overall transcription goals depends on the participation of a few, long-term "super-user" citizen-scientists. Upcoming work will focus on continued digitization among participating herbaria and expanding participation in Notes from Nature (Supported by Virginia Native Plant Society and National Science Foundation, EF-1410086 "The Key to the Cabinets: Building and sustaining a research database for a global biodiversity hotspot."). Author contact: Andrea Weeks, aweeks3@gmu.edu

Posters

INFLUENCE OF PRETREATMENT STRESS ON SUBSEQUENT RESPONSES OF CUCUMBER SEEDLINGS (*CUCUMIS SATIVUS*) TO ALLELOCHEMICALS. Adonel A. Grubb & Mary E. Lehman, Dept. of Biol. & Env. Sci., Longwood Univ. Plant growth can be inhibited by allelochemicals that are released into the soil by surrounding plants, but these inhibitory effects may be reduced if acclimation (increased tolerance) occurs. Using cucumber as a bioassay species, experiments were conducted to evaluate potential acclimation to a phenolic allelochemical when pretreated with a non-inhibitory dose of the same or a different phenol. Cucumber seedlings were pretreated with 0.33 mM of either ferulic or salicylic acid for 7 days in hydroponic nutrient culture before subsequent treatment with 0, 0.2, 0.4, or 0.6 mM salicylic acid. Growth inhibition by increasing concentrations of phenolic treatment was evaluated by change in leaf area and total dry weight. Seedlings that did receive pretreatment were more tolerant to subsequent treatment with salicylic acid, as opposed to control seedlings that were not exposed to the pretreatment stress. This suggests that acclimation can occur, even if the subsequent stress involves a different allelochemical. Further investigation of this acclimation potential may contribute to future development of agricultural practices to improve crop tolerance to environmental stressors. Author contact: Mary E. Lehman, lehmanme@longwood.edu

CURATION, RESEARCH, AND OUTREACH AT VIRGINIA TECH'S MASSEY HERBARIUM. Jordan S. Metzgar. Dept. of Biol. Sci., Va. Polytechnic Inst. & State Univ. The Massey Herbarium is the largest herbarium collection in Virginia with 115,000 catalogued specimens. These holdings are dominated by vascular plants (108,000 specimens) and are also comprised of fungal, bryophytes, lichen, and algal specimens. We are a regional herbarium with over 60% of our material collected in Virginia. The southeastern and mid-Atlantic USA regions account for most of our

remaining collections. We possess numerous new county and state records for the Virginian flora and our material has been cited in over 600 peer-reviewed publications that have received in excess of 12,000 citations. We are actively participating in digitization programs such as the SERNEC (Southeast Regional Network of Expertise and Collections) Portal. We are developing a robust outreach program based on virtual and physical interactions with the community. Our website (masseyherbarium.org) and social media presence (@MasseyHerbarium) allow us to interact with the public and advance botanical knowledge. We have also begun working with school groups, undergraduate organizations, and amateur naturalist societies in the collection, field, and classroom. Author contact: Jordan S. Metzgar, metzgar@vt.edu

Chemistry

INVESTIGATING THE CHEMISTRY AND BIOCHEMISTRY OF RUTHENIUM SUPRAMOLECULAR COORDINATION COMPLEXES. Floyd A. Beckford, Madison B. Niece & Steven M. Shell, Dept. of Nat. Science, The University of Virginia's College at Wise. Evidence in the chemical literature suggests that multinuclear complexes may provide a novel approach to the study of potential metal-based drugs. We have synthesized a number of hexanuclear organometallic ruthenium supramolecular cages by connecting two identical trimeric units via a dipyridylethene linker. The trinuclear units contained a central triazine unit bound to three arene-ruthenium units. The arenes used were benzene, p-cymene, mesitylene and hexamethylbenzene. We will report on encapsulation of 5-fluorouracil, a cytotoxic agent, as well as $Pd(acac)_2$ into the cages. The synthesized compounds have been characterized by elemental analyses, NMR, UV-VIS, fluorescence, powder XRD, and thermal analyses. The complexes are extremely stable in acetonitrile solutions and in buffers at physiological pHs. It was observed that the interaction of the complexes with DNA is somewhat complex. The extent of binding is relatively small but the binding constants are moderate ranging from 7.33×10^3 M^{-1} to 2.92×10^4 M^{-1}. The complexes also seem to stabilize the DNA duplex with approximately 1-2 degrees increase in the melting temperatures in the presence of the complexes containing the hexamethylbenzene and mesitylene arene groups. Preliminary results of the anticancer activity of all the trimer building blocks will also be presented. (This work was supported in part by a Mary Louise Andrews Award for Cancer Research grant from the Virginia Academy of Sciences). Author contact: Floyd Beckford, fab5b@uvawise.edu

THERMODYNAMICS OF ESTERIFICATION. Charles M. Bump, Stephanie N. Chigbu & Ashanti M. Sallee, Dept. of Chem. & Biochemistry, Hampton University. The preparation of esters is a common type of nucleophilic acyl substitution reaction. Acyl halides, acid anhydrides, and carboxylic acids combine with alcohols to give esters as the major organic product. Acyl halides are described as the most reactive carboxylic acid derivative. A base is always added to neutralize the HCl by-product of the reaction. Reactions involving carboxylic acids and alcohols are described as requiring an excess of either the carboxylic acid or alcohol in order to shift equilibria to favor the product (ester). We will look at the thermodynamic basis for the use of excess carboxylic acid or

alcohol in esterification reactions. Author contact: Charles M. Bump, cmbump@aol.com

THERMAL DEHYDRATION OF SODIUM AND POTASSIUM COPPER OXALATE DIHYDRATE. T.C. DeVore & Isatu Kamara, Dept. of Chem. & Biochemistry, James Madison University. The title compounds were precipitated from a saturated solution prepared by dissolving copper oxalate in boiling 1 M alkali oxalate. The blue needle crystals that formed on cooling were harvested using vacuum filtration, washed with water, and air dried. Fourier transform infrared spectroscopy (FTIR) and powder x-ray diffraction (pXRD) were used to characterize the products. Thermal gravimetric analysis indicated that both compounds decomposed in three steps. PXRD and FTIR were used to establish that the first step resulted from the loss of the waters of hydration. The second step was the decomposition of the bis – oxalato cuprate ion to form the alkali oxalate and copper metal or copper oxide depending upon the amount of oxygen in the carrier gas. The final step was decomposition of the alkali oxalate to form the alkali carbonate. Differential scanning calorimetry was used to determine the enthalpy change for each transition under oxidizing conditions. The enthalpy changes for the dehydration step were found to be 103 kJ/ mol and 110 kJ/ mole for the sodium and the potassium salts respectively. The enthalpies of formation were determined to be -2107 kJ/ mole and -2160 kJ/ mole for sodium and potassium bis-oxalato cuprtate respectively and -2695 kJ/ mole and – 2750 kJ/ mole for the respective dihydrates. Author contact: Tom DeVore, devoretc@jmu.edu

DFT MODELING OF THIONE/SELONE-MEDIATED PREVENTION OF BIOCHEMICAL REDOX DAMAGE BY Fe(II). Ana Dreab & Craig A Bayse, Dept. of Chem. & Biochemistry, Old Dominion University. Hydroxyl radicals produced in vivo cause oxidative damage to DNA which increases risk for numerous diseases. Formation of the hydroxyl radical occurs through peroxide reduction involving Fe(II) and Cu(I) (i.e., Fenton Chemistry). Sulfur and selenium compounds have been investigated for their antioxidant properties in preventing this metal-mediated oxidative damage. Density functional theory calculations are used to examine the effect of the coordination of sulfur/selenium derivatives of N, N-dimethylimidazolidinone on the electronic structure and reduction potential of aquated Fe(II) ions isolated or in the presence of guanine. Electron withdrawing and donating groups substituted on the imidazole ring shift the electron density around the S/Se to strengthen coordination to the metal center. The change in HOMO character and energy of formations are discussed and further avenues of investigation into the thione/selone-mediated prevention of DNA redox damage by Fe(II). Author contact: Ana Dread, adrea001@odu.edu

THEORETICAL STUDY OF THE INHIBITION OF ZINC FINGER PROTEINS BY REDUCIBLE SELENIUM AND SULFUR COMPOUNDS. Patricia B. Lutz[1] & Craig A. Bayse[2], [1]Science & Math Department, Regent University and [2]Dept. of Chem. and Biochemistry, Old Dominion University. Zinc fingers (ZFs) are small protein domains that have Zn^{2+} tetrahedrally coordinated to a least 2 Cys and His. Zn^{2+} plays a structural role that produces the correct folding required for function. Zn^{2+} is redox inactive but oxidation of Cys thiolates release the Zn^{2+}. Reducible sulfur and selenium compounds (r-S/Se) have been found to release Zn^{2+} from ZFs. Density functional theory

calculations were used to investigate the strength of interactions between r-S/Se compounds and models of the three types of ZFs, (Cys_2His_2, Cys_3His and Cys_4). The strength of the interaction was shown to increase with the Lewis basicity of the ZF model (Cys_4 > Cys_3His > Cys_2His_2) and the Lewis acidity of the r-S/Se compound. The Lewis acidity was measured by the energy of the S/Se-X antibonding molecular orbital ($\varphi^*_{S/Se-X}$). The correlation of $\varphi^*_{S/Se-X}$ with interaction energy suggest that the $\varphi^*_{S/Se-X}$ energy of a potential r-S/Se compound could be used to test its ability to oxidize ZFs. This work was funded by the National Science foundation (CHE-0750413). Author contact: Patricia B. Lutz, plutz@regent.edu

SYNTHESIS AND CHARACTERIZATION OF POLYETHER ETHER KETONE (PEEK) POLYMER. Reed J. Mingione & Rupak Dua, Dept. of Chem., Hampden-Sydney College. Polyether ether ketone (PEEK) polymer is a class of thermoplastics that have growing applications to the world of medicine. PEEK is radiolucent and has strong thermodynamic properties which allows it to be used as a cage material for spinal fusion surgeries. However, the bio inert nature of the PEEK limits the osseointegration of implant when put in contact with the bone. In order to make the PEEK polymer osteoinductive, we need to have a clear understanding of the synthesis process of PEEK. To accomplish that, we in this project did the synthesis of PEEK using a previous established method and devise a procedure to structurally modify PEEK to make it osteoinductive. PEEK was synthesized via polymerization of 4,4'-difluorobenzophenone (DFPB) and hydroquinone (HQ) in a solution of sodium carbonate and diphenyl sulphone. The nucleophilic aromatic substitution reaction proceeded under high temperatures until a precipitate was formed. The product was washed with acetone and water to remove side products and solvent. The washed product was characterized via ^{1}H and ^{13}C nuclear magnetic resonance (NMR) spectroscopy, melting point analysis, Beer's law experiments, and FT-IR spectroscopy. The data confirmed the synthesis of PEEK with a percent yield of 77.6% in the form of a grey granular powder. Author Contact: Rupak Dua, rdua@hsc.edu

(HYPER)POLARIZABILITIES A MATERIALS DESIGN CRITERION. Edmund Moses N. Ndip, Dept. of Chem. & Biochemistry, Hampton University, Hampton, VA 23668. The effect of extent of conjugation on frequency dependent nonlinear optical properties of model organic semiconductors has been investigated. Semi-empirical calculations of the frequency-dependent linear polarizability, α, the second, β- and third, γ-order hyperpolarizabilities at the fundamental (1028 nm) and other wavelengths were achieved by applying the *ab initio* time-dependent coupled perturbed Hartree -Fock (TDCPHF) method at the Restricted Hartree- Fock (RHF) level using routines contained in MOPAC2016 program for various model systems. Linear absorption spectra were calculated using the CNDO/S with SPD basis set. At the fundamental wavelength (1024 cm^{-1}), the values for the linear polarizability (α) ranged from 110. to 619 A.U.. (polypyrroles – materials for batteries), 184. to 1060. A.U.(poly(3-octylthiophene – materials for solar cells)) and 209. - 1605. A.U. (poly (3,4-ethylenedioxythiophene) – materials for organic light emitting diodes)). The second-order hyperpolarizability values (β) for the various applications range from 0.012 - 3.3325a.u. (batteries), 0.46 – 10073 a.u. (OLEDs), and $5.3521 \times 10^4 - 8.51940 \times 10^5$ a.u. (solar cells). The third-order

hyperpolarizabilities (γ) for the various applications materials range from 2.6747 x 10^4. – 2.409187 x 10^6. a.u.(batteries), 2.40 x 10^6 – 8.05 x 10^9 a.u. (OLEDs), and 3.18 x 10^7 – 1.21 x 10^9 a.u. (solar cells). Maximum absorption wavelengths ranged from 340 nm – 590 nm, 375 nm – 625 nm, and 275 nm – 510 nm for battery, OLEDs, and solar cell applications respectively. The HOMO-LUMO gaps ranged from 6.51 – 4.48 eV, 6.03 – 4.24 eV, and 7.89 – 4.18 eV for battery, OLEDs and solar cell applications respectively. It is well known that semi-empirical methods overestimated these properties. Higher level calculations using first principles *ab initio* methods are planned for the future. This work was supported in part by Hampton University – Brandeis University NSF DMR PREM grant. Author contact: Edmund Moses N. Ndip, edmund.ndip@hamptonu.edu

ENGAGING HIGH SCHOOL STUDENTS IN RESEARCH. Peter N. Njoki, Dept. of Chem. & Biochemistry, Hampton University. Throughout K-12 education, most students only experience science in a classroom setting. The Nanoscience Transforming STEM (Science, Technology, Engineering, and Mathematics) Education at Hampton University (NanoHU) Program has played a prominent role in reversing this trend by hosting high school students to conduct summer research projects with the guidance of faculty mentors. Rising 10^{th} and 11^{th} graders are selected for a six-week (Mon-Fri) non-residential, research-intensive program where they actively engage in Interdisciplinary Nanoscience projects. Performing research alongside a faculty mentor helps students better understand design of experiments, interpretation of data, exploration of the literature, communicating results, and teamwork. This presentation describes research work by six underrepresented minority high school students in a 6-week non-residential summer program at Hampton University. The students synthesized various sizes of gold and silver nanoparticles using conventional heating and microwave irradiation techniques. Compared to conventional heating method, microwave irradiation provided shorter reaction times, better reproducibility, and enhanced reaction control. The students learned to use UV-Vis spectrophotometer to characterize nanoparticles, search literature, and prepare PowerPoint presentation. The summer program culminated with a mandatory poster session where students presented the results of their summer research projects to the parents and university community. (Supported by: NSF HBCU-UP ACE Implementation. HRD-1238838). Author contact: Peter Njoki, peter.njoki@hamptonu.edu

WETTING TRANSPARENCY OF CONDUCTING GRAPHENE. Neda Ojaghlou[1], D. Bratko[1], Alenka Luzar[1] & Mathieu Salanne[2], [1]Dept. of Chem., Virginia Commonwealth University, Richmond, Virginia 23284, and [2]Sorbonne Université, CNRS, Physico-Chimie des Électrolytes et Nanosystèmes Interfaciaux, PHENIX, F-75005 Paris, France. Contact angle measurements revealed that the underlying substrate can exert a significant effect on the contact angle of graphene, a phenomenon called wetting transparency. Experiments, conducted on the suspended graphene compared to the supported one, as well as molecular dynamics simulations on submerged graphene fragment in water have yielded inconsistent results. In addition, contact angle calculations by computer simulations of water on graphene have been determined by ignoring the material's conducting properties. We improved the graphene model by incorporating the conductivity of graphene sheet by applying the fluctuation charge

technique of Constant Potential Molecular Dynamics(CPMD). We evaluated the wettability by measuring the contact angle of cylindrical water drops on a conducting graphene sheet. We found that the contact angle of a water droplet on a graphene sheet submerged on water is about 10° lower than in the absence of water under graphene. In other words, water-graphene adhesion is increased when graphene is wetted from both sides. This difference is important in applications including sensors, fuel cell membranes, and water filtration. Author contact: Alenka Luzar, Aluzar@vcu.edu

A QUANTITATIVE DESCRIPTION OF INTERFACIAL AFFINITY. Joshua D. Patterson, Dept. of Molecular Biology & Chemistry, Christopher Newport University, Newport News, VA 23606. Heterogeneous reactions occurring in atmospheric aerosols are crucial components of multiple chemical reaction cycles. Despite the importance of heterogeneous reactions, our ability to predict the outcomes of these reactions is hindered by the complexity of the interfacial region in which they occur. We use reverse micelles (RMs) in solution as proxies for sea spray aerosols to examine the interfacial properties of ionic species. The tunability and small size of RMs allows for the quantification of ionic partitioning between the interfacial and core regions of the RMs. Interfacial partitioning as a function of RM size (w_0) is well described by a power-law equation. From this equation quantitative interfacial affinity ($\chi_{Int.}$) is derived. Infrared spectroscopy experiments reveal a $\chi_{Int.}$= 0.4618 for nitrate ions in sodium bis(2-ethylhexyl) sulfosuccinate (AOT) RMs. Molecular dynamics simulations indicate that sodium possesses a strong interfacial affinity of 0.81 in AOT RMs and suggest that interfacial affinity is influenced by the charge identity of the surround surfactant molecules within the RMs. (Support by: The National Science Foundation (NSF CHE-1708635). Author contact: Joshua Patterson, joshua.patterson@cnu.edu

TRANSFORMATION OF PINE WOOD BIOMASS INTO PINE 400 BIOCHAR AND ITS OXYGENATION FOR ENHANCING CATION EXCHANGE CAPACITY. Oumar Sacko[1], Rachel Whiteman[1], James W. Lee[1] & Sandeep Kumar[2], [1]Dept. of Chem. & Biochemistry, Old Dominion University and [2]Dept. of Civil & Environmental Engineering, Old Dominion University. Biochar, a pyrolysis product of biomass provides a method of carbon sequestration due to its stability and can also be used as a soil amendment agent. Pine wood biomass was converted to biochar with a highest treatment temperature of 400°C (Pine 400) by slow pyrolysis with a biochar yield of about 30-40% and a water/bio-oil yield of about 30-38%. In order to increase the Cation Exchange Capacity (CEC) of the biochar, the latter was wet-ozonized (in presence of water) and dry-ozonized (in absence of water). The CEC significantly improved going from 9.65 cmol/Kg (non-ozonized control) to 18.01 cmol/Kg (wet-ozonized Pine 400) and 19.46 cmol/Kg (dry-ozonized Pine 400.) The increase in CEC was also marked by a significant drop in pH for the ozonized biochar compared to the control. The Dissolved Organic Carbon (DOC) concentration of the filtrates resulting from the different types of biochar was measured. The ozonization under wet conditions resulted in the highest concentration of DOC/g of biochar; 6.87mg DOC/g of biochar for the wet-ozone treated biochar, 1.06mg DOC/g biochar for the dry-ozone treated biochar and 0.29mg DOC/g of biochar for the non-ozonized biochar. Preliminary studies of the filtrates were undertaken on the cyanobacteria *Synechococcus elongatus* PCC 7942 and showed that the filtrate

from the wet-ozonized biochar was the least inhibitory on the growth of PCC 7942. Author contact: Oumar Sacko, osack001@odu.edu

GENERALIZED FRAMEWORK FOR STUDYING HYDROGEN BOND DYNAMICS. Mahdi Shafiei, D. Bratko & Alenka Luzar, Dept. of Chem., Virginia Commonwealth University. Understanding the translational and rotational dynamics of water molecules in a network of hydrogen bonds that break and reform on a pico-second time scale has been a challenge. Luzar and Chandler presented a method for calculating the rate of hydrogen breaking and reforming between a pair of molecules and Laage and Hynes explained the re-orientation of water molecule during a hydrogen bond exchange. The first formalism focuses on a pair of initially bonded molecules; the second formalism concerns a triplet of molecules involved in the initial bond and in the new bond formed with a different proton acceptor. Our goal is to show that these two approaches are related. We demonstrate that most of the H-bond breakings in Luzar and Chandler formalism coincide with the switching of donated hydrogen to another acceptor. The switching process can be reversed a few times until one of the acceptors leaves the second coordination shell and cannot make a bond any longer. We have tested our generalized approach under a variety of conditions including different water force fields, varied temperatures, different water models, and a range of static and alternating external fields. The characteristic times corresponding to definite switching of hydrogen bond partners in either of the two formalisms conform well to the average frequency of translational steps between dynamic basins of locally trapped water molecules observed in the diffusion coefficient of water in direct Molecular Dynamics simulations. Author contact: Alenka Luzar, Aluzar@vcu.edu

UNDERSTANDING THE EFFECT OF INTRAMOLECULAR AND INTERMOLECULAR INTERACTIONS ON ENERGETIC MATERIAL SENSITIVITY. Ashley L. Shoaf & Craig A. Bayse, Dept. of Chem. & Biochemistry, Old Dominion University. High energy density materials (HEDMs) with improved properties are under investigation to replace hazardous materials currently used in military and aeronautics applications. However, experimental data is limited because detonation is practically instantaneous; thus, information from density functional theory (DFT) could be used to predict energetic properties from bond activation measures. Trigger bonds, activated bonds that break to initiate explosive decomposition, are proposed based on DFT calculations and the Wiberg bond index (WBI), a measure of interatomic electron density. WBIs of HEDM trigger bonds were compared to those in reference molecules (i.e. contain same bond type and hybridization) to determine a relative scale for bond activation (%ΔWBIs). Trigger bonds are expected to be longer, have a lower electron density and be activated by repulsion and steric effects relative to the corresponding bond in reference molecules. Since detonation is a unique solid-state process, gas-phase calculations guide condensed-phase calculations to understand the favorability of certain initiation pathways. Thus, molecular dynamics simulations show how intermolecular interactions change over time with increasing pressure. Correlating %ΔWBIs to experimental data could provide insight into the effect of intramolecular interactions on sensitivity while molecular dynamics can show how intermolecular interactions influence sensitivity. Author contact: Ashley Shoaf, ashoa001@odu.edu

SURFACE INTERACTIONS OF PENTAGRAPHENE WITH VARIOUS LIQUIDS. Margaret E. Thornton, Serban G. Zamfir, Dusan Bratko & Alenka Luzar, Dept. of Chem., Va. Commonwealth University. Pentagraphene is a theoretically predicted material of interest due to its 2:3 ratio of sp^3 to sp^2 carbons, its high heat capacity, and its semi-conductor properties. Since this material has yet to be synthesized, we are interested in predicting additional properties relevant to potential applications. This study investigates surface interactions of pentagraphene with various liquids, specifically water and diiodomethane. Two liquids with different self-interactions were selected for study; water due to its hydrogen bonding that allows it to more readily form droplets, and diiodomethane because its lack of hydrogen bonding. Molecular dynamics (MD) simulations in the NVT ensemble were used to model cylindrical droplets of each liquid on a pentagraphene sheet. Parameters for the sp^2 and sp^3 carbons were based on graphene and diamond surface models, respectively. Resulting data was analyzed in order to calculate the contact angles for each droplet on the sheet. It was expected that the contact angle for the water droplet on the pentagraphene surface would fall somewhere in between the sp^2 and sp^3 literature values if corrugation had no effect on the surface interactions. The resulting value was significantly lower than either of the contact angles for purely diamond or graphene, indicating that the corrugation of the pentagraphene surface plays a role in the resulting contact angle. The diiodomethane droplet resulted in a fully wetted surface. Author contact: Margaret Thorton, thorntonme2@vcu.edu

COMPARISON OF STUDENT LEARNING OUTCOMES IN TRADITIONAL GENERAL CHEMISTRY COURSES TO A BLENDED LEARNING COURSE ENVIRONMENT. Michelle K. Waddell, Brandy Young-Gqamana, Willie Darby, Kesete Ghebreyessus & G. Nwokogu, Dept. of Chem. & Biochemistry, Hampton University. Improving undergraduate student learning outcomes in general chemistry has always been the focus when retention of STEM majors have been the goal. As a prerequisite course, general chemistry sets the foundation for all higher level courses. Over the past ten years, a steady increase in the general chemistry attrition rate has been noted in several sections taught by various instructors. In an effort to improve student comprehension, a blended traditional-flipped teaching model was piloted in two second semester general chemistry courses. The pilot courses used video lectures to enhance traditional lectures in three topic areas. Online quizzes and exam questions were compared between sections which presented traditional lectures versus video enhanced lectures. Results indicated no appreciative benefit for the video enhanced lectures over traditional lectures. However, within one section an improvement in attrition rate was observed. Author contact: Michelle Waddell, michelle.waddell@hamptonu.edu

Posters

LOOP DYNAMICS IN THYROID HORMONE ACTIVATING PROTEINS. Liana G. Brown, Jenna R. Garcia, Eric S. Marsan & Craig A. Bayse, Dept. of Chem. & Biochemistry, Old Dominion University. The selenocysteine-dependent family of iodothyronine deiodinases (Dios) activate and deactivate thyroid hormones through reductive elimination of iodide. Mutations at key residues cause disruptions in developmental and metabolic processes by preventing deiodination. To understand how

structural effects on a critical loop in the protein, multiple μs molecular dynamics simulations have been performed on wild-type Dio3 and several mutants near the active site. Specific hydrogen bonding interactions between residues that have significant effects upon the conformation of the loop, and presumably the activity of the protein, are lost in the mutants. In particular, loss of hydrogen bonding to Ser37/Thr39 can lead to a highly flexible loop which may inhibit substrate binding. Author contact: Craig Bayse, cbayse@odu.edu

SELF DEFENSE OF *ABIES FRASERI* VIA ORGANIC SECONDARY METABOLITES. Taylor L. Darnell, Laura L. Grochowski & Tim C. Durham, School of Natural Sciences & Mathematics, Ferrum College. Through Gas Chromatography-Mass Spectroscopy, GC-MS, analyzations, the compositional differences in terpene production in differing *Abies fraseri* trees can be detected and compared to known spectra of healthy and unhealthy *Abies fraseri* trees. In analyzing the chemical compositional differences in selected *Abies fraseri* trees, subtle differences in secondary metabolite and degradants can be characterized and their insecticidal properties studied. The metabolite structure changes that have been observed in physical stressors has been observed to cause an increase in the production of limonene in said trees. By quantifying the increases in proven secondary metabolites characterized as having insecticidal properties, inferences about the effectiveness of 'self-defense' utilizing the internal chemistry of the tree can be used as a way to reduce the dependence on inorganic and semi-synthetic pesticides. This research has proven that stress levels can be detected in live *Abies fraseri* trees via elevated production of terpenes, and reduced production of certain secondary metabolites, like Bornyl acetate and 3-Carene. This data is also being applied as a way to characterize the relative health of selected Fraser Fir tree stands in an attempt to reduce the dependence on semi-synthetic and inorganic pesticides as the only means of pest control. (Funding provided by Virginia Academy of Science Fall Undergraduate Research Scholarship. Author contact: Taylor Darnell, tdarnell@ferrum.edu

AMINO ACID ANALYSIS OF ALGAE USING HPLC. Ashley O. Moorman, Thomas E. Walker, Todd M. Allen, Addie M. Lauder, & Erik T. Ferenczy, Dept. of Biol. and Chem., Liberty University. Amino acids are the building blocks of proteins within the body. All humans and animals require amino acids for survival. Some of these amino acids are essential, meaning the body cannot produce the amino acid itself and instead must be obtained through diet, while others are nonessential. Due to worldwide food shortages because of the growing population, scientists have proposed supplementing animal feed with algae because of their abundant essential amino acids. Because algae are a cheap addition to animal feed, the goal is to be able to raise more livestock quickly and cheaply, increasing food availability worldwide. Algae cells that produce the greatest amount of protein will have the greatest amount of amino acids. Our research focuses on the development of a reliable and accurate method for the extraction of amino acids in algae cells and the determination of amino acids by high performance liquid chromatography (HPLC). Before analysis, amino acids must be derivatized using dinitrofluorobenzene (DNFB). Specifically, we are focusing on measuring the reaction efficiency of the derivatization for individual amino acids using HPLC and UV-Visible

Spectroscopy. By measuring reaction efficiency, the ability of DNFB to convert amino acids to their derivatized form can be quantized. Additionally, this will provide insight into areas in which our methodology can be changed to produce a higher reaction efficiency. Author contact: Ashley Moorman, amoorman2@liberty.edu

DETERMINING THE EFFECT OF SURFACE DEFECTS ON GRAPHENE-BASED ELECTROCHEMICAL DOUBLE-LAYER CAPACITORS BY AN ELECTROCHEIMCAL QUARTZ CRYSTAL MICROBALANCE STUDY. Alexandra Rosado Carrion, Ronald A. Outlaw, Dilshan Premathilake & Ronald A. Quinlan, Christopher Newport University. Electric double layer capacitors (EDLCs) are traditionally composed of active carbon electrodes. Active carbon is a highly porous material that allows for the high capacitance of EDLCs, however it causes AC line filtering problems. Due to the open morphology of the vertically oriented graphene nanosheets (VOGN), which allows for ingress and egress of the electrolyte, VOGN electrodes are suitable for filtering applications. However, the specific capacitance remains limited. In an effort to further enhance the capacitance, defects in the form of carbon black coatings have been coated on the VOGN material and have increased the specific capacitance to 2.3 mF/cm^2 at 120 Hz. Despite this increase, the interaction between the coating and VOGN support has limited the capacitance to below the theoretical value of ~42 mF/cm^2. Our initial efforts have revealed a dependence on the sonication time and solvent for wetting the material. Using model substrates of HOPG, we are studying the basic interactions at the surface that limit the uniformity of the coatings and possibly the thickness of the Helmholtz layer. These results may increase the understanding of interactions for coatings on these low surface energy materials. Author contact: Ronald A. Quinlan, ronald.quinlan@cnu.edu

COMPARISON OF HPLC AND GC-MS FOR ANALYSIS OF ATRAZINE. Shiloh M. Sooklal & Todd M. Allen, Dept. of Chem., Liberty University. Atrazine is a commonly used herbicide in the mid-western United States with a limit of 3 parts per billion (ppb) allowed in water run-off, despite already being banned in Europe. Previous studies have shown atrazine to be an endocrine disruptor and long-term exposure has the potential to adversely affect an entire ecosystem. Detection of atrazine in ground water samples is difficult due to the low concentrations, ranging from 1 to 200 ppb, typically found in agricultural runoff into local streams and ponds. This study involves the detection of trace concentrations of atrazine ranging from 0.005 to 50ppb using GC-MS and HPLC analysis. After applying Solid Phase Extraction to the trace concentrations of atrazine in spiked water samples, the HPLC detected the lowest concentration of atrazine at 0.005 ppb. Therefore, quantification of atrazine with the SPE method is possible in the range of 0.005 to 50 ppb on the HPLC compared to a range of 0.05 to 50ppb after GC/MS analysis. The extraction and quantification methods were also applied to water samples collected from crayfish tanks. Author contact: Shiloh Sooklal, ssooklal1@liberty.edu

COUNTER-ION IMPACTS ON THE INTERFACIAL PROPERTIES OF NITRATE IONS. Meredith Varmecky, Elizabeth Boycourt, & Joshua D. Patterson, Dept. of Molecular Biology and Chemistry, Christopher Newport University, Newport

News, VA 23606. The structure and local environment of molecules are inexorably linked to their chemistry. Interfaces, the boundaries between chemical phases, possess unique chemical rules that cannot be described by the extension of gas- or liquid-phase properties. As such, the interface has at times been referred to as the "fourth phase"; a distinct chemical environment unto itself. We use reverse micelles (RMs) in solution as proxies for sea spray aerosols to examine the interfacial properties of nitrate ions in the presence of different counter-ions. The tunability of RMs allows for the creation of an aqueous environment that is considered entirely interfacial water. The asymmetric-stretch vibrational mode of nitrate is monitored using infrared spectroscopy. Interfacial nitrate within sodium bis(2-ethylhexyl) sulfosuccinate RMs exhibits higher vibrational frequencies and smaller peak splitting relative to nitrate in aqueous solution. Vibrational frequencies and peak splitting show only modest sensitivity to nitrate counter-ion identity. Observed peak splitting in AOT RMs can be reproduced by creating a hydrogen-bonding deficient environment using NaOH. These observations are consistent with the rigid hydrogen-bonding network of the interfacial region. Interfacial nitrate in cetyl trimethylammoium bromide RMs has a lower vibrational frequency relative to aqueous nitrate indicating that electrostatic interactions with the surfactant headgroups may direct the structural properties of nitrate in RMs. (Support by: The National Science Foundation (NSF CHE-1708635). Author contact: Joshua D. Patterson, joshua.patterson@cnu.edu

NANOCONFINED WATER AND SOLUTION MODELING IN THE PRESENCE OF MULTIBODY POLARIZABILITY EFFECTS. Serban Zamfir[1], Filip Moucka[2], Dusan Bratko[1], Alenka Luzar[1] & Filip Moucka[2], [1]Dept. of Chemistry, Virginia Commonwealth University and [2]Faculty of Science, J. E. Purkinje University. Aqueous molecules and ions in hydrophobic pores are modeled using the gaussian-charge-on-spring BK3-AH representation. This involves nontrivial developments in Expanded Ensemble Monte Carlo simulations for open systems with long-ranged multibody interactions and further improvements for modeling ion exchanges. Our results for the open BK3 model in neat aqueous systems capture the ~10% reduction of molecular dipoles within the surface layer near the hydrophobic pore walls in analogy to reported quantum mechanical calculations at water/vapor interfaces. While we observe only moderate changes in overall thermodynamic properties and atom and charged-site spatial distributions, the Gaussian distribution of atom charges on water and ions in the polarizable model shifts the density amplitudes and blurs the charge-layering effects associated with increased ion absorption in point-charge models. (Supported by: the Office of Basic Energy Sciences U.S. Department of Energy, the National Energy Research Scientific Computing Center and the Extreme Science and Engineering Discovery Environment (XSEDE), which is supported by the National Science Foundation). Author contact: Serban Zamfir, zamfirsg@vcu.edu

Data Science, Computing and Statistics

Not available

Education

Not available

Entomology

COMMUNICATING THE SCIENCE OF ENTOMOLOGY THROUGH SOCIAL MEDIA. Jake E. Bova. Department of Entomology, Virginia Tech, Blacksburg, VA. Two thirds of Americans receive news from social media, and as such, effective communication of the science of entomology on these platforms is incredibly important. Our entomology-oriented Facebook page, "Relax. I'm an Entomologist" has been sharing and discussing entomology related topics from GMO's and invasive species to public health and conservation for the past six years. Insects and arthropods carry with them a charismatic curiosity, from disgust to awe, that resonates with most people. Identifying the most efficient social medium for a scientist or lab can be daunting but highly advantageous. By applying our science to the online discussion, we can reach a wide array of the general public to promote entomological and scientific literacy while fostering an interest in our own work. Author contact: Jbova86@vt.edu

ASSESSING INSECT PEST PRESSURE ON INDUSTRIAL HEMP IN VIRGINIA. Kadie E. Britt & Thomas P. Kuhar, Department of Entomology, Virginia Tech, Blacksburg, VA. An industrial hemp pilot program was initiated in Virginia in 2016. In 2017, hemp field plots from several locations in Virginia were sampled for insects and their damage. Several insect species were commonly encountered on hemp plants including the brown marmorated stink bug (*Halyomorpha halys*), Japanese beetle (*Popillia japonica*), and corn earworm (*Helicoverpa zea*); the latter appeared to cause the most damage to hemp seeds and warrants future IPM research. Additionally, further studies were initiated to assess the effects of insect feeding on yield of industrial hemp. In the first study, greenhouse-grown hemp plants were manually defoliated at levels of 0%, 12.5%, 25%, and 50% to simulate insect leaf feeding, and showed no significant yield differences among treatments. This study will be repeated in field-grown hemp in 2018. The second study examined yield differences between non-treated and insecticide-treated plots and showed noticeable, but not significant, yield increases in insecticide-treated plots. This study will also be repeated in 2018. Author contact: Kadie Britt, kadieb@vt.edu.

THE EFFICACY OF NON-REGISTERED REPELLENTS ON *AEDES ALBOPICTUS*. James A Carver, Dominic Latoma, Benjamin McMilam, Kevin Chan, Jake Bova, & Sally Paulson, Department of Entomology, Virginia Tech. Topical insect repellents are one of the most efficient personal protective measures to reduce the risk of exposure to mosquito-borne pathogens. The Environmental Protection Agency (EPA) has registered multiple active ingredients and compounds known to repel mosquitoes for different amounts of time. All of these products continue to meet safety requirements under the Registration Review Program. As such, the Center for Disease Control and Prevention (CDC) recommends the use of products containing DEET, picaridin, synthesized oil of lemon eucalyptus, and IR353 to repel mosquitoes. However, some consumers choose to utilize untested, non-registered by the EPA products and home-made remedies because of reservations driven primarily by chemophobia. Unfounded beliefs by consumers that these repellents are safer for the user and environment while offering the same level of protection as EPA-registered repellents are perpetuated mainly by word of mouth and through social media online. Many of these products not registered

by the EPA that some consumers claim to repel mosquitoes remain untested. The purpose of this study was to evaluate two EPA-registered repellents and 10 non-registered by the EPA repellents found online for their duration of repellency of nulliparous *Aedes albopictus* females. Five different volunteers topically applied an individual repellent to unprotected skin on their forearms, and the treated area was introduced to 20 mosquitoes via a constructed biting aperture three times per repellent. Duration of repellency was calculated as the time of initial mosquito exposure until the first biting probe by any mosquito. The non-registered by the EPA repellents used in this experiment failed to offer the same duration of protection as EPA-registered products containing DEET and synthetic oil of lemon eucalyptus. We suggest none of them be used in lieu of EPA-registered repellents containing CDC recommended active ingredients by consumers seeking to reduce their exposure to biting mosquitoes. Author contact: spaulson@vt.edu

ASSESSING THE IMPORTANCE OF SOLDIER BEETLES (*CHAULIOGNATHUS* SPP.) AS PREDATORS IN SOUTHWEST VIRGINIA AGRICULTURAL SYSTEMS. Katlyn A. Catron & Thomas P. Kuhar, Department of Entomology, Virginia Tech, Blacksburg, VA. Soldier beetle larvae in the genus *Chauliognathus* are generalist predators in Virginia agricultural systems, with anecdotal evidence suggesting that they prey upon eggs and larvae of several pests of corn and other economically important crops. At least two species of interest, *Chauliognathus marginatus* and *Chauliognathus pensylvanicus*, are present in Virginia, but little has been studied about their phenology, life history, predation habits, or larger role in agroecosystems. Preliminary studies show that *C. marginatus* readily preys upon eggs of multiple pest species and feeds almost exclusively at night. This work expands upon that knowledge to elucidate the roles that *Chauliognathus* spp. larvae play as predators and potentially useful beneficial insects in an integrated pest management context. Author contact: Katlyn Catron, kamos@vt.edu.

SURVIVORSHIP OF BROWN MARMORATED STINK BUG ON SELECT VEGETABLES UNDER LABORATORY CONDITIONS. Adam J. Formella & Thomas P. Kuhar. Department of Entomology, Virginia Tech, Blacksburg, VA. The brown marmorated stink bug (BMSB), is an invasive polyphagous pest that feeds and completes development on a variety of different vegetables. Damage to these commodities results in dimpling and corking of the fruit and can result in significant economic losses for the farmers. To better understand which vegetables these stink bugs can complete development on, the survivorship and development of BMSB nymphs was evaluated on green bean, bell pepper, eggplant, cherry tomato and sweet corn (7 reps each) in a laboratory study. Egg masses containing freshly molted second instar BMSB were collected from the field and were placed in a 30.5 cm collapsible mesh cages with one of the previously mentioned 3-4 week old plants along with their corresponding fruit and a water wick. Survivalship and development time were recorded every other day from second instar to adult. Survival to adult stage was highest on sweet corn (32.9%), followed by bell pepper (25.6%), green bean (23.6%), eggplant (5.9%) and lastly cherry tomato (1.1%). Although there was a significant difference in BMSB survivalship among these vegetables, there was no difference in the development time from second instar to adult. Results from this study will help us better understand how planting certain

vegetables can influence BMSB populations. Author contact: Adam Formella, adam4@vt.edu.

ZIKA MODULATES ARTHROPOD HISTONE METHYLATION IN MOSQUITO CELLS. Telvin L. Harrell[1], Hameeda Sultana[1,2] & Girish Neelakanta[1,2]. [1]Department of Biological Sciences, Old Dominion University, Norfolk, VA. [2]Center for Molecular Medicine, College of Sciences, Old Dominion University, Norfolk, VA. Epigenetics is the heritable series of genomic modifications that affect chromatin structure, gene expression, and protein functionality. These covalent modifications can occur on DNA, histones, and proteins through complex signaling cascades that are still being deciphered. Processes such as methylation, acetylation, ubiquination, and phosphorylation result in the addition of small molecules leading to increased gene expression/transcription, silencing, degradation, and changes in protein functionality, respectively. Such modifications however, have been documented to be extorted by pathogens upon infection. Little is known about the molecular effects Zika exerts human on Host, but even less is known about the molecular effects exerted on mosquito vectors that transmit this virus across the globe. Zika is dependent on methionine for preferential viral gene expression and replication, but the link to epigenetic regulation in vector host has yet to be explored. In this study, we examine the effects of Zika on the S-Adenosyl Methionine (SAM) cycle in C6/36 cells. We observed a forced increase the expression of C6/36 SAM synthetase during Zika infection. An increase in Zika replication also corresponded with increased S-Adenosyl methionine concentration in cell lysate that was indirectly proportional to increases of SAM in cell culture medium. Following increased SAM concentration and zika replication, we also observed an increased histone methylation, specifically on Lysine 27 of histone H3 on Day 1 post infection. Overall, this data supports the influence of Zika on the S-Adenosyl Methionine Cycle of C6/36 cells, leading to increased viral replication and Histone Methylation in vitro. Author contact: gneelaka@odu.edu

MODULATION OF VECTOR HOST CELL SIGNALING BY PATHOGENS. Girish Neelakanta, Center for Molecular Medicine, Department of Biological Sciences, Old Dominion University, Norfolk, VA. In the United States, hard ticks *Ixodes scapularis* transmits several human pathogens including *Anaplasma phagocytophilum*, the agent of Human anaplasmosis. *I. scapularis* ticks ingest *A. phagocytophilum* upon feeding on an infected vertebrate host. Upon ingestion, *A. phagocytophilum* enters gut and then colonizes salivary glands of these ticks. Several studies including our own have provided evidences that *A. phagocytophilum* modulate tick cellular signaling to survive in its vector host. In this study, recent findings from my laboratory on the modulation of organic anion transporting polypeptide and tryptophan pathway by tick-borne pathogens are disucssed. Studies such as this will provide important information in understanding the role of vector molecules in tick-pathogen interactions that will lead in the development of better strategies to target this and other medically important vectors. Author contact: gneelaka@odu.edu

ARTHROPOD EXOSOMES AS MEANS OF VIRAL TRANSMISSION. Hameeda Sultana, Department of Biological Sciences, Old Dominion University, Norfolk, VA. The

transmission strategies used by flaviviruses to exit arthropods and infect human host were envisioned as best approaches to develop transmission-blocking vaccines against molecules or determinants that facilitate pathogen transmission. Research in my laboratory has shown that both tick and mosquito-borne flaviviruses uses exosomes, the small membranous extracellular vesicles for transmission from arthropods to human host. Our studies have revealed that arthropod derived exosomes are important means of communication and transmission between the vector and the vertebrate host. We have found that Dengue virus (DENV), a flavivirus member closely related to mosquito-borne ZIKA viruses are transmitted from vector to the vertebrate host through exosomes as novel modes of transmission. The exosomes containing flaviviruses were viable, secured and highly virulent in all tests such as re-infection kinetics, trans-migration and viral plaque formation assays suggesting exosomes as favorable modes of transmission. Taking together, exosomes serves as protective security vesicles for transmission of vector-borne flaviviruses that escape the vertebrate immune system and cause pathogenesis and perhaps death. Our current efforts are focused on understanding the molecular mechanisms/associated signaling cascades in extracellular vesicles derived from arthropods and from vertebrate cells. Author contact: hsultana@odu.edu

***ANAPLASMA PHAGOCYTOPHILUM* MODULATES TICK OXIDATIVE PHOSPHORYLATION PATHWAYS**. Daniel A. Tiznado, Girish Neelakanta, Hameeda Sultana, Department of Biological Sciences, Old Dominion University, Norfolk, VA. *Anaplasma* phagocytophilum is an obligate intracellular bacterium that is typically transmitted by the tick vector *Ixodes scapularis.* Our data showed that *A. phagocytophilum* directly modulates tick oxidative phosphorylation pathway by actively downregulating the genes involved in the electron transport chain. More specifically, *A. phagocytophilum* infection in tick cells has revealed downregulation of NADH dehydrogenase and other genes. Furthermore, this trend is evident when the tick was either fed (post-feeding) or unfed. The significance of the down-regulation of NADH dehydrogenase or ATP synthase gene expression on *A. phagocytophilum* persistence in ticks is currently not understood. Therefore immediate studies will be performed to elucidate the mechanism by which *A. phagocytophilum* influence fundamental host signaling mechanism for its survival in the arthropod vector for a longer period. Author contact: dtizn001@odu.edu.

***IXODES SCAPULARIS* SRC KINASE IS REQUIRED FOR RICKETTSIAL PATHOGEN SURVIVAL**. Jeremy W. Turck, Vikas Taank, Girish Neelakanta, & Hameeda Sultana, Department of Biological Sciences, Old Dominion University, Norfolk, VA. *Anaplasma phagocytophilum* is an obligate intracellular bacterium that causes disease in humans and Cattles. *A. phagocytophilum* uses various survival strategies to infect both vertebrates and invertebrates. Ticks are the vectors for a means of infection towards other mammalian species. This bacterium has a specific path for infection through the salivary glands of its vector host and to suppress certain cellular functions such as the inhibition of apoptosis and Reactive-Oxygen-Species (ROS) production in order to increase its survival in human neutrophils. Our study identified an important signal transduction pathway that also has an impact on the spread and survival of this pathogen through the tyrosine phosphorylation of proteins. We found that non-receptor protein-tyrosine Src kinase has an impact on the spread and survival of *A.*

phagocytophilum. In *Ixodes scapularis* ticks we show that Src is downregulated in unfed ticks while blood feeding upregulates both the transcript and protein levels of Src kinase. Our inhibition data show that Src kinase is manipulated in the vector, perhaps in order to aid in its evasiveness of the host immune response. Overall, our studies revealed that Src tyrosine kinase plays an important role in *A. phagocytophilum* infection and survival of this bacterium. Author contact: hsultana@odu.edu

Posters

THE ANTS OF VIRGINIA PROJECT. Kal Ivanov, L. Hightower, & J. B. Keiper, Department of Recent Invertebrates, Virginia Museum of Natural History, Martinsville VA. Due to its geographic location, topographic variability, and diversity of physiographic provinces, Virginia ranks as one of the most biodiverse states in the US. The myrmecofauna of Virginia, however, has been insufficiently studied and is not well known. As a result, we initiated the Ants of Virginia Project in late 2014. The goal of this long-term study is to provide a comprehensive list, an up-to-date distributional information, and relevant references for the ant taxa found in the state. With recent taxonomic changes taken into account, review of the published literature revealed that 131 ant species have been previously reported from Virginia. Here we add another 30 species records based on newly collected data, review of museum and personal collections, and online databases. At present, 161 species and morphospecies, including 12 ant exotics, are reliably reported from the state. The most speciose genera in the state are S*trumigenys* (20 species), *Formica* (18), *Lasius* (11), and *Aphaenogaster* (10). Twelve species are provisionally excluded from the list as they represent distribution anomalies, or are based on erroneous records. It is our hope that this work will benefit both amateurs and professionals interested in the study of ants. Author contact: kal.ivanov@vmnh.virginia.gov

EFFICACY OF APRITONE REPELLENT ON *HALYOMORPHA HALYS*. Mika K. Pagani[1], Hayley G. Bush[2] & Thomas P. Kuhar[2], [1]Department of Environmental Science and [2]Department of Entomology, Virginia Tech, Blacksburg, VA. The invasive brown marmorated stink bug (BMSB), *Haylyomorpha Halys* (Stål), is a serious nuisance pest in human dwellings in the U.S. An effective repellent placed on buildings could help reduce the numbers of overwintering BMSB that enter homes in the fall. Prior work found geranyl cyclopentanone (apritone) to effectively repel BMSB in lab and field bioassays. In this study, we evaluated the effectiveness of apritone at different concentrations (0%, 1%, 2.5%, and 5% active ingredient) to prevent BMSB from entering box shelters containing a bell pepper fruit. The repellent was applied to kraft paper, which was then exposed to growth light overtime to determine its longevity. In a four-choice cage experiment, BMSB were released in the center of a cage with the option of entering one of four shelters that incorporated one entry point surrounded by the repellent-applied kraft paper. The number of BMSB entering each box as well as the number of feeding wounds to the pepper fruit were recorded. After the four-week study, there was no significant treatment effect on numbers of BMSB that entered the boxes, and significant BMSB feeding on all pepper fruit. Thus, although apritone has demonstrated BMSB repellency in previous studies, there was no repellency demonstrated when a food stimulus was added to an experiment. (Supported by: Bedoukian Research Inc.). Author contact: mika396@vt.edu.

Environmental Science

Not available

Medical Sciences

BODY FAT COMPOSITION AS A PREDICTOR OF ANAEROBIC EXERCISE PERFORMANCE. Andrea Medero, Kimberly A.P. Mitchell, Matthew F. Lazenka, & Ben N. Kalu, Dept. of Biology and Chemistry, Liberty University. Aerobic activity is high intensity exercise where the muscles do not depend on the presence of oxygen for contraction. The purpose of this study was to determine the relationship between body fat composition and anaerobic activity. There were ten females and seven male participants with an average age of 25.41 years. Participants consented to an InBody analysis and 30 second Wingate anaerobic test. The InBody analysis provided information regarding body fat mass (BFM), and percent body fat (PBF), while the Wattbike provided measurements of average power, and fatigability. There was a significant negative correlation between PBF and average power, $r(15)=0.90$ with a regression equation of $F(1,15)=62.66$, $p=<.001$, $r^2=0.81$. There was a significant negative correlation between BFM and average power $r(15)=0.78$ with a regression equation of $F(1,15)=23.90$, $p=<.001$, $r^2=0.61$.The relationships between BFM and fatigability, and PBF and fatigability were non-significant with negative correlations. PBF and BFM can be used as strong predictors of average power, with PBF having a stronger correlation with average power than BFM. Author contact: Andrea Medero, amedero@liberty.edu

FOXC2 IS A KEY REGULATOR OF MELANOMA CELL ADHESION TO THE EXTRACELLULAR MATRIX AND LYMPHATIC ENDOTHELIAL CELLS. Coleman E. Johnson & Kristian M. Hargadon, Dept. of Biol., Hampden-Sydney College. Melanoma is a highly aggressive form of skin cancer characterized by its propensity to invade regional lymph nodes and metastasize to other vital organs. We have recently demonstrated that the FOXC2 transcription factor plays a key role in lymph node invasion by melanoma cells To gain insights into this phenomenon, we assessed how disruption of the *Foxc2* gene in the B16-F1 melanoma cell line influences tumor cell adhesion to extracellular matrix (ECM) proteins and lymphatic endothelial cells. We also investigated how overexpression of the FOXC2 transcription factor regulates these processes in the D5.1G4 melanoma cell line that normally expresses the *Foxc2* gene at low levels. Disruption of the *Foxc2* gene in B16-F1 melanoma increased tumor cell adhesion to the ECM proteins fibrinogen and fibronectin while decreasing tumor cell adhesion to SV-LEC lymphatic endothelial cells, suggesting that in wild-type B16-F1 cells FOXC2 promotes loss of adhesion to the ECM and improved adherence to lymphatic endothelium. Interestingly, we observed the opposite phenomenon in D5.1G4 melanoma cells, where overexpression of FOXC2 enhanced tumor cell adhesion to fibrinogen and fibronectin. These data indicate that FOXC2 is a key regulator of tumor cell adhesion but that factors that remain to be explored, such as subcellular localization of FOXC2, ultimately dictate its gene regulatory functions . (Supported by: Commonwealth Health Research Board, Jeffress Trust Awards Program in

Interdisciplinary Research, H-SC AV Davis Endowment, and Mr. Michael Hargadon & Mrs. Patricia Hargadon). Author contact: JohnsonC19@hsc.edu .

FOXC2 REGULATES EXPRESSION OF THE INTEGRINS ITGA5 AND ITGA9 IN MELANOMA. Corey J. Williams & Kristian M. Hargadon, Dept. of Biol., Hampden-Sydney College. Melanoma is a highly aggressive cancer derived from melanocytes of the skin. Using a murine model system, we have previously shown that the FOXC2 transcription factor is overexpressed in the highly aggressive B16-F1 melanoma cell line as compared to the poorly tumorigenic D5.1G4 melanoma cell line and that disruption of the *Foxc2* gene in B16-F1 melanoma limits the outgrowth and lymph node invasive potential of this tumor. To better understand how FOXC2 regulates melanoma progression, we investigated how *Foxc2* gene disruption in B16-F1 melanoma and FOXC2 overexpression in D5.1G4 melanoma influence the expression of cell adhesion molecules that might influence tumor progression. Our findings show that melanoma-associated FOXC2 regulates the expression of the integrins ITGA5 and ITGA9. Interestingly, while FOXC2 down-regulated expression of ITGA5 and ITGA9 in B16-F1 melanoma overexpression of this transcription factor in D5.1G4 melanoma promoted expression of these same integrins, suggesting that FOXC2-mediated regulation of ITGA5 and ITGA9 may ultimately be determined by the subcellular localization of this transcription factor. (Supported by: Commonwealth Health Research Board, Jeffress Trust Awards Program in Interdisciplinary Research, Hampden-Sydney College A.V. Davis Endowment, and Mr. Michael Hargadon & Mrs. Patricia Hargadon). Author contact: williamscj19@hsc.edu

CORRELATION BETWEEN BODY MUSCLE COMPOSITION AND POWER, FATIGUE AND CADENCE PRODUCED DURING THE WINGATE ANAEROBIC TEST. Emily J. Pocius, Kimberly A. P. Mitchell, Matthew F. Lazenka & Ben N. Kalu, Dept. of Biology & Chemistry, Liberty University. Athletic performance in many high intensity sports is dependent upon anaerobic exercise. To study how best to improve anaerobic exercise, we examined the correlation between body muscle composition and anaerobic physical performance: specifically, the power produced, the fatigue experienced, and the cadence performed by the participants. The results were collected with ten female participants and seven male participants, ranging from 22-33 years of age. Lean body mass, dry lean mass, and skeletal muscle mass were measured using an Inbody 770 analyzer.

A modified Wingate test was performed on a Wattbike Cycle Ergometer to analyze the participants' power, fatigue and cadence during anaerobic exercise. Using a correlation with regression analysis we found that skeletal muscle mass was the best predictor of anaerobic performance and had a significant positive correlation with average power, , $r(15)=0.50$ with a regression equation $F(1,15)=4.89$, $p=0.05$, $r^2=.25$; and fatiguability, $r(15)=.61$ with a regression equation $F(1,15)=8.95$, $p=0.05$, $r^2=.37$. These correlations between body muscle composition and anaerobic athletic performance can aid in optimizing athletic training. Author contact: Emily Pocius , ejpocius@liberty.edu

ROLE OF MU-OPIOID AGONIST EFFICACY ON ANTINOCICEPTIVE INTERACTIONS BETWEEN MU-OPIOID AGONISTS AND THE NOCICEPTIN

OPIOID PEPTIDE RECEPTOR AGONIST RO 64-6198 IN RHESUS MONKEYS. Jeremy C. Cornelissen & Matthew L. Banks, Dept. of Pharmacology & Toxicology, Virginia Commonwealth University. Mu-opioid receptor (MOR) agonists are effective for pain management, but also limited by undesirable effects including sedation. One approach to enhance the therapeutic effects and minimize the undesirable effects of MOR agonists may be to combine MOR agonists with an adjunct targeting a different receptor system. The nociceptin opioid peptide (NOP) receptor system has emerged as one possible target. The present study determined whether MOR agonist efficacy was important for MOR/NOP antinociceptive interactions. Rhesus monkeys (*Macaca mulatta*) were utilized in a warm water tail-withdrawal procedure (n=3-4) to assess antinociceptive effects and an assay of schedule-controlled responding (n=3-4) to assess sedative effects. Six MOR agonists (NAQ<buprenorphine<nalbuphine<morphine<oxycodone<methadone) that varied in *in vivo* efficacy were evaluated alone and following pretreatment with the NOP agonist Ro 64-6198. Buprenorphine, nalbuphine, morphine, oxycodone, and methadone alone produced dose-dependent antinociception. Nalbuphine, morphine, oxycodone, and methadone alone also produced dose-dependent behavioral suppression. Ro 64-6198 pretreatment selectively potentiated the antinociceptive potency of buprenorphine, nalbuphine, and methadone under a narrow range of experimental conditions. Results suggest limited clinical utility of MOR/NOP agonist combinations for pain management. (Supported by NIH DA037287 and DA007027, VCU). Author contact: cornelissejc@vcu.edu

EFFECTS OF CAFFEINE CONSUMPTION ON ANAEROBIC EXERCISE PERFORMANCE UTILIZING THE WINGATE TEST. Joshua E. Ibanez, Ben N. Kalu, Kimberly A. Mitchell & Matthew F. Lazenka, Dept. Of Biol., Liberty University. The proposed propensity of caffeine to elicit ergogenic effects among athletes has been widely debated. While some studies have shown evidence of its effectiveness on athletic performance, other reports suggest its impact on exercise is negligible. This study aims to evaluate the ergogenic effects of caffeine on anaerobic exercise performance. The study was conducted with 13 volunteers (6 males and 7 females) assessing their anaerobic exercise performance using the 30s Wingate Test on a Wattbike. Our hypothesis was that caffeine would increase average power and decrease modified fatigue factor. Our results showed that caffeine significantly increased power output in the last 5s of the test $t(13) = 3.099$, $p=0.009$. Modified fatigue factor (%) was significantly decreased with caffeine intake; $t(13)=-2.60$, $p=0.023$. <0.05 Total power and power average over 30 seconds showed no statistically significant increases, but both results showed a trend of increase in the experimental group vs. control. Based on this association we can infer that anaerobic athletic performance would improve with caffeine intake. While further investigation is needed with a larger population size, studies into the ergogenic effects of caffeine versus its metabolic half-life could determine how long these effects last and further aid in sports that increase oxygen deficit and require anaerobic respiration. . Author contact: Joshua Ibanez, jeibanez@liberty.edu

THE IMPACT OF CHRONIC ADOLESCENT STRESS ON THE ADULT STRESS RESPONSE. Jacqueline Ninkundiye[1], Molly M. Hyer[1], Sydney Rowson[2],

Samya Dyer[1], Mandakh Bekhbat[1,2], & Gretchen N. Neigh[1]. [1]Department of Anatomy and Neurobiology, Virginia Commonwealth University and [2]Neuroscience Graduate Program, Emory University. Stress-induced depression can cause alterations in the hypothalamic–pituitary–adrenal (HPA) axis which regulates the stress response. Chronic adolescent stress (CAS) can cause long term effects on the HPA axis. Activation of the HPA axis causes elevated concentrations of corticosterone - the primary hormone released during the stress response – in a sex-dependent manner. In our experiment, we used male and female non-stressed and stressed Wistar rats to examine how CAS impacts the adult response to an acute stressor – the forced swim test (FST). Performance in the FST assesses depressive-like behavior by quantifying patterns of mobility – more immobility is indicative of more depression. We hypothesized that CAS would increase immobility in the FST. Blood was collected to determine the concentrations of corticosterone 15, 30, or 120 minutes after the FST. Our hypothesis was that non-stressed rodents who underwent the FST would present increased concentrations of corticosterone immediately following the FST, but then quickly return to baseline concentrations. For rats that underwent CAS, we expected a similar initial peak followed by a prolonged elevation of corticosterone. This work can provide a better understanding of the mechanisms that link stress to depressive behavior while accounting for sex differences that can impact presentation as well as response to treatment. R25GM102795. Author contact: jn22137@email.vccs.edu

MODELING THE INTERACTION OF F-ACTIN FILAMENTS. Melissa A. Riddle & Callie Miller, James Madison University. F-actin networks have different structures throughout the cell depending on f-actin location or their mechanical role. For example, at the leading edge of a migrating cell, F-actin is organized in the lamellipodia as a branched network responsible for pushing the membrane outwards. Behind the lamellipodia is a lamellar actin network where focal adhesions and stress fibers originate, and then within the cell cortex, actin is arranged in a gel-like network. Stress fibers are an important organization of F-actin and how they arise from either the branched lamellipodia network or the gel-like cortex network is poorly understood. Our approach is to create a computational simulation to model a mechanism of spontaneous parallel bundling by specifically modeling the interaction of two cylindrical rods (individual F-actin filaments). We have created a 2D simulation of two cylindrical rods in MATLAB that "bump" into each other at the plus ends. We specify the initial speeds of the rods, and plot their location after impact based on the principles of linear momentum. Our method and approach will allow us to integrate the interaction of F-actin into previously published emergent models for F-actin dynamics to further prove or disprove the spontaneous emergence of parallel F-actin filaments from the gel-like cell cortex. Grant aid provided from the Department of Engineering, James Madison University. Author contact: Melissa Riddle, riddlema@dukes.jmu.edu

EFFECTS OF RED BULL CONSUMPTION ON COMMON CAROTID ARTERY BLOOD FLOW. Kanika Khanna, Ben N. Kalu, Matthew F. Lazenka, & Kimberly A.P. Mitchell, Department of Biology and Chemistry, Liberty University. Our study assessed the effect of caffeine ingestion on common carotid artery (CCA) blood flow. Vasodilation due to adenosine inhibition of excitatory neurotransmitter release may be

the trigger for migraines. Since caffeine is an adenosine receptor antagonist, and therefore will block the effects of adenosine and cause vasoconstriction, we hypothesized that blood flow would decrease in the CCA. Eight participants ingested 12oz of Red Bull Energy Drink, and after 30 minutes, the peak systolic velocity (PSV) and end diastolic velocity (EDV)
were measured at proximal and distal locations of the left and right CCA using Doppler ultrasound. While we saw a significant decrease in EDV and PSV in the right distal CCA ($p < 0.05$), there was an increase in blood flow seen in the left distal. Interestingly, EDV in the left and right proximal CCA decreased while PSV increased at those locations. Though our results do not support our hypothesis, they do support a selective decrease in blood flow through the distal right CCA, and further research on this topic may give us more insight as to how caffeine could help relieve pain from migraines. Author contact: Kanika Khanna, kkhanna@liberty.edu

ROLE OF EPIGENETIC REMODELING IN SENSITIZING TRIPLE-NEGATIVE BREAST CANCER CELLS TO TREATMENT THROUGH ENHANCED CHEMOTHERAPY-INDUCED AUTOPHAGY. Liliya Tyutyunyk-Massey, Nga Dao, Syed Haqqani, Joseph Landry & David Gewirtz, Virginia Commonwealth University. Dysregulation of the epigenome is implicated in initiation and progression of variety of cancers and their resistance to chemotherapy. Targeting epigenetic regulators can modulate cancer cell biology and sensitivity to chemotherapy and/or radiation. Our studies demonstrate that silencing of the epigenetic regulator Nucleosome Remodeling Factor (NURF) sensitizes breast tumor cells to chemotherapy and enhances the anti-tumor immune response. NURF knock down (KD) cells are sensitized to doxorubicin and etoposide, as well as paclitaxel. NURF KD increases DNA damage and autophagy in cells exposed to doxorubicin (Dox) and enhances growth inhibition. Increased autophagy as well as sensitization to Dox were observed using a small molecule inhibitor of NURF, suggesting that NURF can also be targeted pharmacologically. Our studies suggest that enhanced autophagy may be a primary contributor to chemo-sensitivity in NURF KD cells. Studies are underway to confirm the role of autophagy in enhanced immune response *in vivo* using autophagy deficient cells (through ATG silencing). Increased cell autonomous antitumor effects and increased cell immunogenicity could help to achieve tumor regression and possibly promote long term remission in breast cancer. Author contact: tyutyunykmals@vcu.edu

GENE CO-EXPRESSION IN 2 AND 24 MONTH MOUSE CD3+ SPLENOCYTES: A NETWORK APPROACH. Megan L. Mair & Tarynn M. Witten, Center for the Study of Biol. Complexity, Va. Commonwealth Univ. Gene co-expression networks (GCNs) were derived for 130 immune-related genes obtained from CD3+ splenocytes extracted from mice at ages 2 and 24 months. Structure of the two age-group networks was analyzed in order to understand potential age-related changes in network properties and their influence on immunosenescence. The GCN constructed for the 2 month old mice was composed of 64 nodes and 85 edges, while the GCN for the 24 month old mice had 102 nodes and 302 edges. Power curve analysis demonstrated the younger mouse GCN followed a power law behavior implying small world structure, while the older mouse group showed a weak power law behavior. The small world network structure of

the young CD3+ cells indicates the transcription of genes is tightly regulated within the splenocytes of 2 month old mice. Weak small world dynamics of the 24 month old mouse GCN suggest that this control is decreased with age. This finding has implications for the regulatory behavior of genes in older T cells. Gene co-expression correlates with a number of biological processes, including cell signaling, protein complex formation, and transcription pathways. That the 24 month old mouse GCN sees an increase in correlation at the expense of more robust network structures suggests T cell regulation and immune behavior is diminished, indicating the need for further investigation into gene regulation in older T cells. Author contact: mairml@vcu.edu

MODELING THE INTERACTION OF F-ACTIN FILAMENTS. Melissa A. Riddle & Callie Miller, Dept. of Engineering, James Madison University. F-actin networks have different structures throughout the cell depending on f-actin location or their mechanical role. For example, at the leading edge of a migrating cell, F-actin is organized in the lamellipodia as a branched network responsible for pushing the membrane outwards. Behind the lamellipodia is a lamellar actin network where focal adhesions and stress fibers originate, and then within the cell cortex, actin is arranged in a gel-like network. Stress fibers are an important organization of F-actin and how they arise from either the branched lamellipodia network or the gel-like cortex network is poorly understood. Our approach is to create a computational simulation to model a mechanism of spontaneous parallel bundling by specifically modeling the interaction of two cylindrical rods (individual F-actin filaments). We have created a 2D simulation of two cylindrical rods in MATLAB that "bump" into each other at the plus ends. We specify the initial speeds of the rods and plot their location after impact based on the principles of linear momentum. Our method and approach will allow us to integrate the interaction of F-actin into previously published emergent models for F-actin dynamics to further prove or disprove the spontaneous emergence of parallel F-actin filaments from the gel-like cell cortex. Grant aid provided from the Department of Engineering, James Madison University. Author contact: Melissa Riddle, riddlema@dukes.jmu.edu

ENZYMOLOGY AND INHIBITION STUDIES OF THE L205R MUTANT OF cAMP-DEPENDENT PROTEIN KINASE. Nicole Luzi, Darrell Peterson, & Keith C. Ellis, Department of Medicinal Chemistry, Virginia Commonwealth University. Cyclic-AMP dependent protein kinase (PKA) is involved in many biological processes and is made up of four subunits: two regulatory and two catalytic subunits. When the catalytic subunits are released they engage in phosphorylation events leading to the production of cortisol. When PKACα undergoes a single amino acid change in the substrate-binding site, the L205R-PKACα protein becomes constitutively active leading to increased cortisol production in a subset of ACTH-Independent Cushing's Syndrome patients. In order to develop selective inhibitors of the L205R-mutant, we need to study the kinetics and inhibition from known PKA inhibitors of both wt- and L205R-PKACα prior to testing novel compounds. The kinetics of the substrate-binding site for both wt- and L205R-PKACα were determined using a novel, fluorophore-labeled substrate peptide in a endpoint assay followed by detection of substrate and product by HPLC. This assay allowed for direct determination of K_M for both proteins. The K_M[peptide] for L205R-PKACα was determined to be 6-fold higher compared to wt-PKACα. The K_M[ATP] for

the mutant was determined to be ~1.6-fold higher compared to the wild-type enzyme. In our inhibition studies using the same assay, the IC_{50} of H89 was equipotent against both proteins ($IC_{50} \cong 62$ nM). The IC_{50} for PKI(5-24) was found to be 250-fold higher against L205R-PKACα ($IC_{50} \cong 1800$ nM) compared to wt-PKACα α ($IC_{50} \cong 7$ nM). Work developing L205R selective inhibitors will also be presented. Author contact: nluzi035@gmail.com

DEVELOPMENT OF PROTEIN DEGRADATION PROBES (PROTACS) FOR MIS-REGULATED ISOFORMS OF PKACα. Nicole Luzi & Keith C. Ellis, Department of Medicinal Chemistry, Virginia Commonwealth University. Proteolysis degradation chimeras, or PROTACs, are synthetic compounds that induce protein degradation. PROTACs are composed of two binding ligands bound together by a linker. One ligand binds to the target protein of interest, while the other ligand binds an E3 ligase. When these compounds bind to both the target protein and the E3 ligase, the E3 ligase complex will ubiquitinate the target protein, which is then recognized by the proteasome and degraded. Our goal is to design a PKACα PROTAC by utilizing the ATP-competitive small molecule inhibitor H89 to bind PKACα and the immunomodulatory small molecule pomalidomide to bind to the E3 ligase cereblon. Synthesis of the pomalidomide fragment has been performed in two high yielding steps affording a glycine-substituted pomalidomide fragment. The synthetic plan for making the H89 fragment is to synthesize two smaller fragments: an isoquinoline fragment and an amino styrene fragment. To synthesize the isoquinoline fragment, isoquinoline-5-sulfonic acid was converted to the sulfonyl chloride followed by a substitution with aminoacetaldehyde dimethyl acetal. Synthesis of the amino styrene fragment utilized a Wittig reaction and the completed fragment is being reacted with the isoquinoline sulfonamide aldehyde in a reductive amination reaction to obtain the completed H89 fragment. The H89 fragment and pomalidomide fragment will then be appended together using an aliphatic linker. Once completed, the PROTAC will be tested in various biological assays. Author contact: nluzi035@gmail.com

ACTIVITY, STABILITY AND STRUCTURAL STUDIES OF G2.2, A SMALL MOLECULE SELECTIVE INHIBITOR OF CANCER STEM CELLS. Shravan Morla, Elsamani Abdelfadeil, Daniel K. Afosah & Umesh R. Desai, Dept. of Med. Chem. & ISB3D, VCU. We recently discovered that a novel non-saccharide GAG-mimetic, G2.2, demonstrates highly selective cancer stem-like cells (CSCs). To advance its in-vivo anti-cancer potential, we obtained 20g of material from contract research organization (CRO). Evaluation of CRO-synthesized G2.2, labelled as G2.2CRO, in HT-29 xenograft mouse model showed significant reduction in tumor volume and CSC markers, as expected, but unexpected bleeding. Similar studies with G2.2 synthesized in our laboratory, labelled as G2.2Lab, had shown no bleeding effects. To investigate the difference between the two samples (G2.2Lab and G2.2CRO) we performed UPLC-MS characterization and found that G2.2CRO was actually a 85:15 mixture of two compounds. Elemental, NMR and MS data showed that G2.2Lab was fully sulfated flavonoid derivative, as expected, but G2.2CRO's 15% contaminant contained one less sulfate group. We tested both agents for their inhibition of various coagulation factors and found that G2.2CRO inhibited FXIa 2-fold better than G2.2Lab. Activated partial

thromboplastin time assay indicated that G2.2Lab is 3-4-fold less anticoagulant than G2.2CRO. This implied that a loss of just one sulfate induced significant side effects and prompted to us to conduct additional studies on G2.2Lab sample to access its stability. We found that G2.2Lab sample is stable, and doesn't lose sulfate groups, at 37°C over a wide range of pH (4-9) for at least 72 hours. These results show that subtle structure-activity relationships and challenges in synthetic chemistry are important to understand. Author contact: morlas@vcu.edu

CAFFEINE AND ALTITUDE AFFECT CARDIAC AUTONOMIC REGULATION. Vhuthuhawe T. Madzinge & Michael Broussard, Dept. of Biology and Chemistry, Liberty Univ. The heart is innervated by the sympathetic cardiac plexus to increase heart rate and force of contraction, and by the parasympathetic vagus nerve to decrease heart rate and force of contraction. The study was conducted on the effects of altitude-induced hypoxia and caffeine (sympathetic stimulants) on heart rate variability (HRV), which is a noninvasive evaluation of the balance between the parasympathetic and sympathetic responses. HRV, the standard deviation of normal RR intervals (SDRR), evaluates the balance between the sympathetic component - low-frequency (LF) and the parasympathetic components, namely the root mean square of RR intervals (RMSSD), high-frequency (HF), and the percentage of normal RR intervals that differ by 50ms (pRRx%). A crossover trial was conducted to measure HRV at 4000m before and after the consumption of 200mg of caffeine using a CAT altitude chamber. We hypothesized an increase in HRV. The data was analyzed using a two-tailed t-test. The results indicated that caffeine consumption at 4000m decreased HR ($t(13) = 1.252$) but increased SDRR ($t(13) = -0.496$). RMSSD ($t(13) = -1.353$) and pRRx% ($t(13) = -1.1339$) decreased at 4000m and increased with caffeine consumption at 4000m. Also LF/HF ($t(13) = 0.721$) increased at 4000m, but decreased with caffeine consumption at 4000m compared to baseline. These results indicate that HRV increases when the sympathetic nervous system is overstimulated; however, this also suggests complications may arise with individuals with cardiovascular diseases. Author contact: vmadzinge@liberty.edu

Natural History and Biodiversity

MERGENCE OF ALTERNATIVE MALE MORPHOTYPES IN BLUEGILL SUNFISH (*LEPOMIS MACROCHIRUS*) MASKS DIFFERENCES IN PARASITISM. Candace E. Ashworth & Michael R. Zimmermann, Dept. of Biol., Shenandoah University. Bluegill sunfish (*Lepomis macrochirus*) are a sexually dimorphic sport fish distributed throughout North America. Additionally, there are multiple male morphotypes that exhibit differences in territoriality, diet, and behavior. The larger size of α-males results in dominance in these aspects, in addition to enhancing their reproductive success, as they invest heavily in courtship and parental care. Contrarily, subordinate β-males partake in mutant mating strategies in which they either participate in sneaking or mimicking behaviors in order to gain access to the α-male nests. These distinct morphotypes have not been factored into previous studies regarding parasitism in *L. macrochirus*. This study investigated whether these behavioral differences influenced parasitism and if combining these morphotypes, as has been done

in previous studies, actually masks potential differences between sexes of *L. macrochirus* hosts. In total, 1,257 *L. macrochirus* were collected from 13 lakes and ponds in northwestern Virginia and assessed for parasites infecting the different morphotypes. Significant differences in parasite abundance between male morphotypes were observed in 13 parasite species, while differences between at least one male morphotype and females was found in 16 parasite species. Conversely, when the male morphotypes were combined, only 3 parasite species differed between males and females, indicating that combining male morphotypes in analyses of parasitism in *L. macrochirus* actually masks the differences, not only between the male morphotypes, but between sexes. Future studies regarding parasitism in *L. macrochirus* must take the male morphotypes into account because combining them may result in missing key explanatory variables. Warrington 2018 Grant. Author contact: Candace E. Ashworth, cashwort16@su.edu

A STREAM CONTINUUM ANALYSIS OF BACTERIA COMMUNITY ASSEMBLY IN ASSOCIATION WITH CRAYFISH AND THEIR SYMBIONTS. Matthew Cooke, Luke Fischer, Kaleb Bohrnstedt, Thomas Keplar, Matthew Becker, and Kyle Harris, Liberty University. Microbial community assemblages have long been understood as key components within freshwater ecosystems. However, patterns of microbial presence and persistence along stream continuums, in relation to specific host organisms, have been understudied. One such pattern involves microbial assemblages on crayfish with ectosymbionts (branchiobdellidans). In this study, patterns of microbial community assembly in the stream environment (water and sediment) and on crayfish in a local stream are evaluated. It is hypothesized that the presence of ectosymbionts will influence patterns and persistence of microbial assemblages. Bacterial samples from crayfish and the environment were collected using aseptic technique at five different collection sites along Opossum Creek in central Virginia. DNA was extracted using a Qiagen Blood and Tissue Kit and qPCR was performed for quantitative analysis of microbial abundance. Initial qPCR results suggest that stream order, location, and other environmental factors may have effect on microbial abundance. PCR for microbial 16s gene amplification, and bioinformatics analysis with QIIME is being used to look for patterns in relation to microbial assemblages with crayfish ecotosymbionts. Author contact: Kyle Harris, kjharris@liberty.edu

PEN TRIAL OF ESTROGEN-INDUCED EGG AVERSION IN RACCOONS (*PROCYON LOTOR*). Raymond D. Dueser[1,2,3], Joel D. Martin[1], & Nancy D. Moncrief[3], [1]Dept. of Wildland Resources, Utah State Univ., Logan, UT 84322, [2]Virginia Museum of Natural History, Martinsville, VA 24112, and [3]Dept. of Environmental Sciences, Univ. of Virginia, Charlottesville, VA 22904. Aversive conditioning is a promising but unproven non-lethal approach to reducing mammalian predation on the eggs of ground-nesting birds, terrapins, and sea turtles. We tested the efficacy of oral estrogen (17 alpha-ethinyl estradiol) deployed in chicken eggs as an aversive agent for raccoons (*Procyon lotor*). Nine treatment raccoons received 6 treated eggs (injected with 10 mg of estrogen) every other day for 14 days, followed by a combination of 2 treated and 4 untreated eggs every other day for 14 days. Nine control animals received 6 untreated eggs on the same schedule. None of the 9 treatment animals showed signs of illness immediately following estrogen ingestion. Nevertheless, all became averse and reduced egg consumption by

50% after 1-8 feedings. The control animals ate 99.7% of all eggs presented and never reduced egg consumption. The aversion was neither absolute (1 treatment animal ate 91.7% of the 84 eggs presented) nor persistent (all of the animals later "sampled"). Raccoons could not distinguish between treated and untreated eggs. We observed no changes in behavior and no detrimental health effects, except for the death of 1 pregnant female, which was almost certainly a consequence of the estrogen. These results suggest that a full-scale field trial of estrogen is likely to be productive under circumstances where all of the target population is subject to treatment. Author contact: Nancy Moncrief, nancy.moncrief@vmnh.virginia.gov

SURVEILLANCE OF FUNGAL AND VIRAL PATHOGENS IN VIRGINIA HERPETOFAUNA. Rachel M. Goodman, Biol. Dept., Hampden-Sydney College. I summarize findings of surveys for herpetofauna and two associated pathogens in Prince Edward County, Virginia. Students, collaborators, and I found 10 species of amphibians and 16 species of reptiles during formal and informal surveys. We sampled tissues and collected skin swabs from the five most common frogs, *Lithobates catesbeianus*, *Pseudacris crucifer*, *Anaxyrus fowleri*, *Lithobates palustris*, *Acris crepitans*, and five most common reptiles, *Chrysemys picta*, *Sternotherus odoratus*, *Terrapene carolina*, *Sceloporus undulatus*, and *Carphophis amoenus*. We conducted DNA tests for presence of two emerging infectious diseases, ranaviruses (which infect both taxa) and the fungus *Batrachochytrium dendrobatidis* (Bd; which only infects amphibians). Among amphibians, we found no evidence of ranaviruses. We found Bd in three of five frog species and at each of three water bodies sampled. Prevalences were 5.6%, 9.5%, and 17.2% in *L. palustris*, *A. crepitans*, and *P. crucifer*. Among reptiles, we detected ranavirus in three of five species, with prevalences of 22.0%, 36.1%, and 20.0% in *C. picta, T. carolina,* and *S. undulatus*. We did not detect ranaviruses in *S. odoratus*, possibly due to our sampling method. Standard genetic protocols for ranavirus testing did not work for our single snake species, *C. amoenus*. These surveys supplement existing range information for species that were known to carry and suffer mortality from Bd and ranaviruses. Additionally, we documented the first occurrence of ranaviruses in a wild, terrestrial lizard population. Author contact: Rachel Goodman, rgoodman@hsc.edu

FUNCTIONAL CORRELATION BETWEEN PREDATOR ESCAPE PERFORMANCE AND MATERIAL PROPERTIES OF THE VERTEBRAE IN YELLOW PERCH, *PERCA FLAVESCENS* (PISCES: PERCIDAE): INTRASPECIFIC DIVERGENCE IN FUNCTIONAL DESIGN. Takashi Maie, Dept. of Biol., Lynchburg College. Bones in teleosts are not prone to exchange calcium for homeostatic regulation, but can respond to changes in mechanical loads through adaptive modeling and remodeling. The teleost vertebral column experiences the mechanical loads as strain-related stimuli from not only steady undulatory motion of the body but also the most vigorous behavior during predator-prey interactions (C-start behavior). Using highspeed videography, kinematics and performance of the escape response in *P. flavescens* from two distinct habitats (a spring-fed lake vs. a mining-influenced lake) were examined. Material properties of their vertebrae were examined for evaluating how the mechanical capacity of the vertebrae would contribute to locomotor biomechanics in *P. flavescens* naturally exposed to the different environmental

conditions. This study presents evidence of intraspecific divergence in kinematics and performance of predator escape responses in *P. flavescens*. The results suggest that the vertebral bones, through adaptive modeling and remodeling, increase mineralization and Young's modulus regardless of ambient calcium bioavailability. Elevated material properties, such as strength and Young's modulus, would augment recoilability of the vertebral column, and consequently, increase angular velocity and acceleration during the escape response. In addition, decreased visibility of the water may be indirectly inducing the adaptive response in skeletal structures that contribute to locomotor performance in *P. flavescens*. Author contact: Takashi Maie, maie.t@lynchburg.edu

G.I.S MAPPING IN THE BIG HORN BASIN OF WYOMING. Natalie A. Romine, David R. Perault, & Brooke W. Haiar, Department of Environmental Science, Lynchburg College. The Morrison Formation is a Late Jurassic aged rock deposit that houses a diverse flora and fauna. The Two Sisters Quarry is located in the Morrison Fm. near Greybull, Wyoming. Excavations of sauropod dinosaur material have been uncovered from this quarry for over 10 years. Using Esri GIS and Adobe Illustrator, I created a map of the recovered elements from the 2016 field season. I first used field pictures and traced the bones using Illustrator, then uploaded those images onto Esri GIS to create a map. The purpose of this project is to allow future excavators to be able to predict where certain bones may be, and see the position that the sauropod was in when it died. This summer, I am going back to Wyoming and hope to apply my research there. Author contact: Natalie Romine, romine_n@lynchburg.edu

Psychology

Not available

Structural Biology, Biochemistry and Biophysics

DESMOPLAKIN AC MUTATIONS' AFFECT ON STRUCTURE AND STABILITY OF ITS NH2-TERMINUS. Taylor L. Albertelli[1], Heather Manring[2], Maegen A. Ackermann[2], Stuart Campell[3] & Nathan T. Wright[1], [1]Department of Chemistry & Biochemistry, James Madison University, 901 Carrier Dr, Harrisonburg, VA 22801, [2]Department of Physiology & Cell Biology, The Ohio State University, 333 W. 10th Ave, Columbus, OH 43210, [3]Department of Biomedical Engineering, Yale University, New Haven, CT 06520. Desmoplakin is a large (260 kD) protein in the desmosome, a subcellular structure that links the cytoskeleton of one myocyte to that of its neighbor. In the heart, the desmosome works to propagate the contractile force and allows for the synchronized, strong contractions of the human heart. The N-terminal third of desmoplakin is composed of multiple tandem spectrin repeat (SR) domains, with a single SH3 domain positioned on top of one of the SR domains. Previously published studies suggest that this SH3 domain may be a hotspot for variants linked to arrhythmogenic cardiomyopathies (AC). While some of these variants are associated with decreased amounts of desmoplakin protein, their molecular mechanism of action remains undefined. Here, we examine these specific variants *in silico* and *in vitro*. CD and fluorescence analysis show that these mutations do not significantly perturb the global desmoplakin structure and stability. However, MD simulations suggest significant

changes to local stabilizing interactions within the SH3 domain. Thus, these studies provide a compelling molecular mechanism of action for at least a subset of AC cases. (Supported by: Research Corporation, NSF REU CHE-1461175 & NSF RUI MCB-1607024). Author contact: Taylor Albertelli, alberttl@dukes.jmu.edu

PERSISTENCE OF KEY LONG-RANGE INTERACTIONS DURING GB1 UNFOLDING SIMULATIONS. John T. Bedford, Jennifer Poutsma, & Lesley H. Greene, Old Dominion University. One of the essential components of life is that of proteins. They are responsible for a plethora of different functions and as such need to be both structurally stable and functionally flexible. Long-range interactions help to achieve this duality. We define a long-range interaction as one that is shared between two amino acids that are separated by seven or more residues in the primary structure and are within five angstroms in the tertiary structure. We hypothesize that a sub-set of these long-range interactions are key to determining the overall structure, function, and stability of a protein. The immunoglobulin-binding domain of protein G (GB1) was selected as our model protein because it is a small, 56 residue protein comprised of one α-helix and one four-stranded β-sheet that are symmetrical. Four molecular dynamics simulations were ran to assess the persistence of long-range interactions. We define persistence as the likelihood for a long-range interaction to be present at any point during a simulation. Upon analysis of all 72 long-range interactions in GB1 it was determined that 19 were highly persistent. In comparison with pre-existing experimental data from Baker and co-workers (U. Washington), it seems that the residues comprising these long-range interactions are involved more with protein stability than the protein folding process. Author contact: jbedford@odu.edu

A COMPUTATIONAL STUDY OF ASPARAGINE 79 IN UBC13. Katherine L. Elliott & Isaiah Sumner. Department of Chemistry and Biochemistry, James Madison University. Ubiquitin (Ub) is a regulatory protein with the ability to flag proteins to be degraded. Ub is covalently attached to a lysine on the target protein by a series of reactions catalyzed by three types of enzymes: ubiquitin activating enzymes, E1; ubiquitin conjugating enzymes, E2; and ubiquitin ligases, E3. We are using molecular dynamics (MD) and QM/MM simulations to elucidate the mechanism of the E2 enzyme, Ubc13, which forms polyubiquitin chains. Our MD simulations contradict a popular hypothesis that a conserved asparagine in Ubc13 stabilizes a reaction intermediate. Instead we show this is unlikely unless an E3 is present. Furthermore, we show with QM/MM that a conserved glutamic acid in the target ubiquitin and a conserved aspartic acid in Ubc13 are equally likely to deprotonate the substrate lysine. (Supported by the National Science Foundation Research Experience for Undergraduates (NSF-REU) grant number CHE-1461175, The Thomas F. and Kate Miller Jeffress Memorial Trust, Bank of America, N.A., Trustee, and the James Madison University Department of Chemistry and Biochemistry). Author contact: sumneric@jmu.edu

INVESTIGATION OF THE REUSABILITY OF AFFINITY COATED SURFACES FOR CELL CAPTURE AND ANALYSIS. Eric Hurwitz, Tara Anderson, and Randall D. Reif, Department of Chemistry, University of Mary Washington, Fredericksburg, VA, 22401. The use of affinity-coated surfaces to

immobilize cells is commonly applied to cellular separations and microfluidic devices. The goal of this study was to assess the reusability of affinity coated microfluidic devices previously used to capture Jurkat T-lymphocytes for real-time analysis. The reusability of the affinity surface of these microdevices was assessed by measuring the binding efficiency (number of cells bound post-wash/number of cells bound pre-wash) after cleaning the devices with various reagents. Results indicate that devices cleaned with ethanol after being used to capture cells can be recoated with the affinity surface proteins and maintain a high binding efficiency (~95%). Devices cleaned with ethanol but not recoated with the affinity surface showed an initial binding efficiency of 96.2% ± 3.3% that dropped to 24.8% ± 14.8% after cleaning with ethanol. The results indicate that ethanol significantly reduces the affinity of the surface for the cells. Lastly, experiments conducted with anti-CD71 were repeated using anti-CD95 for cell capture. Overall, the results indicate that affinity surfaces can be cleaned and reused which could save money and time for research involving affinity coated microfluidic devices in the future. (Supported by: UMW Mahoney Research Fellowship) Author contact: rreif@umw.edu

FOLDING OF THE INTRINSICALLY DISORDERED PAR-4 TUMOR SUPPRESSOR AND ITS ROLE IN CISPLATIN TREATMENT OF CANCER. Andrea M. Korell, Komala Ponniah, Meghan S. Warden & Steven M. Pascal, Department of Chemistry and Biochemistry, Old Dominion University. The field of structural biology plays a key role in the advancement of cancer research and the development of innovative therapeutics. Prostate apoptosis response-4 (Par-4) is a 38kDa tumor suppressor protein. Par-4 down-regulation is observed in many forms of cancer while Par-4 up-regulation is characteristic of neurodegenerative conditions such as Alzheimer's disease. As a largely intrinsically disordered protein, full length Par-4 does not form a well-defined three-dimensional structure. Cleavage of Par-4 by caspase-3 activates tumor suppression via formation of an approximately 23kDa fragment (cl-Par-4) that enters the nucleus and inhibits pro-survival genes such as TOPO-1 and NF-□B that serve a role in tumor proliferation. Additionally, Par-4 confers cancer cell-specific sensitivity to the chemotherapeutic drug cisplatin. Consistent with this finding, cisplatin exerts a stabilizing effect on cl-Par-4 and increases cellular cl-Par-4 levels. We are investigating the structure of cl-Par-4 using circular dichroism (CD) and NMR spectroscopy, under varying conditions. We have identified specific pH and ionic strength conditions that stabilize the conformation of cl-Par-4. In addition, we have begun to characterize changes in cl-Par-4 conformation upon interaction with cisplatin. Author contact: Andrea Korell, akorell@odu.edu

DESIGN OF A DISABLED-2-DERIVED PEPTIDE TO IMPAIR PLATELET-MEDIATED CANCER CELL EXTRAVASATION. Wei Song[1], Anne M. Brown[2], Shuyan Xiao[1], Andrew Biscardi[1], Daniel G. S. Capelluto[1] & Carla V. Finkielstein[1], [1]Department of Biological Sciences, Virginia Polytechnic Institute and State University and [2]Department of Biochemistry, Virginia Polytechnic Institute and State University. Disabled-2 (Dab2) targets cellular membranes and triggers a wide range of biological events, including endocytosis and platelet aggregation. The N-terminal region drives Dab2 to the platelet membrane surface by binding to sulfatide through two sulfatide-binding motifs (SBM). A Dab2 peptide, representing SBM, can reversibly bind to

sulfatide with moderate affinity, and when added to a platelet mixture, reduces the number and size of sulfatide-induced aggregates. Molecular docking studies show that Arg 42 of SBM likely interacts with the head group of sulfatide through hydrogen bond interactions and the second sulfatide binding motif is possibly involved in sulfatide acyl chain interactions. Also, Ser 24 phosphorylation of SBM is found to be significant for membrane-bound sulfatide recognition. Moreover, tumor cells are reported to have the ability of aggregating platelets, which facilitates tumor cell migration, invasion and arrest within the vasculature. Contributions of platelets aggregation to tumor cell survival and spread suggest platelets as a new avenue for therapy. (Supported by American Heart Association Grant and 4-VA grant). Author contact: wsong317@vt.edu

THE FUNCTIONAL BASIS OF PHAFIN2 IN AUTOPHAGY. Tuo-Xian Tang & Daniel G. S. Capelluto, Dept. of Biol., Virginia Tech. Autophagy is a highly conserved cellular pathway in eukaryotic cells. A portion of the cytosol, which contains invading pathogens and long-lived proteins, is taken up by an autophagosome. This double-membrane organelle fuses with lysosomes, where the contents were digested by the lysosomal enzymes. Previous data showed that Phafin2 was involved in the induction of autophagy. The lysosomal accumulation of Phafin2 and Akt is a critical step in the induction of autophagy. Phafin2 has two domains, N-terminal PH (Pleckstrin Homology) domain and C-terminal FYVE (Fab 1, YOTB, Vac 1, and EEA 1) domain. Both domains can bind the phospholipid phosphatidylinositol 3-phosphate (PtdIns(3)P). In this study, we showed that Phafin2 is stable, showing a melting temperature of 48.4°C. The binding affinity between PtdIns(3)P and Phafin2 was studied by surface plasmon resonance. Results showed that PtdIns(3)P and Phafin2 had a strong binding, triggering minor conformational changes in the protein. Another interesting finding is that Phafin2 can cause membrane curvature, which may be required for tethering of lysosomes to autophagosomes, and consequently initiating autophagy. Author contact: tangtx@vt.edu

EXPERIMENTAL AND COMPUTATIONAL STUDIES OF OBSCURIN'S FLEXIBILITY. Jake A. Whitley, Daniel R. Marzolf, Oleksandr Kokhan, & Nathan T. Wright, Department of Chemistry and Biochemistry, James Madison University, 901 Carrier Dr., Harrisonburg, VA 22807. Obscurin is a giant modular muscle protein that functions to connect the sarcoplasmic reticulum to the contractile apparatus. Obscurin is made up of multiple Ig domains in a chain connected by short linkers. Previous structural papers show that short linkers are less flexible, yet MD papers show these linkers to be very flexible. Our research reconciles these divergent data. Here, we test the flexibility of 5 dual obscurin domain systems. Using NMR and SAXS, we show that these domains all adopt an extended architecture. However, MD and SMD data demonstrate obscurin to be significantly flexible. Therefore, we believe obscurin to be an extended, flexible protein, despite its short linkers. (Supported by: James Madison University Department of Chemistry and Biochemistry, Research Corporation, NSF REU (CHE-1461175), NSF RUI: MCB-1607024). Author contact: Jake Whitley, whitleja@dukes.jmu.edu

STRUCTURAL BASIS OF LIGAND RECOGNITION BY THE ENDOSOMAL ADAPTOR PROTEIN TOM1. Wen Xiong[1], Anne Brown[2] & Daniel G. S. Capelluto[1], [1]Department of Biological Sciences, Biocomplexity Institute, Virginia Tech,

[2]University Libraries, Virginia Tech. The target of Myb 1 (Tom1) plays a role in membrane trafficking by serving as an alternative endosomal sorting complex required for transport (ESCRT)-0 component. Tom1 possesses a N-terminal VHS domain followed by a central GAT domain. Tom1 has been shown to serve as a new phosphatidylinositol 5-phosphate (PI(5)P) effector at signaling endosomes through its VHS domain, delaying cargo degradation in a bacterial infection model. However, Tom1 itself unexpectedly does not bind to PI(5)P. Therefore, we propose that Tom1 may exhibit an autoregulation mechanism on the regulation of its function in the endosomal trafficking pathway. Our heteronuclear single quantum coherence (HSQC) data, lipid binding overlay assay, and molecular dynamic simulations revealed that Tom1 VHS interacts with PI(5)P following a fast-exchange regime, with the PI(5)P binding site identified to be at a region of the α-helix 6 and 8. Furthermore, Tom1 may exhibit an autoinhibition mechanism via a highly conserved DXXLL motif. Given the important role of the Tom1 protein in the immune system, clarification of its biological functions will contribute to the design of novel anti-bacterial strategies targeting specific protein trafficking events. Author contact: wxiong@vt.edu

COMPARING THE TEMPORAL DYNAMICS OF CASPASE ACTIVITY BETWEEN DIFFERENT INDUCTION PATHWAYS. Catherine Zwemer, Sean Morris, and Randall D. Reif, Department of Chemistry, University of Mary Washington, Fredericksburg, VA, 22401. Apoptosis, a process in which a cell systematically triggers its own death through a family of enzymes called caspases, is widely utilized in the body. Malfunction of apoptosis may lead to serious health problems including cancer. While the stages of apoptosis are known, the timing is poorly understood. The goal of this research is to examine the temporal dynamics of the intrinsic and extrinsic pathways of apoptosis with respect to caspase enzyme activation. Using an affinity microfluidic device, a known apoptosis inducer (hydrogen peroxide) and various rhodamine 110 based fluorescence caspase probes, the fluorescence of individual Jurkat T lymphocytes was monitored via fluorescence microscopy over a six hour period. The fluorescence of the cells indicated the level of caspase activity in the cell. This allowed for the determination of various parameters including the onset time and duration of caspase activity for all caspases as well as caspase-3 specifically. The intrinsic pathway showed consistent caspase activation between 4.3 to 5.3 hours after induction. The extrinsic pathway showed varying onset times with an average around 4 hours post induction. Analysis of the intrinsic pathway showed that caspase-3 activity started 5.3 hours after induction. Future studies will focus on caspase-3 activity in the extrinsic pathway. Knowledge of the timing of caspase activation and duration could be helpful when designing therapies that affect apoptosis. (Supported by: UMW Undergraduate Research Grant) Author contact: rreif@umw.edu

Virginia Journal of Science
Volume 69, Issue 1 & 2
Spring & Summer 2018
doi: 10.25778/DB6R-4R32

Compositional Changes in Two Small Mammal Communities During Succession in Southeastern Virginia

Robert K. Rose[1], Robyn M. Nadolny[1,2], Jay Kiser[1], Stephen E. Rice[1], Heather Green Salamone[1], Jana Eggleston[1], and Holly D. Gaff[1]

[1]Department of Biological Sciences, Old Dominion University, Norfolk, Virginia 23529-0266
[2]Army Public Health Center, Aberdeen Proving Ground, Maryland 21010

Corresponding author: brose@odu.edu

ABSTRACT

Changes in the composition of two small mammal communities were studied during 8 and 9 years of ecological succession in southern Chesapeake. Virginia. Using monthly live-trapping on grids of similar size and history since their abandonment as agricultural fields, we learned that house mice were early colonists on one grid but not the other. Two species of herbivorous rodent and the granivorous eastern harvest mouse were numerically dominant on both grids across the study. Some species disappeared early on one grid but persisted to the end at the other. The two arboreal small mammals, golden and white-footed mice, were most predictable between sites, showing up at year 8, after significant woody elements were present on the grids. The greatest abundances of small mammals (and probably greatest total biomass too) were seen between years 4 and 6 of ecological succession.

Key Words: community composition, small mammals, succession, Virginia

INTRODUCTION

Ecological succession, including of small mammals, begins immediately after an agricultural field is abandoned. In eastern North America, succession (as originally outlined by Clements, 1916, and best understood with plants) usually begins with the establishment of grasses and, to a lesser extent, herbaceous dicotyledonous plants (forbs); the seeds of these fast-growing plants are present in the soil seed bank. Later, woody elements such as shrubs and tree saplings are added, their composition being determined by proximity to seed sources, wind direction and intensity for carrying seeds to the field, seed transport and sometimes storage by seed-eating mammals such as squirrels or other rodents, among other factors. Eventually the shade provided by the leaves of woody plants eliminates the once-dominant herbaceous vegetation, and although some plant species able to live in low light do become established on the forest floor, the mature forest has much lower plant diversity than earlier stages of succession. As these changes in plant composition occur, the composition of almost every other

group of organisms in this dynamic habitat changes too, whether mycorrhizal fungi (e.g., Boerner et al., 1996; Hartnett and Wilson, 1999), insects (e.g., Martinko et al., 2006), spiders (e.g., Hurd and Fagan, 1992), or small mammals (e.g., Foster and Gaines, 1991; Kirkland, 1977; Larkin et al., 2008).

The speed with which an abandoned farm field becomes a mature forest depends on a number of factors, including the length of the growing season, the harshness of winters or duration of a drought, the amount and distribution within the year of rainfall, such physical factors as the water-holding capacity and richness of the soil, among others (Cramer and Hobbs, 2007). In southeastern Virginia, where our field studies of small mammals were conducted, many factors are particularly favorable for a rapid conversion from field to forest: a long growing season, hot summers, 1.3 m of rainfall uniformly distributed across the months of the year, a large number of cloud-free days, rich organic soils, and mild winters (Southeast Regional Climate Center: www.sercc.com; see Wallaceton-Lake Drummond site) .

The purpose of this research was to examine the changes in the numbers and kinds of small mammals present during the different stages of ecological succession, from habitats dominated by grasses to those with little herbaceous vegetation. We expected to see (1) dominance by herbivorous rodents early in succession, (2) gradual or sharp loss of herbivores when the grasses disappeared, and (3) the late appearance of arboreal small mammals when trees and shrubs came to dominance. To record these changes, we monitored the small mammals by monthly live trapping during which we caught, ear-tagged, and released small mammals on permanent grids of live traps. Thus, we were able to determine the abundance and residence periods of the several small mammal species across a range of years of study on two areas of similar history in their conversion from farm field to forest. Using this information, we hoped to be able to predict which small mammal species would be present in habitats of a particular stage of development along the grass-to-forest continuum in the coastal plain of our mid-Atlantic region.

MATERIALS AND METHODS

Descriptions of the two study sites

One study site was last used as a farm field in 2000, two growing seasons before we began our field studies. Now owned by The Nature Conservancy, the Su tract, named after its former owner, is located near Benefit Road in southern Chesapeake (36°37'N, 76°19'W), Virginia. In our first month of study at the Su tract, December 2002, the 11.5-ha field was dominated by 1.3-m tall little bluestem (*Schizachyrium scoparium*), other grasses, mostly panic grasses (*Panicum* spp.), and with some volunteer trees, mostly < 1-m loblolly pines (*Pinus taeda*) and with a few 1.5-m planted swamp chestnut oaks (*Quercus michauxii*). The field was bordered on two sides by mature hardwood forest, and by a freshwater marsh and a nearby mature (25-m) pine forest on the other sides. The small mammal study grid, placed about 30 m from the access road, was bisected by a meter-wide and 0.5-m-deep drainage ditch, typical of the ditching network of southern Chesapeake that makes agriculture possible in land formerly part of the Great Dismal Swamp, the distinctive geological feature of southeastern Virginia. The high water table of the region is due in part to moderate rainfall and low evapotranspiration during

winter. The Su tract lies about 4 km east of the 50,000-ha Great Dismal Swamp National Wildlife Refuge. Southern Chesapeake averages 247 frost-free days and 10 cm of snow annually, has 8-13 cm of rainfall each month, and the ground is rarely frozen for more than a few days in winter (www.sercc.com) . In brief, the growing season is long and the winters are mild and wet.

The other study site, called the Stephens tract after its former owner, is also owned by The Nature Conservancy. Located north of Cornland Road at 36° 39'N, 76° 21' W, this 60-ha former corn field was removed from cultivation in 2002, two growing seasons before we established a similar grid of traps for studying small mammals. Our 1-ha study grid was placed in similar grass-dominated vegetation, with a row of about 8 planted 2.0-m sycamore (*Platanus occidentalis*) trees along its eastern margin and with about 10 planted 1.5-m bald cypress trees (*Taxodium distichum*) scattered throughout the grid. Later, other trees were volunteers, mostly sweet gum (*Liquidambar styraciflua*), bayberry (*Myrica cerifera*), and red maple (*Acer rubrum*), which later came to dominate the site.

Field methods

We trapped for 3 days each month from December 2002 through July 2005 on the Su grid, except for June 2003 when extreme predator disturbance required closing the traps. After the numbers of small mammals plummeted, we trapped intermittently to monitor the arrival times of forest species of small mammals and to document the disappearance of resident species. We trapped three days each month from April 2005 through September 2012 on the Stephens grid.

Our study grids were 8 by 8 with 12.5-m intervals, producing a grid with an effective trapping area of 1 ha (Stickel, 1954). At each grid coordinate we placed 1 Fitch live trap (Rose, 1994) baited with a mixture of wild bird seed and sunflower seeds, with fiberfill added in winter for insulation. We set traps in the late afternoon, usually during the new moon phase, and checked them early for the next 3 mornings. From April through October, we locked the traps open after checking them in the morning and reset them just before sundown to prevent heat-related mortality. Using this approach, mortality for rodents was nearly zero. At the Su tract, we used only one trap per coordinate because the modest densities of small mammals precluded the need for more traps. However, when the meadow vole population at the Stephens tract increased greatly in density (June 2006), we added a second trap at each coordinate; after the meadow vole density declined, we continued to use two traps per station there.

At its first capture, each rodent was given a right ear tag with unique number, which, if lost, was replaced with a tag in the left ear, and the animal was synonymized to avoid inflating numbers of individuals. Although we recorded detailed information on reproductive condition for both sexes, for this report we are interested primarily in the numbers of different tagged individuals (an estimate of relative abundance) and in the presence, persistence, and disappearance of a species in the community of small mammals, or later, in the appearance of forest-dwelling small mammals. Our goal was to individually mark all animals living on the grid and to monitor the changes in the composition of the small mammal community as ecological succession progressed.

We initiated our studies before the Old Dominion University Institutional Animal Care and Use Committee required their approval for field studies of wild mammals, and have had annual ODU IACUC approvals (#10-010, #11-012, #13-017, #16-003) since 2010. Our methods followed the guidelines for the use of mammals in research and education, as outlined by the American Society of Mammalogists (Sikes et al. (2016).

RESULTS

During the only month of trapping in 2002 at the Su grid, hispid cotton rats (*Sigmodon hispidus*) dominated the small mammal community (Table 1); large numbers of house mice (*Mus musculus*) were present too but these disappeared in 2003. Cotton rats increased in numbers, flourished, and then declined sharply in number from 2005 to 2006, and remained in low numbers as the pines came to dominate the site. Among the herbivorous rodents, meadow voles (*Microtus pennsylvanicus*) appeared early in 2003, increased greatly in numbers, and then disappeared after three good years. Marsh rice rats (*Oryzomys palustris*), another herbivorous rodent, disappeared the same year as meadow voles, and exactly when cotton rats numbers dropped sharply too. This was the time when herbaceous vegetation, especially grasses, had mostly disappeared. (A 10 m by 10 m depression, dug as a breeding pool for amphibians and located near the center of the grid, remained free of pines; the obligate wetland grasses, sedges, and soft rushes growing there provided some habitat and food, enabling cotton rats and eastern harvest mice [*Reithrodontomys humulis*] to persist.)

Colonizing eastern harvest mice, an 8-g seed-eating rodent, found the site early and increased substantially in numbers and then declined but persisted for years, longer than for most other rodents (Table 1). The two forest species, white-footed mouse (*Peromyscus leucopus*) and golden mouse (*Ochrotomys nuttalli*), appeared much later, in years 8 and 9 of succession, respectively. The only other small rodent of forests, the woodland vole (*Pitymys pinetorum*) was represented by one individual that appeared in year 9 of succession.

The pattern was different at the Stephens site where in the first year of trapping substantial numbers of the three dominant herbivores (meadow voles, rice rats, and cotton rats) already were present (Table 2). The same was true in the second year, when large numbers of harvest mice also were added to the community of small mammals. The next year, house mice, which had been totally absent, appeared and were numerous then and in 2008; then house mice declined in number and they almost disappeared after 10 years of succession. This pattern of appearance and disappearance for house mice was drastically different than at the Su site. Also different was the persistence of both meadow voles and rice rats on the Stephens grid; true, their numbers declined but even after 9 years of succession, 20 meadow voles and 15 rice rats were tagged in 2012. The one pattern similar to that observed on the Su site was the late appearance of both golden and white-footed mice: both first appeared in the 8th year of succession and seemed to increase slowly in abundance later.

Despite the between-grid differences in the speed of succession to forest, a correlation analysis, using the MNA totals for each year, revealed a significant correlation ($r = 0.72$, $n = 6$, P

< 0.05). The greatest numbers of small mammals were during years 4 to 6 (or 7), after which numbers declined, dramatically so on the Su grid.

DISCUSSION

We began our field studies of small mammals two growing seasons after the farm fields had been abandoned. During those early stages of ecological succession, grasses dominated the vegetation, and the common herbivorous rodents quickly found these sites and established populations there. In both fields, little bluestem and panic grasses were the dominant grasses, and goldenrods (*Solidago* spp.), asters (*Aster* spp.), and horse nettle (*Solanum carolinense*) were common dicots. We have detailed information on the diets of cotton rats and rice rats in southeastern Virginia. In winter and spring, monocots comprised the majority of the diet for cotton rats but dicots were dominant in summer and autumn (Walker and Rose, 2010). Dicots were present in all 103 rice rat stomachs and monocots in 82 percent of stomachs (Rose and McGurk, 2006). Meadow voles have even more exclusively plant diets where they have been studied (e.g., Zimmerman, 1965).

On the Su grid, house mice and rice rats colonized the site quickly (Table 1), but both were later replaced (or displaced) by other small mammals; house mice remained one more year and rice rats three more years, then disappeared. Hispid cotton rats, also early colonizers, quickly became numerically dominant for a few years and persisted as long as eastern harvest mice. Meadow voles were co-dominants with cotton rats and eastern harvest mice from 2003 to 2005, and then disappeared after 2005, a time when total numbers of all small mammals dropped sharply, by nearly 90 percent. (This was when shading by the maturing pines extinguished most of the grasses.) During years 8 and 9 of succession (2009, 2010), golden mice, absent for the first seven years, outnumbered all other species combined. By 2010, when the grid was a pine forest with only patches of herbaceous vegetation, the herbivorous rice rats and meadow voles had been absent for five and four years, respectively, but the equally herbivorous cotton rat persisted in small numbers almost to the end, as did the granivorous eastern harvest mouse. It is particularly noteworthy that the insectivorous shrew, *Blarina*, was never abundant and none was caught during the last five years. By contrast, in pine plantations of four different ages in nearby Isle of Wight County, *Blarina* was fifth in abundance among the nine small mammals collected with both pitfall and live traps (Dolan and Rose, 2007). (Southeastern Virginia has two species of short-tailed shrew: *Blarina carolinensis*, the 6-10 g southern short-tailed shrew averages 100 mm and lives mostly in open habitats, whereas *B. brevicauda telmalestes*, the Dismal Swamp [and largest] subspecies, is found mostly in forests. We have lumped these as *Blarina* spp.) Interestingly, no meadow vole or rice rat was trapped in the Dolan study, even in grassy 1-year-old pine plantations, in a multi-year study with 67,950 trap nights.

The pattern of change in composition was more erratic on the Stephens grid, where all 8 species still were present in small to moderate numbers in 2012, after 10 years of succession (Table 2). One of the surprises was that house mice were absent for the first two years of study, then had modest numbers for two years and lower numbers thereafter; but they persisted with the populations of native mammals, unlike in many studies (e.g., Lidicker, 1966; Stickel, 1979). House mice usually are among the first colonizers of abandoned fields (e.g., Gentry, 1966) but often they are displaced when native species establish populations (DeLong, 1966; Lidicker,

1966). The most numerous herbivore, the cyclical meadow vole, reached highest abundance in year 2 (2006), sustained relatively high numbers for three more years, and never disappeared; on the Su grid, meadow voles were absent for the last four years. Marsh rice rats and cotton rats also had their years of abundance, years of moderate numbers, but they too persisted to the end of study at the Stephens grid, when cotton rats were the most numerous of the 8 species. Unlike other species, the harvest mouse showed a similar pattern on both grids: it arrived early and thrived every year, showing an ability to tolerate a wide range of habitat types, and was present at the end of the field studies. At the Stephens grid, a few *Blarina* were present every year, also different from the pattern on the Su grid, where this shrew was absent for the last five years. On both grids, white-footed mice and golden mice first appeared after 7 years of succession, when the woody components of the plant community had become well established.

Thus, succession to forest went much more quickly on the Su grid than on the Stephens grid, mostly because of its proximity to a seed source: a mature pine forest with 25-m trees was located about 40 m west of the Su grid. Meter-high pine seedlings already were present in December 2002 when the trapping began. We measured and counted the pine trees on the grid in 2005, 2008, and 2010. Of the more than 15,000 seedlings/saplings we counted early in 2005, about 12 percent of mortality was due to girdling by cotton rats, mostly in late winter and spring of 2005 (Nadolny and Rose, 2015); consumption of bark was confirmed by Walker and Rose (2010). By 2008 and certainly by 2010, some pines were sufficiently mature, with diameters greater than 15 cm, to produce cones. In brief, succession to pine forest happened quickly due to the nearby source of pine seeds and to the innate rapid growth of loblolly pines, the dominant pine species in southeastern Virginia.

By contrast, we placed the grid at the Stephens tract more than 100 m from any forest edge and more than 200 m from the western edge of this much larger field. Pine seedlings and saplings were rare on the Stephens grid, where the majority of volunteer trees were sweet gum and red maple. Further, because the sycamores and cypresses planted by The Nature Conservancy grew relatively slowly, much more time was required before significant shading reduced the herbaceous ground cover. In addition, large patches of wool grass, *Scirpus cyperinus*, and soft rushes, *Juncus* spp., were present throughout the grid and these persisted until deciduous trees were sufficiently well established to lower the water table and shade out these obligate wetland plants. Thus, succession went much more slowly at the Stephens site than at the Su site, resulting in the much slower progression to forest there. Because grasses and forbs were present for several years, food was available to sustain all small mammal populations at modest densities on the Stephens grid. Even the shrews persisted to the end of the study on the Stephens grid.

Cotton rats were numerically dominant at the Su site with meadow voles second in total abundance of tagged animals; on the Stephens grid, their rank-order was reversed. Surprisingly, eastern harvest mice were third in abundance on both grids, the result of their modest but persistent annual populations. Their third-place status is due in part to the versatility of eastern harvest mice: in southeastern Virginia, it is the only species that might be trapped in any habitat, from the barest grassy habitat to the most mature deep-woods forest. In ecological terms, it has the broadest niche among the rodents in southeastern Virginia.

Perhaps the most consistent feature between grids was the timing of the appearance of the forest-dwelling species: the arboreal golden and white-footed mice. Vertical structure must be available before arboreal species can be accommodated and thus their late arrival on the grids was expected. Golden mice often are associated with forest edge, where shrubs and vines form the interface between forest and a more open habitat type, whether old field or crop field. Golden mice often build their spherical nests in thickets of brush and feed on invertebrates, fruits and seeds in these productive edge habitats (Rose, 2008), but they also nest in boxes placed on trees in a mature forest (Rose and Walke, 1988) and probably also in tree holes. Golden mice appeared on both Su and Stephens grids during the 8th year in succession. Golden mice were present only in the 8-year-old pine plantations (and absent in 18- and 24-year-old pines—Dolan and Rose, 2007), the same age as when they were present on both grids. The narrow habitat tolerances and low abundances of golden mice are best illustrated in the quote of Dueser and Shugart (1979): "The golden mouse [near Oak Ridge, Tennessee] has low variability in niche configuration, occurs in low abundance even in its optimal site, and is highly susceptible to influence by external and successional habitat alterations."

In southeastern Virginia, *Peromyscus leucopus* seems to require older and larger trees, because it was never abundant even during the last year of study on either grid. Only 1 had been caught on the Su grid after 10 years of succession and 10 on the Stephens grid, the fewest of any species at both sites. Although regarded by some investigators as an arboreal species nesting in holes of large trees in maturing or mature forest (e.g., Linzey et al., 2012), some populations of white-footed mice are excellent colonizers, as seen in the study of small mammals on nine 1-ha grassy grids on reclaimed surface mines in eastern Kentucky (Larkin et al. 2008), where *P. leucopus* was overwhelmingly dominant (n = 295); only 5 individuals of other species were caught. By contrast, in a field study on the upper coastal plain of Virginia, *P. leucopus* was equally common in all five macrohabitats, ranging from old fields through pine forests and oak-hickory forests (Bellows et al., 2001). It is unclear why one species should show such varying results in its habitat affinities. Our results indicate that at least in southern Chesapeake, Virginia, *P. leucopus* is a forest mammal and definitely neither a good colonizer of newly created habitat nor versatile in occupying differing habitats along the grass-forest continuum.

In southeastern Virginia, the first small mammals to find a newly abandoned farm field often are house mice and eastern harvest mice (Cawthorn and Rose, 1989). In Cawthorn's study, these two species comprised 90 percent of captures in a grassy oldfield. Numerous field studies (e.g., DeLong, 1966; Kaufman and Kaufman, 1990) report the early presence of house mice, including on disturbed sites with little covering vegetation. Later, house mice, an introduced species, often are replaced by native species of small mammals; Lidicker (1966) describes the extinction of a house mouse population as a population of California vole expanded and DeLong (1966) also reported house mice being displaced by *Microtus*. On a dredge spoil site in Portsmouth, Virginia, house mice and meadow voles coexisted for 13 months, during which time house mice dropped from 104 per ha to 37 per ha, while meadow voles increased from 8 to 41 per ha in a *Phragmites* marsh (Rose and Kratimenos, 2006). But sometimes house mice persist, as they did on the Stephens grid, and seemingly coexist with populations of native small mammals.

Our studies of small mammal communities in southeastern Virginia indicate that herbivorous rodents will find grassy sites quickly but can either disappear nearly as quickly when grasses are shaded out by canopy closure or persist longer if canopy closure proceeds more slowly. House mice quickly found one grid but not the other, and their responses differed too, for they abruptly disappeared on one grid when populations of native mammals had become established but coexisted for years with populations of the same native species on the other grid. The three herbivores showed similar differential responses, as did *Blarina*, disappearing in mid-succession on the Su grid but persisting to year 10 on the Stephens grid. Although white-footed mice are sometimes excellent colonizers or have similar abundances in a range of habitats, on our two study grids in southeastern Virginia, they were truly forest species, appearing only after 8 or 9 years of biological succession, when substantial trees and shrubs were present. The golden mouse also was predictable, appearing around year 8, and flourishing at least a year or two. In brief, although most information on small mammal communities is derived from inferences based on short-term trapping studies in a range of habitats in a region, such as those conducted across Wisconsin (Stephens and Anderson, 2014), our long-term studies at nearby locations with similar succession histories indicate that the composition of small mammal communities was less predictable and more variable than we expected.

Although the sites were not studied contemporaneously and thus cannot be considered to be replicates, the significant correlation of total MNA and years since abandonment from agriculture indicates that the patterns of greatest abundances of small mammals (from ages 4 to 6 [or 7]) were similar. The Su site transitioned so quickly to pine forest that the numbers of the three dominants dropped by nearly 90 percent from year 6 to year 7, whereas on the Stephens grid total numbers of these three dominants actually increased by about 20 percent from year 6 to year 7, and their numbers did not drop until year 8. Thus, a slow progression toward forest gives herbivorous rodents a longer residence time in southeastern Virginia and somewhat delays the appearance of the arboreal species of small mammals.

ACKNOWLEDGMENTS

We thank The Nature Conservancy for the use of their land for research, fellow graduate students for occasional field assistance, our department for its support, and the suggestion of one reviewer to use correlation analysis to see patterns in changing numbers.

LITERATURE CITED

Bellows, A. S., J. F. Pagels, and J. C. Mitchell. 2001. Macrohabitat and microhabitat affinities of small mammals in a fragmented landscape on the upper coastal plain of Virginia. American Midland Naturalist 146:345-360.

Boerner, R. E. J., B. G. DeMars, and P. N. Leicht. 1996. Spatial patterns of mycorrhizal infectiveness of soils along a successional chronosequence. Mycorrhiza 6:79-90.

Cawthorn, J. M., and R. K. Rose. 1989. The population ecology of the eastern harvest mouse (*Reithrodontomys humulis*) in southeastern Virginia. American Midland Naturalist 122:1-10.

Clements, F. E. 1916. Plant succession: An analysis of the development of vegetation. Carnegie Institute of Washington, Publication 242.

Cramer, V. A., and R. J. Hobbs, eds. 2007. Old fields: dynamics and restoration of abandoned farmland. Island Press, Washington, D. C.

DeLong, K. T. 1966. Population ecology of feral house mice: interference by *Microtus*. Ecology 47:481-484.

Dolan, J. D., and R. K. Rose. 2007. Depauperate small mammal communities in managed pine plantations in eastern Virginia. Virginia Journal of Science 58:147-163.

Dueser, R. D., and H. H. Shugart, Jr. 1979. Niche pattern in a forest-floor small mammal fauna. Ecology 60:108-118.

Foster, J., and M. S. Gaines. 1991. The effects of a successional habitat mosaic on a small mammal community. Ecology 72:1358-1373.

Gentry, J. B. 1966. Invasion of a one-year abandoned field by *Peromyscus polionotus* and *Mus musculus*. Journal of Mammalogy 47:431-439.

Hartnett, D. C., and G. W. T. Wilson. 1999. Mycorrhizae influence plant community structure and diversity in tallgrass prairie. Ecology 80:1187-1195.

Hurd, L. E., and W. F. Fagan. 1992. Cursorial spiders and succession: age or habitat structure? Oecologia 92:215–221.

Kaufman, D. W., and G. A. Kaufman. 1990. House mouse (*Mus musculus*) in natural and disturbed habitats in Kansas. Journal of Mammalogy 71:428-432.

Kirkland, G. L., Jr. 1977. Responses of small mammals to the clearcutting of northern Appalachian forests. Journal of Mammalogy 58:600-609.

Larkin, J. L., D. S. Maehr, J. J. Krupa, J. J. Cox, K. Alexy, D. E. Unger, and C. Barton. 2008. Small mammal response to vegetation and spoil conditions on a reclaimed surface mine in eastern Kentucky. Southeastern Naturalist 73:401-412.

Lidicker, W. Z., Jr. 1966. Ecological observations on a feral house mouse population declining to extinction. Ecological Monographs 36:27-50.

Linzey. A. V., A. W. Reed, N. A. Slade, and M. H. Kesner. 2012. Effects of habitat disturbance on a *Peromyscus leucopus* (Rodentia: Cricetidae) population in western Pennsylvania. Journal of Mammalogy 93:211-219.

Martinko, E. A., R. H. Hagen, and J. A. Griffith. 2006. Successional change in the insect community of a fragmented landscape. Landscape Ecology 21:711-721.

Nadolny, R. N., and R. K. Rose. 2015. Girdling by the hispid cotton rat as a significant source of mortality in a loblolly pine (*Pinus taeda*) successional forest. American Midland Naturalist 174:74-86.

Rose, R. K. 1994. Instructions for building two live traps for small mammals. Virginia Journal of Science 45:151-157.

Rose, R. K. 2008. Population ecology of the golden mouse. Pp. 39-58 *in* Barrett, G. W., and G. A. Feldhamer (eds). The Golden Mouse. Springer, New York.

Rose, R. K., and G. E. Kratimenos. 2006. Population dynamics of meadow voles and feral house mice on a dredge disposal site. American Midland Naturalist 156:376-385.

Rose, R. K., and S. W. McGurk. 2006. Year-round diet of the marsh rice rat, *Oryzomys palustris*, in Virginia tidal marshes. Virginia Journal of Science 57:115-121.

Rose, R. K., and J. W. Walke. 1988. Seasonal use of nest boxes by *Peromyscus* and *Ochrotomys* in the Dismal Swamp of Virginia. American Midland Naturalist 120:258-267.

Sikes, R. S., and Animal Care and Use Committee of the American Society of Mammalogists. 2016. 2016 Guidelines of the American Society of Mammalogists for the use of wild mammals in research and education. Journal of Mammalogy 92:663-688.

Stephens, R. B., and E. M. Anderson. 2014. Habitat associations and assemblages of small mammals in natural plant communities of Wisconsin. Journal of Mammalogy 95:404-420.

Stickel, L. F. 1954. A comparison of certain methods of measuring home range of small mammals. Journal of Mammalogy 35:1-15.

Stickel, L. F. 1979. Population ecology of house mice in unstable habitats. Journal of Animal Ecology 48:871-887.

Walker, L. A., and R. K. Rose. 2010. Seasonal variation in diet of a marginal population of the hispid cotton rat, *Sigmodon hispidus*. Virginia Journal of Science 60:3-12.

Zimmerman, E. G. 1965. A comparison of habitat and food of two species of *Microtus*. Journal of Mammalogy 46:605-612.

Table 1. Numbers of individuals of small mammal species taken during monthly live trapping at the Su site in southern Chesapeake, Virginia, starting in year 3 of ecological succession after abandonment as a farm field. MNA refers to the number of individuals given uniquely numbered ear tags and mammals per trap night is the catch rate/100 traps.

Common Name	**2002**	**2003**	**2004**	**2005**	**2006**	**2007**	**2008**	**2009**	**2010**	**Total**
Short-tailed shrew	0	1	7	3	0	0	0	0	0	11
Eastern harvest mouse	1	51	73	63	12	0	8	2	1	211
Golden mouse	0	0	0	0	0	0	0	10	7	17
Hispid cotton rat	69	302	273	153	21	5	7	3	0	833
House mouse	22	30	0	0	0	0	0	0	0	52
Marsh rice rat	9	6	8	6	0	0	0	0	0	29
Meadow vole	0	50	87	95	2	0	0	0	0	234
Pine vole	0	0	0	0	0	0	1	0	0	1
White-footed mouse	0	0	0	0	0	0	1	0	0	1
Total mammal MNA	101	440	448	320	35	5	17	15	8	1389
Total number trap nights	256	1600	2432	1216	448	64	576	192	192	6976
Total mammals/trap night	0.39	0.28	0.18	0.26	0.08	0.08	0.03	0.08	0.04	.20

Table 2. Numbers of individuals of small mammal species taken during monthly live trapping at the Stephens site in southern Chesapeake, Virginia, starting in year 3 of ecological succession after abandonment as a farm field. MNA refers to the number of individuals given uniquely numbered ear tags and mammals per trap night is the catch rate/100 traps.

Common Name	**2005**	**2006**	**2007**	**2008**	**2009**	**2010**	**2011**	**2012**	**Total**
Short-tailed shrew	5	6	5	7	8	11	4	31	77
Eastern harvest mouse	9	37	59	71	67	56	43	29	371
Golden mouse	0	0	0	0	0	2	4	6	12
Hispid cotton rat	19	33	37	120	250	103	34	53	649
House mouse	0	0	57	62	11	5	0	2	137
Marsh rice rat	39	84	47	6	21	24	4	15	240
Meadow vole	109	516	206	136	129	27	25	20	1168
White-footed mouse	0	0	0	0	0	1	2	7	10
Total mammal MNA	181	676	411	402	486	229	116	163	2664
Total number trap nights	1280	4480	5504	4608	4736	4096	3456	3584	31744
Total mammals per trap night	0.14	0.15	0.07	0.09	0.1	0.06	0.03	0.05	0.08